CHARACTERIZATION OF MATRIMONY'S ROLE AS A POLO KINASE REGULATOR DURING *DROSOPHILA* FEMALE MEIOSIS

BY

S. Kendall Smith

Submitted to the graduate degree program in Molecular and Integrative Physiology and the Graduate Faculty of the University of Kansas Medical Center in partial fulfillment of the requirements for the degree of Doctor of Philosophy.

_____

Chairperson, R. Scott Hawley, Ph.D.

Committee Members

_____

David Albertini, Ph.D.

_____

Joan Conaway, Ph.D.

_____

Roy Jensen, M.D.

_____

Liskin Swint-Kruse, Ph.D.

Date defended: 6/29/11

The Dissertation Committee for S. Kendall Smith certifies that this is the approved version of the following dissertation:

CHARACTERIZATION OF MATRIMONY'S ROLE AS A POLO KINASE REGULATOR DURING *DROSOPHILA* FEMALE MEIOSIS

_____

Chairperson, R. Scott Hawley, Ph.D.

Date approved: 7/25/11

Abstract

Regulatory interactions that occur between Polo-like kinase 1 (Plk1) and its protein partners are critical for promoting many different cell division events. Indeed, Plk1 is found mis-regulated in a diverse set of human cancers and has been clinically validated as a drug target in cancer. Here, we use *Drosophila* as a model to understand how a 217 amino acid protein called Matrimony (Mtrm) regulates the *Drosophila* homolog of Plk1, Polo kinase, during female meiosis. By analyzing the functionality of a variety of Mtrm mutants, we find that Mtrm and Polo appear to engage in a non-canonical mechanism of interaction *in vivo* relative to previously described Polo protein interactors. Furthermore, we have identified a Mtrm mutant that separates function during meiosis, suggesting that Mtrm may differentially interact with Polo kinase by at least two different pathways or mechanisms. Thus, in addition to furthering our understanding of the role of Mtrm as a regulator of Polo in *Drosophila* female meiosis, these studies address a larger, more fundamental question of how Polo interacts with its protein partners *in vivo*. Elucidating such non-canonical mechanisms of Polo regulation *in vivo* may contribute to the development of novel and innovative strategies for selective Plk1 inhibition in cancer.

Dedication

This thesis is dedicated to my mother, Mary Drew Myer, and in loving memory of Nancy Cooper Maier.

Acknowledgments

I wish to thank my advisor, Scott Hawley, for providing me with a solid foundation in genetics and the highest level of training imaginable. Scott has been particularly supportive as I pursue a combined MD-PhD degree. In addition, his advocacy for women leaders in science is truly remarkable. Thank you, Scott, for your constant guidance, support and profound inspiration.

I would like to thank all of the Hawley Lab members for their patience, advice and excellent training. Those that contributed to this thesis including Youbin Xiang, Jennifer Chisholm, Amanda Wilson and our collaborators Sue Jaspersen, Laurence Florens, Michael Washburn, Selene Swanson, Arcady Musheigan, Jay Unruh, and Brian Slaughter deserve a special '*nod*.' In addition, a special thanks goes out to Stephanie Kong and Charles Banks. Overall, this work would not have been possible without all of your enormous contributions.

Thanks to my Committee members, David Albertini, Joan Conaway, Roy Jensen, and Liskin Swint-Kruse for their helpful advice and valuable time. In addition, members of the KUMC MD-PhD Program, in particular Tim Fields, Joe Bast and Janice Fletcher have been particularly supportive over the years.

I wish to thank Jim and Virginia Stowers for their enormous generosity and advocacy for basic scientific research. The Stowers Institute has changed countless lives and will continue to do so in ways beyond my comprehension.

Finally, I want to thank my family. You have provided me with unconditional love, support and inspiration throughout this process and beyond.

Table of Contents

List of Figures

List of Tables

List of Abbreviations

°C……..…degrees centigrade

AD……..……activation domain

bp……..…….base pair

BD……..…..binding domain

BSA……..…..bovine serum albumin

C. elegans.……*Caenorhabditis elegans*

Cdc25……Cell division cycle 25

Cdk1……..Cyclin-dependent kinase 1

CDks……..Cyclin-dependent kinases

cDNA……....complimentary deoxyribonucleic acid

CIN……..…chromosomal instability

cm……..…centimeter

co-IP……..co-immunoprecipitation

D. melanogaster…..Drosophila melanogaster

DNA……deoxyribonucleic acid

dNTP……..…..deoxynucleotide triphosphate

FCS……fluorescence correlation spectroscopy

FCCS……..…fluorescence cross correlation spectroscopy

EDTA……..….ethylenediaminetetraacetic acid

EGTA……...….ethylene glycol tetraacetic acid

FL……....full length

g……..…gram

GAL……galactose

GSK-3β……....Glycogen synthase kinase 3 beta

GFP……..……green fluorescent protein

hr……..…….....hour

HEPES……..…N-[hydroxyethylpiperazine –N ‘-[2-ethanesulphonic acid]

IP……immunoprecipitation

Kb……..…..kilobase

kDa…….kiloDalton

LiOAc……....lithium acetate

Map205……..Microtubule-associated protein 205

mg……..…...milligram

MKlp2……Mitotic kinesin-like protein 2

mins……minutes

ml……milliliter

mM…….millimolar

MOPS……..…....3-(N-morpholino)propane sulphonic acid

mRNA…….……..messenger RNA

MS…….mass spectrometry

MudPIT…….multidimensional protein identification technology

Mtrm……..…Matrimony

NDJ…….…….nondisjunction

NE…….nuclear envelope

NEB……...…..nuclear envelope breakdown

ng…….nanogram

NP-40……..ethylphenyl-polyethylene glycol

NSAF……..normalized spectral abundance factor

PBD……..……..Polo-box domain

PBS……...…..phosphate buffered saline

PCR……..…..polymerase chain reaction

PEG……..…...polyethylene Glycol

PLGEM……..power law global error model

Plks……..…..Polo-like kinases

Plk1……...……Polo-like kinase 1

PTM……...posttranslational modification

o/n……...…..overnight

RNA……..…ribonucleic acid

RNAi……....RNA-mediated interference

rpm……..revolutions per minute

S. cerevisiae...*Saccharomyces cerevisiae*

S. pombe…...*Schizosaccharomyces pombe*

SAM……...Sterile Alpha Motif

SDS……..….sodium dodecyl sulfate

TCA……...trichloroacetic acid

Tris……tris[hydroxymethyl aminomethane]

UAS……..upstream activation sequence

WT……...wild-type

X. laevis…..*Xenopus laevis*

Y2H……..yeast two-hybrid

YPD……....yeast peptone dextrose

Chapter 1. Introduction

1.1 Why study Polo kinase regulation?

Successful cell division requires a series of carefully coordinated events to occur in time and space including DNA replication, alignment of sister chromosomes on the spindle, segregation of genetic material to each of the daughter cells, and then disassembly of the spindle and cytokinesis. Temporal and spatial control of these events is achieved in part by the coordinated action of multiple kinases. One such kinase is the highly conserved Polo-like kinase 1 (Plk1), which is increasingly recognized as a master promoter of many cell division events (for reviews, see [1-4]). Furthermore, Plk1 is mis-regulated in human cancers of diverse origins and has been clinically validated as a selective drug target in cancer [5-8]. Therefore, we reason that understanding how Plk1 is regulated *in vivo* is important for elucidating how this kinase performs its numerous roles during cell division. In addition, this work may also contribute to the development of innovative strategies for targeted Plk1 inhibition as an anti-cancer therapy.

1.1.1 Polo kinase—"The Multi-tasking kinase"

The discovery of Plk1 began with the isolation of a mutant in *Drosophila melanogaster* that displayed abnormal mitotic spindle poles [9]. The mutation was mapped to a gene (later named *polo*) encoding a serine/threonine kinase that is highly conserved from budding yeast (Cdc5) to humans (Plk1) [10]. Since its discovery in 1988, the known roles of Plk1 orthologs (hereafter collectively

called Polo kinases) in cell division have rapidly expanded to include proper mitotic/meiotic entry, regulation of centriole duplication and centrosome maturation, biorientation of chromosomes, regulation of cohesion, control of mitotic exit and cytokinesis (Figure 1-1). The various functions of this multi-tasking kinase have been the subject of many extensive reviews [1-4].

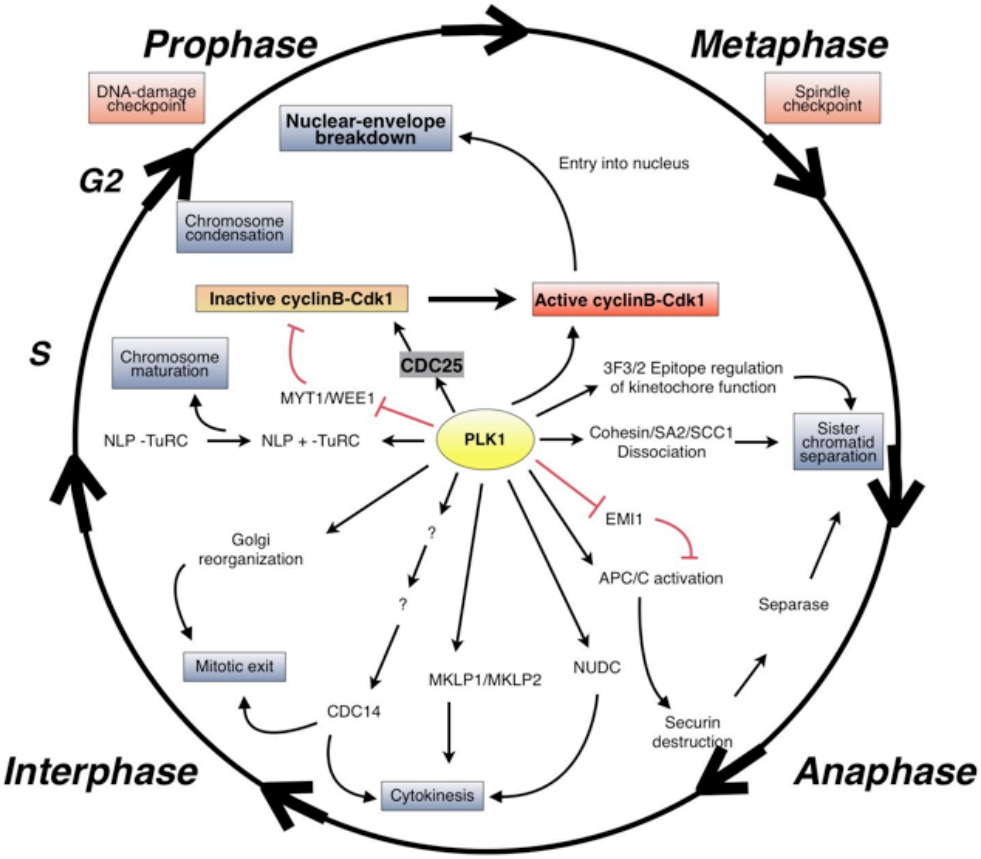

Figure 1-1 Summary of Plk1 functions in the cell cycle.

This figure, adapted from [11], summarizes the functions of Plk1 during various aspects of mitotic progression including mitotic entry, centriole and centrosome maturation, proper chromosome segregation, mitotic exit and cytokinesis. Inhibitory interactions are shown in red and stimulatory interactions are shown as black arrows.

While these initial studies pointed to a clear role for Polo in promoting mitotic and meiotic events during cell division, they also raised an interesting question: how can Polo perform such a diverse array of tasks from the beginning to the end of cell division? The answer, in part, involves its dynamic post-translational regulation aside from transcriptional control and targeted degradation (reviewed in [1-4]). Not only is Polo kinase able to phosphorylate its targets, it also engages in noncatalytic phosphoprotein interactions that facilitate its dynamic subcellular localization within the cell. The ability of Polo kinase to participate in two major mechanisms of signal transduction—phosphorylation and phosphoprotein binding–is a remarkable property that has only been shown to exist for only a handful of signaling proteins thus far [12]. Proper subcellular localization of Polo through noncatalytic means effectively gives the kinase access to its catalytic targets at the proper time and place during cell division. Conversely, such localization would also effectively restrict the kinase from its substrates at the wrong time and place. This special aspect of Polo kinase will be described in more detail in Sections 1.2 and 1.3.

1.1.2 Clinical Implications

From a clinical standpoint, this work is important because Plk1 is found dramatically mis-regulated in a diverse set of human cancers. It is not surprising that mis-regulation of such a central protein kinase could override critical checkpoints leading to improper cell division and aneuploidy, which is linked to tumorigenesis [13,14]. Plk1 overexpression has been observed in a number of

human cancers including non-small-cell lung cancer [15], head and neck cancer [16], esophageal cancer [17], gastric cancer [18], melanomas [19], breast cancer [20], ovarian cancer [21], cervical cancer [22], colorectal cancer [23], glioma [24], papillary carcinoma [25], pancreatic cancer [26,27], prostate cancer [28,29], leukemias and lymphomas [30-32], bladder cancer [33] and thyroid cancer [34], among others (for list and reviews, see [35-37]).

Paradoxically, Plk1 down-regulation has also been implicated in tumorigenesis. Increased tumor development has been observed in *Plk1*$^{+/-}$ mice [38]. However, this observation may reflect the essential role of Plk1 during embryogenesis, when Plk1 expression is required for rapid cellular proliferation and differentiation [38]. Nevertheless, the observation that both overexpression and down-regulation of Plk1 may lead to tumorigenesis suggests that the tight regulation of this kinase is essential for proper cell division (for review, see [35]).

Many studies have clinically validated Plk1 as drug target in cancer [5-8]. Currently, two general strategies are being pursued for selective Plk1 inhibition by small molecules. The first involves a classical method of kinase inhibition by targeting the ATP-binding pocket responsible for rendering the kinase catalytically active. Indeed, considerable success has been achieved using this approach [39,40] (for review, see [41]). However, due to the high degree of structural conservation among ATP-binding pockets, identifying inhibitors that selectively target the Plk1 ATP-binding pocket has proven challenging.

The second approach involves targeting the unique domain of Polo responsible for mediating the noncatalytic protein-protein interactions that facilitate its dynamic subcellular localization. One potential advantage to the second approach is that, unlike the ATP-competitive inhibitors, targeting this unique Polo domain may minimize undesirable off-target effects. On this front, progress has also been made in identifying small molecules that inhibit Polo activity via this domain [42-44] (for review, see [41]). However, as we continue to advance our basic understanding of how Polo noncatalytically interacts with its protein partners *in vivo*, we are finding that the mechanisms of interaction are more varied and complex than previously thought. This suggests that identifying new and innovative approaches for non-competitive Polo inhibition is entirely plausible, and perhaps even likely. Advancing our basic knowledge of how Polo interacts with its protein partners *in vivo* may help to drive those discoveries.

1.2 Evolutionarily conserved structure of Polo kinase

Further discussion requires a more detailed examination of the structure of Polo kinase, which is highly conserved from budding yeast (Cdc5) to humans (Plk1) (Figures 1-2 and 1-3). Polo kinase is comprised of two functional domains—a canonical N-terminal serine/threonine kinase domain and a unique C-terminal Polo-box domain (PBD) separated by a flexible linker region (Figure 1-2). While the crystal structure of each domain has been determined

individually, a complete structure of the entire protein has not been reported to date (see [41] for review).

The N-terminal kinase domain of Polo targets proteins that contain the consensus motif (D/E-X-pS/pT-Ø-X-D/E), in single amino acid code, where X is any amino acid, p denotes phosphorylation, and Ø is any hydrophobic amino acid. Crystal structures of the kinase domain of Polo reveal typical kinase domain topology, where phosphorylation of its activation loop occurs at T210 of human Plk1 (T182 in *Drosophila* Polo) (Figure 1-3). While the kinase topology is grossly canonical, several modest structural modifications within the Polo ATP-binding pocket are observed. These changes may contribute to the success in developing selective ATP-competitive inhibitors such as BI 2536, which shows high selectivity for Plk1 versus other serine/threonine kinases [39,47].

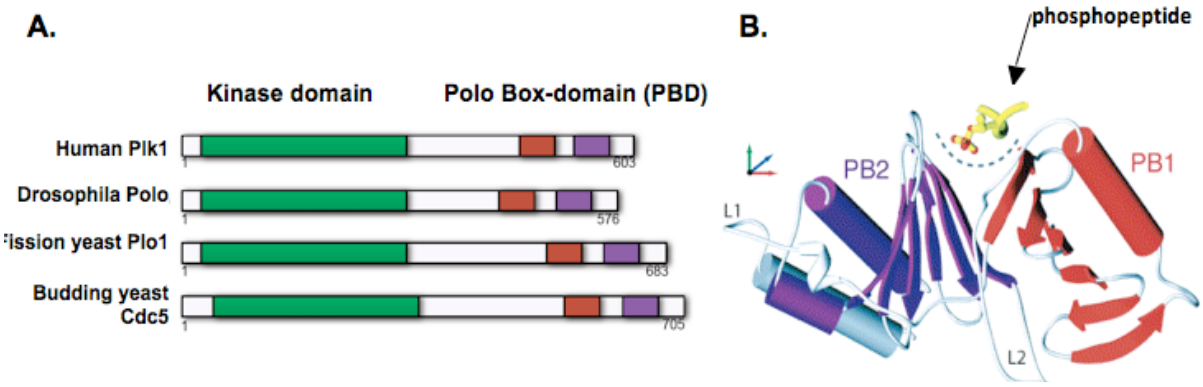

Figure 1-2 Structure of Polo kinase.

(A) Plk1 is comprised of an N-terminal kinase domain and a C-terminal noncatalytic PBD separated by a flexible linker region. (B) Adapted from [48]. Two Polo boxes, PB1 and PB2, form the C-terminal PBD. The PBD is thought to bind phosphopeptides comprised of a specific core consensus motif, which functions to spatially and temporally regulate the protein's catalytic activity during cell division [45,46].

The C-terminal noncatalytic Polo box-domain (PBD) is unique to Polo and mediates protein-protein interactions that allow the kinase to multi-task within the cell. The C-terminal PBD consists of two Polo boxes, PB1 and PB2, which function as a single protein-binding unit. A shallow, positively charged cleft is formed at the interface of the two Polo boxes, which has been reported to selectively bind phosphopeptides containing a specific core consensus motif (S-pS/pT-P/X), where p denotes phosphorylation and X is any amino acid (Figure 1-2) [45,46].

Moreover, multiple studies in several organisms have identified several mutations that abrogate the ability of the PBD to selectively bind proteins. The classic 'pincer mutant' was first identified as an H538A/K540M double mutant residing within PB2 [46]. Additional studies have revealed several mutations within PB1 that also abrogate PBD selectivity including W414F, V415A and L427A of human Plk1 [48]. The equivalent mutations in *Drosophila* Polo are W395F, V396A, and L408A and have been shown to abrogate function within this organism [49]. Because these mutations ablate PBD specificity, they often largely impair Polo function within the cell.

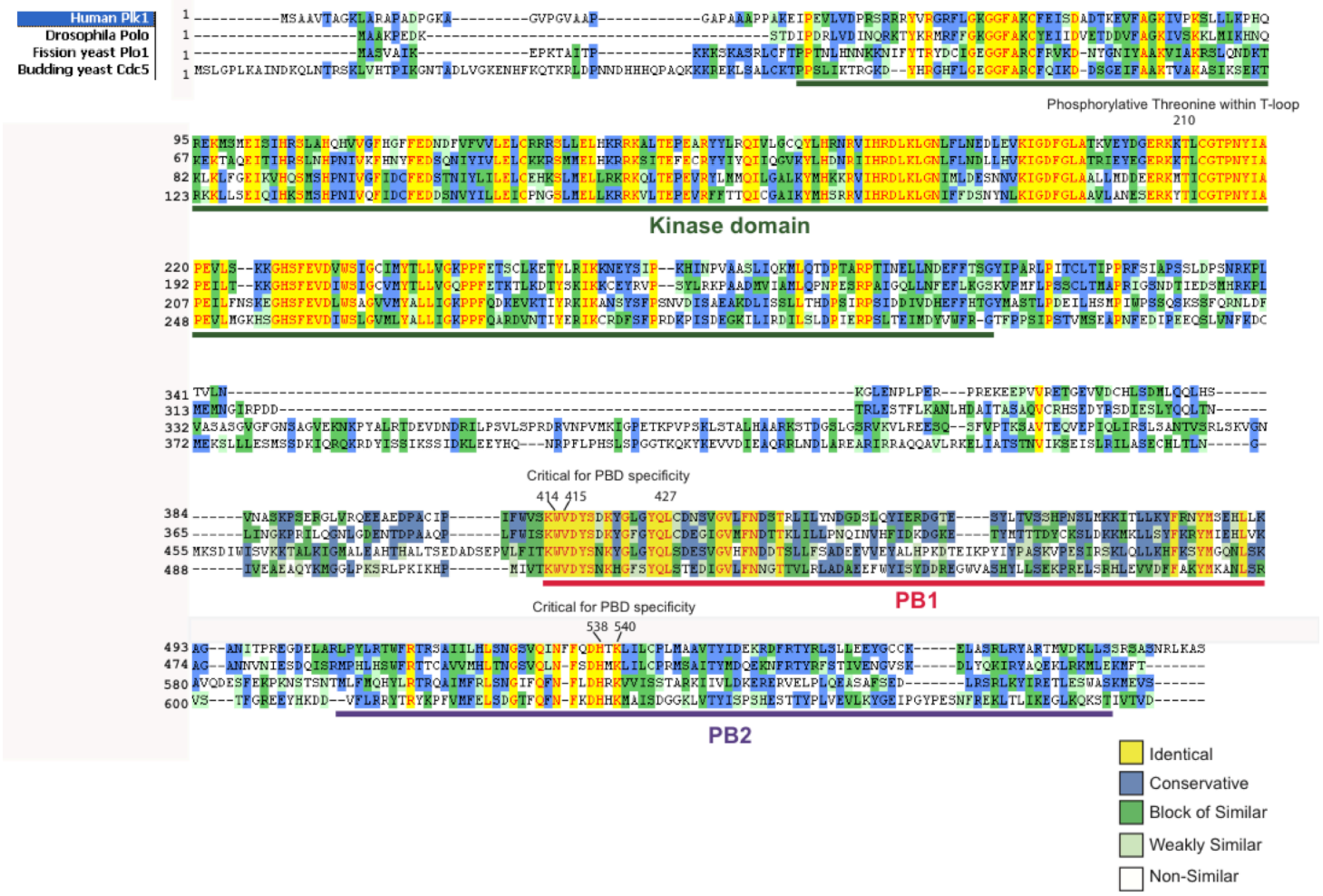

Figure 1-3 Amino acid sequence alignment of Polo homologs from yeast to humans.

(A) Plk1 is comprised of an N-terminal kinase domain and a C-terminal noncatalytic PBD separated by a flexible linker region. (B) Adapted from [48]. Two Polo boxes, PB1 and PB2, form the C-terminal PBD. The PBD is thought to bind phosphopeptides comprised of a specific core consensus motif, which functions to spatially and temporally regulate the protein's catalytic activity during cell division [45,46].

1.3 Polo Regulation via the C-terminal Polo-box domain

Although early studies suggested that the C-terminal PBD of Polo strictly interacts with phosphopeptides containing a canonical S-pS/pT-P/X motif [45,46], it is becoming increasingly clear that the PBD can interact with regulatory proteins via non-canonical mechanisms as well (for review, see [50]). This emerging view of the PBD as a versatile mediator of several types of protein-protein interactions may more accurately explain the intricacies of how this kinase is able to multi-task so efficiently during cell division. It also suggests that PBD function is not fully understood and will be a worthwhile endeavour for years to come. Furthermore, certain Polo functions could be reduced or abrogated while leaving others intact, opening up the possibility for novel therapeutic strategies.

1.3.1 Canonical mechanisms of interaction

Several reports have validated the canonical method of Polo-protein interaction that is dependent on a S-pS/pT-P/X motif within the Polo protein interactor. One such example involves the interaction between Plk1 and Bub1 in mitotic HeLa cells, where phosphorylation of Bub1 at a threonine within a conserved S-pT-P PBD binding motif is critical for proper localization of endogenous Plk1 to kinetochores during mitosis. Furthermore, this interaction is dependent on the PBD, as the Plk1 H538A/K540M 'pincer mutant' is unable to co-immunoprecipitate (co-IP) with Bub1 [51]. Another example involves PICH, a centromere-associated SNF2 family ATPase. PICH is thought to recruit Plk1 to

kinetochores during prometaphase in HeLa cells through phosphorylation of a threonine within a canonical PBD binding motif by Cdk1 [52]. Several other examples have been reported and are thoroughly reviewed in [50], but probably the most thoroughly characterized canonical PBD dependent Polo-protein interaction is that of Plk1 and Cdc25C. Phosphorylation of Cdc25C of an S-pT-P PBD binding motif residing within the protein allows for PBD binding and subsequent activation of Cdc25C via Plk1-mediated phosphorylation—a critical event for mitotic entry [46].

1.3.2 Non-canonical mechanisms of interaction

Although Polo binding to the S-pT-P motif of Cdc25C is one of the first characterized examples of PBD-phosphoprotein interaction, additional studies have reported contradictory findings. More specifically, Elia *et al.* reported that phosphorylation of this site is necessary for interactions with the PBD, however, a second report demonstrated that the PBD can functionally bind equally well to a nonphosphorylated version of Cdc25C [46,53]. The nature of this discrepancy is not clear; however, it is the first of several published works suggesting that the PBD can interact with proteins in a more complex manner than initially proposed. A similar mechanism of non-canonical interaction with the PBD was demonstrated in *Drosophila* S2 cells. In these cells, Polo kinase robustly interacts with microtubule-associated protein, Map205, during interphase of the cell cycle by a phospho-independent mechanism, which is thought to allow for proper timing of mitotic entry [49].

In addition to the proposed phosphorylation requirement of the central residue within the PBD binding motif, several reports demonstrated that the serine at the – 1 position relative to the central residue is also critical for binding [46,54]. Nevertheless, exceptions have been discovered. One such example is the interaction between Plk1 and MKlp2 in HeLa cells, which serves to localize Plk1 to the central spindle/midbody in order to regulate cytokinesis [55]. While this particular interaction does appear to be phospho-dependent (in fact, Plk1 is thought to phosphorylate its own PBD binding site in this case), the determined sequence for PBD binding is H-pS-L within MKlp2.

Other cases exist where robust PBD binding to target proteins is reported despite the lack of a recognizable S-pS/pT-P/X motif. For example, the yeast protein Dbf4 has been described to interact with the yeast homolog of Polo (Cdc5) that potentially facilitates proper mitotic exit under certain circumstances via a non-canonical mechanism [56]. Interestingly, Dbf4 appears to phospho-independently interact with the Cdc5 PBD through a novel R-S-I-E-G-A Dbf4 amino acid sequence. Moreover, the PBD 'pincer mutant' robustly interacts with Dbf4 as assayed by yeast two-hybrid (Y2H), suggesting that Dbf4 may use a distinct binding surface to interact with the PBD. Other examples of non-canonical Polo-protein interactions include Bora and Plk1, which act together with Aurora A kinase to regulate mitotic entry in HeLa cells. The specific PBD binding site on Bora has not been determined. However, the interaction appears

to occur independently of phosphorylation. Furthermore, Bora appears to be capable of interacting with both the kinase domain and the PBD of Plk1 [57].

Perhaps the most intriguing aspect of Polo regulation via the C-terminal PBD involves auto-regulation (reviewed in [58] and [50]). Currently the intramolecular basis of how the PBD domain interacts with the kinase domain remains unclear. The kinase domain lacks a recognizable PBD binding motif, suggesting that the mechanism of interaction is non-canonical. Furthermore, dephosphorylation of the T-loop within the kinase domain may facilitate self-interaction with the PBD resulting in a closed, inactive configuration state. Phosphorylation of the T-loop may relieve this mutually inhibitory interaction, returning Polo kinase to an open configuration state, where the kinase domain is active and the PBD is free to bind other regulatory partners. Overall, these and other examples (reviewed in [50]) serve to illustrate the complexity of noncatalytic Polo-protein interactions. Clearly, future studies are necessary to elucidate how these varied regulatory interactions influence Polo activity within the cell.

1.4 Evolutionarily conserved structure of Matrimony (Mtrm)

The *mtrm* gene was isolated in a deficiency screen for *Drosophila* mutants that fail in homologous achiasmate chromosome segregation—a process that normally ensures proper homolog segregation in the absence of genetic exchange [59]. Importantly, this phenotype is fully suppressed by simultaneously reducing the dosage of the *polo* gene, suggesting that Mtrm may regulate Polo

during *Drosophila* female meiosis. Furthermore, Mtrm and Polo physically interact *in vivo* as assayed by biochemical and proteomic analysis in the fly [60]. Of note, this finding is consistent with an independent study, which identified Mtrm and Polo kinase as interactors in a global Y2H study that screened 102 *D. melanogaster* bait proteins orthologous to human cancer-related and/or signaling proteins against high-complexity fly *cDNA* libraries [61]. This topic will be further discussed in Section 1.5. Here we address our goal of understanding precisely how Mtrm may physically interact with Polo by first examining its predicted structure.

Mtrm is a 217 amino acid protein that is evolutionarily conserved throughout the genus *Drosophila*. Indeed, Mtrm homologs have been identified in the 11 other sequenced species of *Drosophila*, indicating that this protein has been conserved for approximately 30 million years. Using an amino acid sequence alignment of the homologs, we observed that Mtrm can be parsed into three blocks of sequence that are conserved throughout the 12 sequenced *Drosophila* species. One block surrounds an S-T^{40}-P sequence that fits a canonical PBD consensus motif (S-pT/pS-P/*X*) hereafter named the 'STP region', one is located just proximal to the C-terminal sterile alpha motif (SAM) domain, and one coincides with the SAM domain itself (Figure 1-4).

Previous work has shown that mutating MtrmT40 to alanine both ablates Mtrm function and its ability to interact with Polo kinase [60]. However, whether the PBD binding motif alone is sufficient to mediate the interaction between Mtrm

and Polo remained unclear. Moreover, the use of NetPhosK software revealed several other potentially important consensus motifs within Mtrm [62] (see top of Figure 1-4). Two nearby serines, MtrmS48 and MtrmS52, fall within a consensus motif for Glycogen synthase kinase 3 β (GSK-3β) phosphorylation (pS/pT-X-X-X-pS), which has been shown to play important roles in cell division [63]. Other motifs include a partially conserved cyclin B-Cdk1 phosphorylation motif (pS/pT-P-X-R/K), where the phospho-residue would be MtrmS66. In addition, MtrmS137 falls within a near perfect consensus motif for Polo phosphorylation (D/E-X-pS/pT-Ø-X-D/E). This of interest as Polo has been proposed to phosphorylate its own PBD targets such as MKlp2.

We also find that key residues within the C-terminal SAM domain are conserved, however, the functionality of the Mtrm SAM domain remains unclear. Intriguingly, proteins that harbour SAM domains are involved in a set of remarkably diverse functions that result from SAM domain-mediated interactions between other proteins, DNA and RNA [64-66].

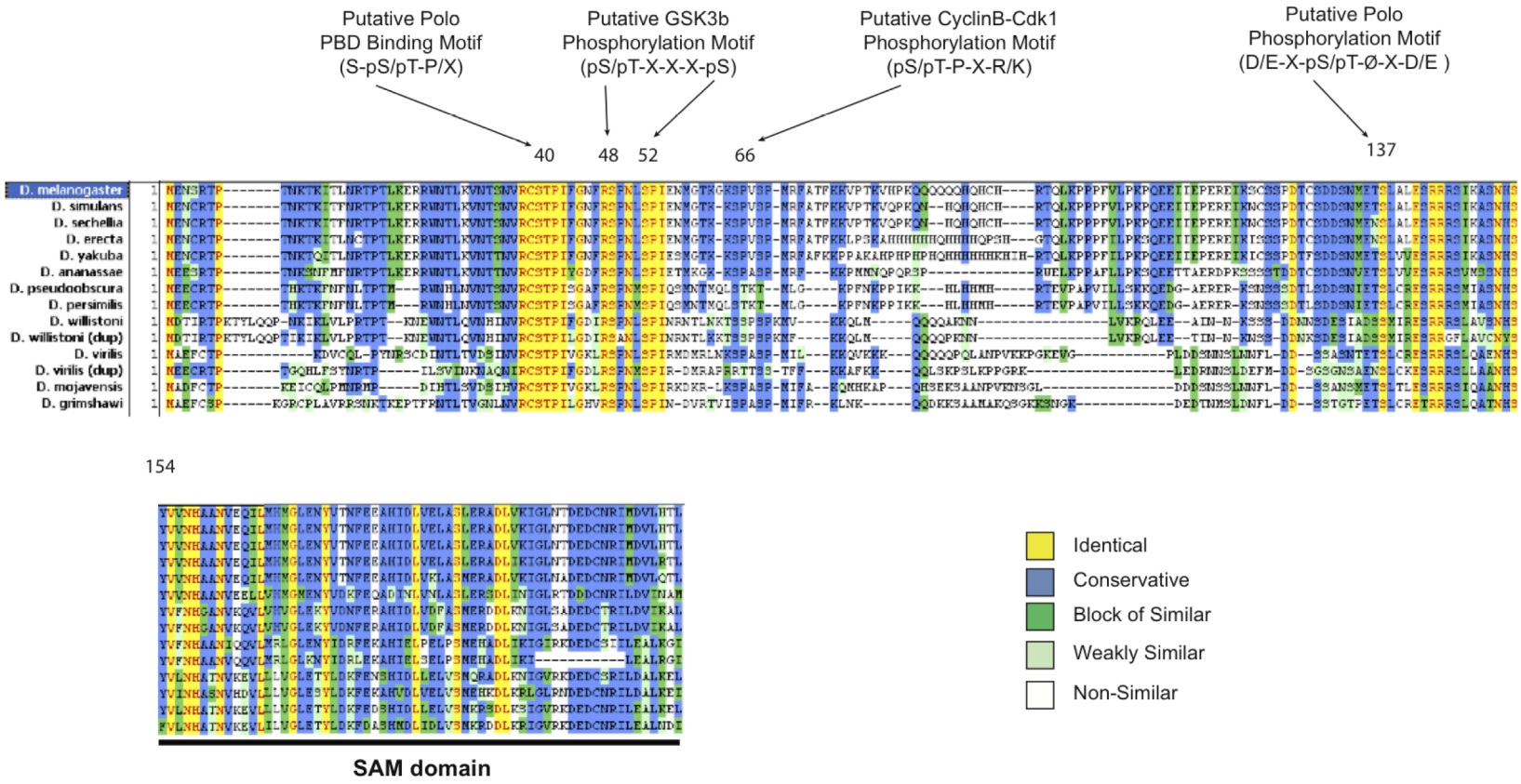

Figure 1-4 Amino acid sequence alignment of Mtrm homologs from 12 sequenced species of *Drosophila*.

D. melanogaster represents the top row in the alignment. Residues in yellow are absolutely conserved throughout all 12 species, while residues in blue are partially conserved and residues in green are functionally similar. Potentially significant motifs identified either by NetPhosK software or experimentally are listed above the alignment.

Examination of the amino acid sequence and the predicted secondary structure of the region proximal to the SAM domain prompted speculation that part of Mtrm may be intrinsically unstructured. Intrinsially unstructured proteins are both abundant and functionally important in eukaryotes—their inherent lack of secondary and/or tertiary protein structure confers increased flexibility, which allows for a wide range of functions including many processes during cell division [67]. We utilized FoldIndex to predict whether this may be the case for Mtrm, and we found that the entire protein proximal to the SAM domain is predicted to be intrinsically unstructured [68] (Figure 1-5). For comparison, the program also correctly predicted several smaller intrinsically unstructured regions within Polo, particularly the flexible linker region between the N-terminal kinase domain and the C-terminal PBD, which is consistent with previous structural analyses. (Figure 1-5). The likelihood of Mtrm being intrinsically unstructured allows us to speculate how this protein may be physically capable of interacting with Polo. In addition, this analysis also supports a rational strategy for site-directed mutagenesis of residues within the region of Mtrm proximal to the SAM domain. Lower structural complexity confers structural permissiveness, which decreases the probability that a given mutation within this region will cause protein misfolding and subsequent degradation [69].

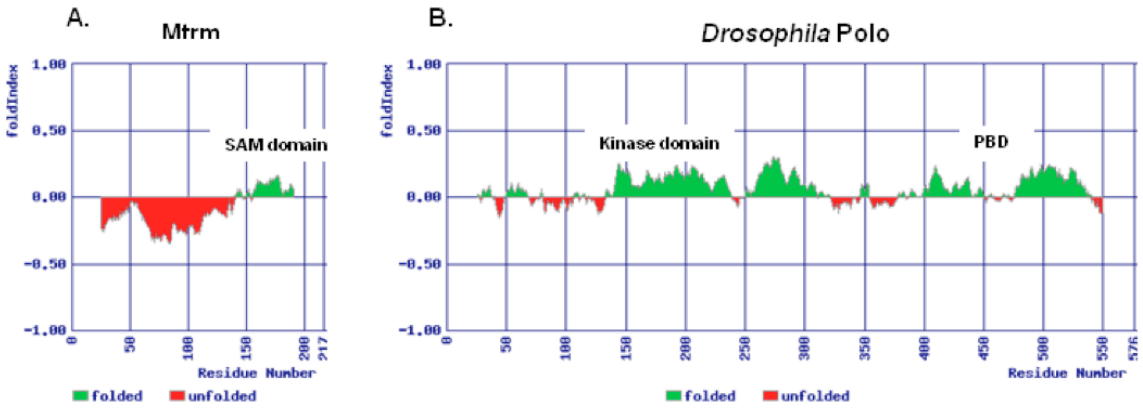

Figure 1-5 FoldIndex predicts Mtrm to contain a large intrinsically unstructured region.

(A) Mtrm contains a large unstructured region proximal to the C-terminal SAM domain. Because lower structural complexity confers structural permissiveness, site directed mutagenesis within this region of the protein is likely to be permitted without protein misfolding and subsequent degradation. (B) For comparison, *Drosophila* Polo was predicted to have an unstructured linker region separating the N-terminal kinase domain and the C-terminal PBD, which is consistent with structural studies of Polo.

1.5 The role of the *mtrm* gene product in *Drosophila* female meiosis

Perhaps one of the more interesting aspects of this work is our focus on examining the physical interaction between Mtrm and Polo in its native context—*Drosophila* female meiosis. *Drosophila* female meiosis is an ideal model for exploring Polo regulation *in vivo*. Depletion of the *mtrm* gene causes several well-described meiotic consequences *in vivo*. More importantly, evidence suggests that the meiotic defects observed in females lacking the proper dosage of *mtrm* are a consequence of Polo misregulation.

1.5.1 Female meiosis—a specialized form of cell division

Meiosis is a specialized form of cell division that differs from mitosis since DNA replication is followed by two rounds of cell division: Meiosis I (MI) and Meiosis II (MII). The first division, MI, separates homologous chromosome pairs, and the second division, MII, separates sister chromatids resulting in a haploid cell ready for fertilization. For many years, female meiotic cells (oocytes) have been successfully used to elucidate the basic mechanisms of cell division for several reasons. First, oocytes are characteristically larger than other cells, often providing easily accessible material for biochemical and cytological analysis. Secondly, unlike cells undergoing mitosis or male meiosis that quickly complete division upon M phase entry, the vast majority of female meiotic systems undergo two pre-programmed mid-cycle arrests. In a way, one can imagine these arrests as exaggerated versions of what happens during mitosis and male meiosis. Thus, in essence, female meiosis could be viewed as a specialized form of cell division that provides a larger window of opportunity by which to study the mechanisms of cell division control (for reviews, see [70,71]).

Drosophila female meiosis is an ideal model for understanding the basics of cell division. First, *D. melanogaster* carries the obvious advantage of being a highly genetically tractable model organism with a long history of focus on chromosome segregation during MI of female meiosis, when homologous chromosome pairs align and separate. Much more concise than the human genome, which is comprised of 23 homologous pairs of chromosomes, the

Drosophila genome is comprised of only 4 chromosome pairs. Nevertheless, in *Drosophila* oocytes, like most organisms, genetic exchange or chiasmata formation between homologous chromosome pairs during MI serves to physically lock them together, thus facilitating their proper alignment and co-orientation on the metaphase plate [72-74].

Surprisingly, cases also exist where genetic exchange (or recombination) either fails or occurs at a lower frequency, and yet proper homologous chromosome segregation remains intact. This observation led to the discovery and characterization of a remarkably efficient 'back-up' mechanism that facilitates proper chromosome segregation in the absence of exchange or chiasmata formation. This system was initially discovered in *Drosophila* and coined 'the distributive system' by Rhoda Grell in 1962 [75], and is now recognized more generally as 'homologous achiasmate segregation' [76] (Figure 1-6). Studying the mechanism by which non-exchange chromosome are faithfully segregated is of importance as recent reports indicate that approximately 1 in 5 human oocytes that contain an extra chromosome 21 have failed to recombine with its homolog [77,78]. Trisomy 21 is the most common chromosomal abnormality observed in humans, and yet the rate is significantly lower than 1 in 5 births, strongly suggesting that an achiasmate system may also exist in humans.

Since its discovery in 1962, the biology of homologous achiasmate segregation has been observed in several other meiotic systems, but remains most extensively studied in the fly (for review, see [79]). This is at least partly due to several convenient aspects of *Drosophila* chromosomal biology as well our ability to readily manipulate the *Drosophila* genome. For example, the fourth chromosomes of *Drosophila* are always achiasmate during female meiosis.

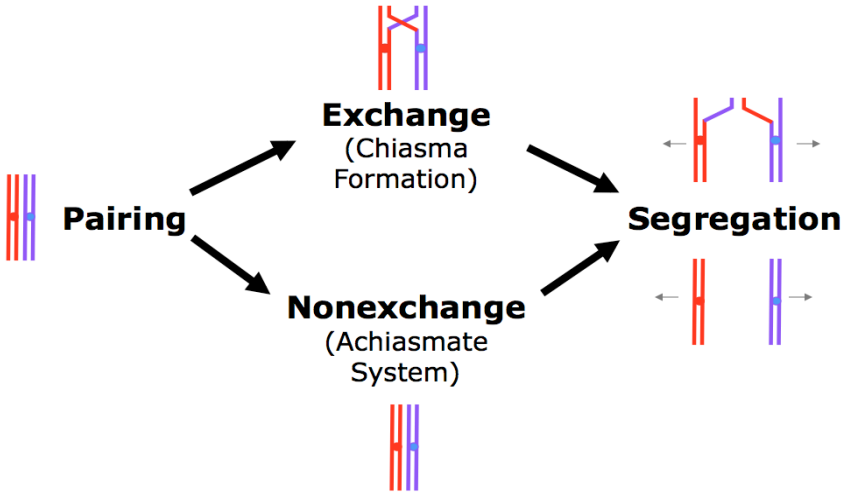

Figure 1-6 Homologous chromosome segregation during female meiosis.

Genetic exchange serves the important mechanistic role of facilitating the segregation of homologous chromosomes at M1 of female meiosis. However, chromosome pairs that fail to undergo exchange for one reason or another may still faithfully segregate through the process of homologous achiasmate segregation.

Additionally, the *X* chromosomes can be genetically manipulated to be obligately achiasmate by creating flies heterozygous for a normal sequence *X* chromosome and a chromosome containing multiple inversions, known as a balancer chromosome. Inversions within the balancer chromosome (such as *FM7*)

effectively suppress exchange or recombination with the normal sequence homolog. Due to the process of homologous achiasmate segregation, both the genetically manipulated *X* homologs and the fourth homologs are still able to faithfully segregate away from each other during MI [76]. This observation has allowed us to perform large genetic screens to identify genes critical for achiasmate chromosome segregation.

Drosophila female meiosis is also an ideal model for understanding the basic mechanisms of cell cycle control since they undergo similar pre-programmed developmental arrests as other female meiotic systems (for review, see [70]. While the second arrest in *Drosophila* female meiosis occurs at metaphase of MI rather than metaphase of MII in humans, the first arrest at prophase of MI is the same as humans as well as the vast majority of all other female meiotic systems. Moreover, the unique anatomy of the *Drosophila* ovariole allows for the simultaneous characterization of oocytes in all stages of development up to the second arrest, when all four homologous chromosome pairs must be properly aligned and co-oriented on the metaphase plate (Figure 1-7).

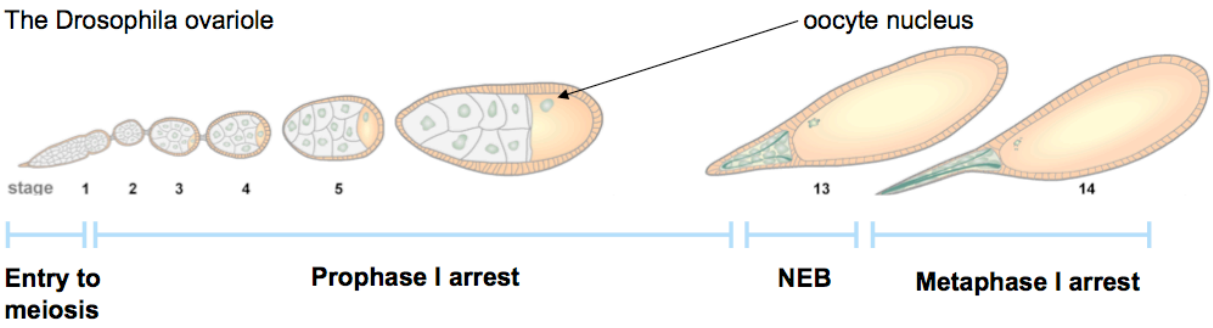

Figure 1-7 The *Drosophila* ovariole provides a snapshot of oocyte development.

Adapted from [60]. The unique anatomy of the *D. melanogaster* ovariole allows us to examine oocytes in all stages of development including those stages in which the pre-programmed and highly conserved Prophase I arrest occurs. The termination of Prophase I arrest is defined by nuclear envelope breakdown (NEB), which normally occurs at stage 13 of *Drosophila* oocytes development.

1.5.2 Effects of mtrm depletion

Just before the global Y2H screen identified the gene product *CG18543* as a putative Polo kinase interactor [61], it was isolated in a *Drosophila* screen of autosomal deficiencies for dominant effects on homologous achiasmate segregation [59]. *CG18543* was subsequently renamed *matrimony (mtrm)* since it appeared to be critical for holding chromosome pairs together for a substantial period of time. In 2007, the critical role for *mtrm* in homologous achiasmate segregation was functionally linked to *polo* [60]. The high levels of achiasmate chromosome nondisjunction (NDJ) observed in *Drosophila* females heterozygous for a null allele of *mtrm* could be fully rescued by simultaneous reduction of the *polo* gene by one copy. Furthermore, as mentioned previously, mutating the central residue of the PBD binding motif within Mtrm, MtrmT40, to alanine both

ablates Mtrm function (as assayed by homologous achiasmate segregation) and its ability interact with Polo kinase [60].

Additionally, Xiang *et al.* found that *Drosophila* females heterozygous or homozygous for a null allele of *mtrm* also exhibited precocious nuclear envelope breakdown (NEB) in a dosage-dependent manner, suggesting that the timing of the cessation of prophase I arrest was perturbed [60]. Furthermore, this defect was also rescued by simultaneous reduction of the *polo* gene or by simultaneous reduction of Polo's downstream target, Cdc25 (*twine*) [60] (for review, see [80]). These data are consistent with a large collection of reports implicating Polo kinase as the 'trigger' kinase leading to CyclinB-Cdk1 activation, which acts to dismantle the nuclear envelope in many organisms or to promote mitotic/meiotic entry in those organisms that undergo 'closed' cell division with an intact nuclear envelope [81-83]. For example, work in *S. cerevisiae, S. pombe*, and *X. laevis* revealed that Polo kinase promotes mitotic entry by phosphorylating Cdc25, which in turn activates Cyclin B-Cdk1 [81-83]. A similar theme is also seen in female meiosis. In *C. elegans* oocytes, silencing of *plk-1* expression in by RNA-mediated interference (RNAi) significantly delays NEB, which can be phenocopied by silencing the *C. elegans* Cdk1 ortholog via RNAi [84]. Furthermore, work in *X. laevis* oocytes revealed that Plx1 (Polo kinase in *X. laevis*) functions to activate Cdc25 and CyclinB-Cdk1 [85].

Considering these two phenotypes, it seemed possible that the achiasmate chromosome nondisjunction phenotype could be a direct

consequence of the precocious NEB phenotype. Thus, in addition to testing whether *D. melanogaster* oocytes simultaneously heterozygous for a null allele *mtrm* and a null allele of the meiotic version of Cdc25 (*twine*) rescued the NEB phenotype, Xiang *et al.* also examined whether these oocytes exhibited suppression of the achiasmate nondisjunction phenotype. Surprisingly, they found that while the NEB phenotype could be rescued in this genetic background, the achiasmate NDJ phenotype could not. These data suggest that the two phenotypes observed in oocytes lacking the proper dosage of *mtrm* may be functionally separate albeit both Polo-mediated, potentially serving to highlight the high degree of complexity of Polo regulation *in vivo.*

1.5.3 Mtrm as a negative regulator of Polo kinase

As stated above, previous work in yeast and flies demonstrates that Mtrm physically interacts with Polo kinase. Importantly, both meiotic phenotypes observed in females lacking sufficient levels of *mtrm* are suppressed by simultaneously reducing the dosage of *polo*, which suggests that Mtrm is a negative regulator of Polo kinase. Thus, considering that Mtrm and Polo physically interact via Y2H and by co-IP in *Drosophila* ovarian lysates, it is possible that Mtrm may negatively regulate Polo kinase during *Drosophila* female meiosis via direct physical interaction.

1.6 Summary

Polo kinase is a critical promoter of multiple events during cell division, is overexpressed in many human cancers, and has been validated as a selective target for inhibition as an anti-cancer therapy. Therefore, understanding the mechanisms of its regulation *in vivo* is fundamentally important. Although initial studies suggested that post-translational Polo regulation largely occurs by a specific type of non-catalytic interaction between the C-terminal Polo PBD and phosphoproteins containing a specific S-pS/pT-P/X motif, more recent studies suggest that 'non-canonical' interactions between Polo and its regulatory partners also exist. Understanding the mechanisms of these 'non-canonical' interactions may lead to novel strategies for targeted Polo inhibition in cancer.

Mtrm is a 217 amino acid protein that post-translationally regulates Polo kinase during *Drosophila* female meiosis. An amino acid sequence alignment of Mtrm homologs from 12 sequenced *Drosophila* species representing approximately 30 million years of evolution reveals that this protein can be parsed into three blocks of highly conserved sequence. One block surrounds an S-T^{40}-P sequence that fits a canonical PBD consensus motif, one is located just proximal to the C-terminal sterile alpha motif (SAM) domain, and one coincides with the SAM domain itself. Previous work showed that the central residue of the PBD binding motif is critical for Mtrm function and physical interaction with Polo kinase *in vivo*, but whether this motif alone is sufficient for physical interaction *in vivo* remains unclear. Furthermore, it appears that the functions of Mtrm during

Drosophila female meiosis may be separable, albeit both Polo-related, raising the intriguing possibility that Mtrm could regulate Polo kinase by multiple pathways or mechanisms.

1.7 Scope of this thesis

1.7.1 Examining the interaction between Mtrm and Polo *in vivo*

This work addresses whether the physical interaction between Mtrm and Polo is 'canonical' or 'non-canonical' with respect to other known Polo protein interactors. We first utilize *S. cerevisiae* as a means by which to explore the effects of multiple Mtrm and Polo mutants on their ability to physically interact via Y2H. We then further validate our findings by *in vivo* studies in the fly using newly available site-specific transgenic techniques. By studying this interaction in *D. melanogaster*, we are able to examine various Mtrm related meiotic phenotypes observed in *Drosophila* females lacking sufficient levels of the *mtrm* gene.

1.7.2 Questions to be addressed

This thesis begins with experiments utilizing *S. cerevisiae* as an *in vivo* test tube to demonstrate that Mtrm and Polo may interact by a 'non-canonical' mechanism. The validity of these findings is demonstrated by creating the same series of Mtrm mutants integrated into a specific site in the *D. melanogaster* genome and then examining the ability of these mutants to physically interact with endogenous Polo kinase during female meiosis via proteomic analysis. We

then address whether Mtrm separation-of-function mutants can be identified by screening for the ability of a large class of Mtrm mutants targeting evolutionarily conserved residues to rescue the homologous achiasmate segregation defects observed in *Drosophila* females heterozygous for a null allele of *mtrm* and/or the sterility defects observed in *Drosophila* females homozygous for a null allele of *mtrm*. This is achieved by usage of well-established *Drosophila* genetic techniques designed to specifically examine both homologous achiasmate segregation and oocyte development.

Chapter 2. Analysis of the physical interaction between Mtrm and Polo kinase in *S. cerevisiae*

2.1 Introduction

As mentioned in Chapter 1, the physical interaction between Mtrm and Polo was initially reported in a global yeast two-hybrid (Y2H) screen for *Drosophila* interacting proteins [61], and experiments in the fly verified the interaction to be functionally critical for several aspects of female meiosis [60]. The Y2H system offers many advantages. Most importantly, it offers a means to study protein-protein interactions in a live, eukaryotic environment with greater speed than would be possible in the fly. Thus, we returned to analysis in yeast to dissect the nature of the physical interaction between Mtrm and Polo. This chapter will describe a study that identifies specific residues/regions of Mtrm and Polo that may be important for their interaction during *Drosophila* female meiosis. The results of the study allowed us to focus on point or deletion mutants of Mtrm that potentially have the most effect on *Drosophila* female meiosis, the topic of Chapters 3, 4 and 5.

Because Polo kinase is highly conserved, we also addressed the question of whether Mtrm is able to physically interact with the budding yeast homolog of Polo, Cdc5.

2.2 Yeast two-hybrid analysis of Mtrm mutants

Y2H is a method to analyze protein-protein interactions in a eukaryotic cell, namely the budding yeast *Saccharomyces cerevisiae*. The results discussed in this section use two sets of chimeric proteins, one chimera that is a fusion with the DNA-binding domain (BD) of the yeast transcription factor, Gal4, and the other that is joined with the Gal4 activation domain (AD). In the Y2H system used in the following experiments, the BD binds to the *GAL1* upstream activation sequence (UAS), which contains four Gal4 binding sites. The AD, derived from the C-terminal 113 amino acids of Gal4, facilitates transcription via RNA polymerase II. As the BD and the AD activities are separate and independent, the two domains only need to be in close proximity to each other to activate gene transcription. Therefore, the interaction between two proteins of interest fused to a BD and an AD respectively can be determined by whether or not gene transcription occurs. Here, the *GAL1* UAS is used to drive expression of a reporter gene, *HIS3*. When a functional interaction occurs, *HIS3* is transcribed, and cells are able to grow on media lacking histidine. If no binding occurs, *HIS3* is not produced and the yeast cells die. In addition, growth of cells is assayed on media lacking leucine and tryptophan, which ensures presence of the 2u plasmids containing the AD and the BD fusion proteins, respectively.

As shown in Figure 2-1, the growth of diploid yeast cells with plasmids encoding Mtrm-AD and Polo-BD on SC-His-Leu-Trp plates demonstrates that the yeast-two hybrid assay confirms the interaction between full-length Mtrm and

Polo. Strains carrying *mtrm-AD* or *polo-BD* genes in addition to the respective *AD* or *BD* (vector only) control genes are unable to grow. Thus, Mtrm-AD does not bind significantly to the Gal4 binding site, nor does Polo-BD act as an activator (Figure 2-1).

In order to determine which Mtrm residues/regions are required for Polo interaction via Y2H, we constructed a C-terminal truncation deleting the Mtrm SAM domain. In addition, a series of point mutants were made that would disrupt Mtrm residues predicted to fall within known phosphorylation motifs (MtrmS48A, MtrmS52A, MtrmS66A and MtrmS137A) and/or previously shown to be potentially significant in the fly (MtrmT40A).

As shown in Figure 2-1, the lack of colony growth of strains expressing Polo-BD and MtrmSAMDEL-AD on the SC-His-Leu-Trp medium suggests that the C-terminal SAM domain of Mtrm contributes to the physical interaction between Mtrm and Polo via Y2H. Furthermore, strains expressing Polo-BD and MtrmS48A-AD or MtrmS52A-AD (mutants of residues that fall within a putative GSK-3β phosphorylation motif and that have been found reproducibly phosphorylated in the fly) also showed reduced growth (Figure 2-1). Therefore, we conclude that these residues play a role in Mtrm's interaction with Polo.

By contrast, colony growth of strains carrying Polo-BD and MtrmS66A-AD or MtrmS137A-AD is robust under selective conditions and resembles that of the positive control, Mtrm-AD (Figure 2-1). These results suggest that neither

MtrmS66, which lies within a putative CyclinB-Cdk1 phosphorylation, nor MtrmS137, which is located within a near perfect Polo phosphorylation motif have significant roles in Mtrm-Polo binding. Lastly and surprisingly, the strains expressing Polo-BD and MtrmT40A-AD, which disrupts an absolutely conserved core PBD-binding motif previously shown to be critical for homologous achiasmate segregation in the fly, are able to grow on selective media (Figure 2-1). Therefore, in the context of the Y2H system, MtrmT40 appears dispensable for its binding to Polo kinase.

Taken together, these data provide the first evidence that Mtrm may interact with Polo in a fashion that does not solely depend on a canonical PBD-binding motif, but may also depend on the C-terminal SAM domain and other phosphorylatable residues such as MtrmS48 and MtrmS52.

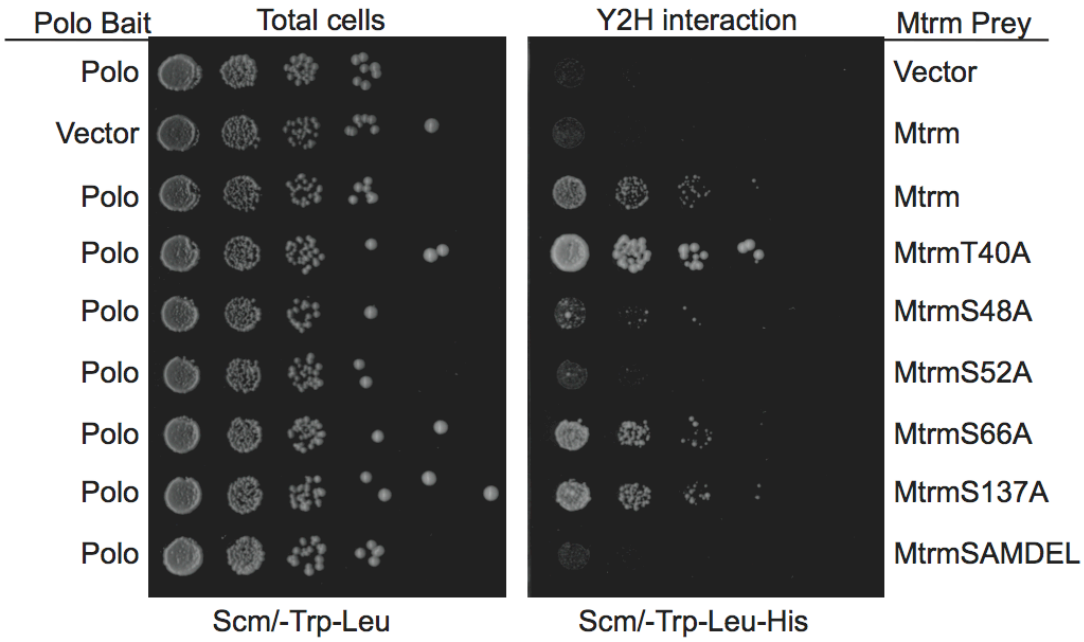

Figure 2-1 Y2H reveals key Mtrm residues/regions required to physically interact with Polo.

Mtrm residues either predicted to be post-translationally modified by NetPhosK software or determined to be important experimentally were mutated to alanine and then tested for a Y2H interaction with Polo. 10-Fold serial dilutions of saturated cultures were spotted onto SCM/-Trp-Leu plates to visualize cells and confirm presence of both plasmids and Scm/-Trp-Leu-His to score the two-hybrid interaction.

2.3 Yeast two-hybrid analysis of Polo mutants

We took a similar approach in order to determine whether specific Polo residues were required for physical interaction with Mtrm via Y2H. We targeted amino acids within the T-loop of the protein's kinase domain and the C-terminal PBD that have previously shown to be essential for Polo activity *in vivo*. Replacement of the phosphorylatable residue of the T-loop, PoloT182, with alanine is predicted to yield a kinase dead mutant. The mutations PoloH518A and PoloK520M disrupt the selectivity of the PBD and are equivalent to the 'pincer mutant' identified in Plk1. Additionally, we constructed a PoloH518A/K520M double mutant (Polo-HK) and a PoloT182A/H518A/K520M

triple mutant (Polo-THK). Surprisingly, while PoloT182A appears to have a diminished ability to interact with Mtrm, the mutants that are known to disrupt PBD selectivity (PoloH518A, PoloK520M and Polo-HK) as well as the triple mutant, Polo-THK, which has both the kinase domain and the PBD altered, were all able to interact with Mtrm-AD. (Figure 2-2). Considering that the 'pincer mutant' is predicted to ablate PBD specificity, these results suggest that Mtrm and Polo may interact by some non-canonical mechanism, perhaps similar to what has been described between Dbf4 and the yeast Polo homolog, Cdc5 [56].

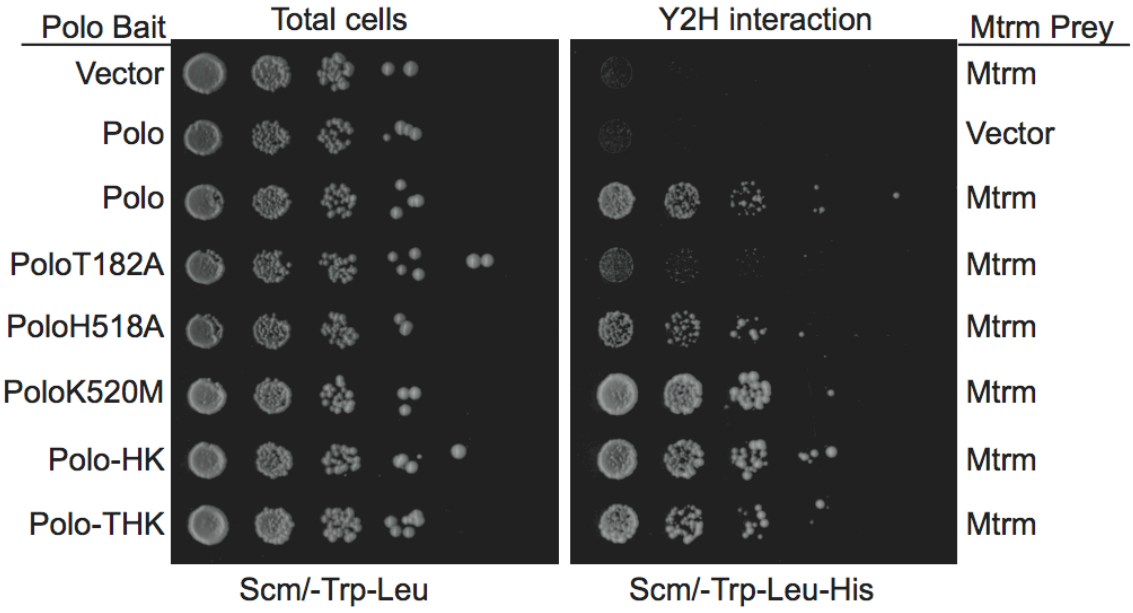

Figure 2-2 Y2H reveals Polo residues critical for PBD selectivity are dispensable for interaction with Mtrm.

Polo residues critical for functionality were mutated and then tested for a Y2H interaction with Mtrm. 10-Fold serial dilutions of saturated cultures were spotted onto SCM/-Trp-Leu plates to visualize cells and confirm presence of both plasmids and Scm/-Trp-Leu-His to score the two-hybrid interaction.

2.4 Heterologous Mtrm expression in *S. cerevisiae*

Several possible explanations exist as to why Mtrm might interact with kinase dead versions of Polo, such as Polo-THK. First, the budding yeast homolog of Polo Cdc5 may be able to phosphorylate Mtrm and therefore bypass the requirement for Polo phosphorylation. Alternatively, other kinases may modify Mtrm to allow for interactions between Mtrm and Polo in yeast. Finally, a yeast protein might bridge the interaction between Mtrm and Polo, one possible candidate being Cdc5 itself.

To address these possibilities, we purified a Mtrm-3xFLAG fusion protein from yeast cells that expressed the protein from the galactose-inducible *GAL1* promoter using FLAG resin. These cells also contained a Myc-tagged version of Cdc5 under the control of its endogenous promoter (SLJ917, gift of the Jaspersen Lab). Our initial co-immunoprecipitation experiments suggested that perhaps a very weak interaction existed between Mtrm-3xFLAG and Myc-Cdc5 (see Section 2.4.1). However, multidimensional protein identification technology (MudPIT) mass spectrometry analysis more supported the view that Mtrm does not appear to robustly interact with Cdc5. Moreover, MudPIT analysis also demonstrated that Mtrm-3XFLAG does not appear to interact with any other yeast protein (see Section 2.4.2). Furthermore, post-translational modification analysis of purified Mtrm-3XFLAG reveals that Mtrm is phosphorylated similarly in yeast as in the fly (see Section 2.4.3). Overall, these data ultimately support

the view that the Y2H interaction between Mtrm and Polo likely reflects a direct, physical interaction.

2.4.1 Co-immunoprecipitation assays of Mtrm and Cdc5 in yeast

In order to determine whether Mtrm is able to interact with the yeast homolog of Polo, Cdc5, we performed reciprocal co-immunoprecipitation assays by inducibly expressing and immunoaffinity purifying a Mtrm-3XFLAG protein from a WT yeast strain (SLJ001, gift of the Jaspersen Lab) and a strain containing Myc-tagged version of Cdc5 under the control of its endogenous promoter (SLJ917, gift of the Jaspersen Lab). Mtrm-3XFLAG appeared to non-specifically bind to Myc immunoaffinity beads in a WT background, (see Figure 2-3 panel A Lane 1), rendering the results observed in panels C and D, Lanes 1 likely an artifact. Utilization of FLAG immunoaffinity beads appeared to potentially co-immunoprecipitate a small amount of Myc3-Cdc5. (see Figure 2-3, panels C and D, Lanes 3). Furthermore, Myc3-Cdc5 did not appear to non-specifically bind to FLAG beads alone (Figure 2-3, panels C and D, Lanes 4).

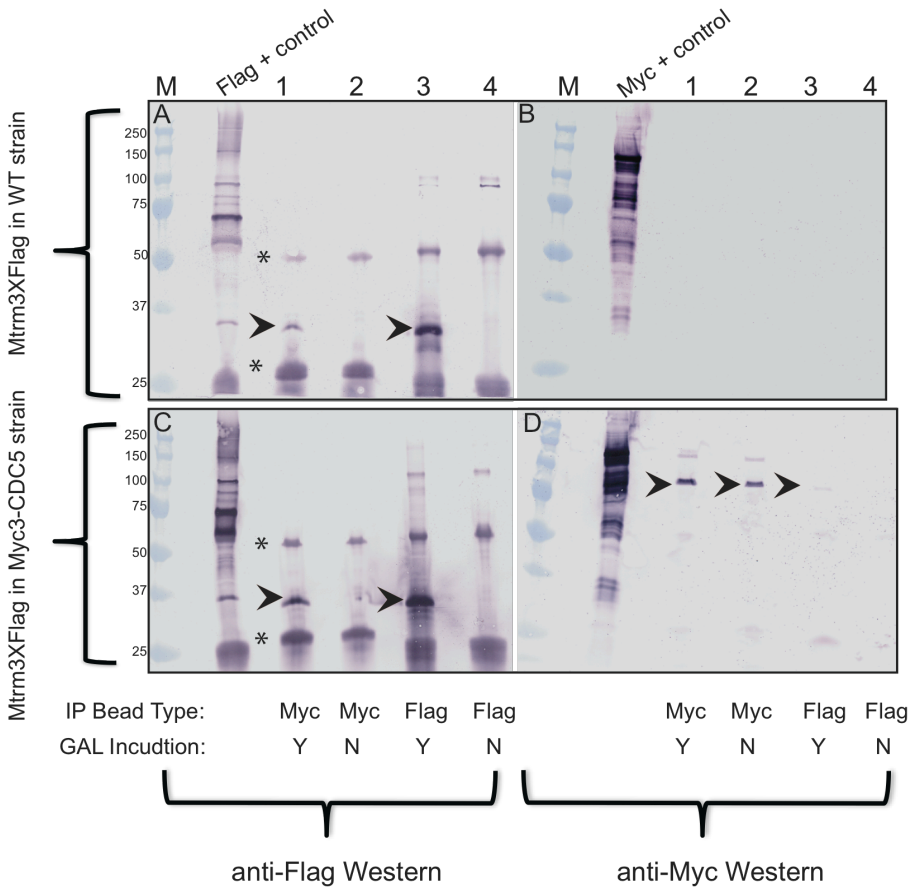

Figure 2-3 Co-Immunoprecipitation assays of Mtrm-3XFLAG and Myc3-Cdc5 in yeast.

Cell lysates from either a WT strain or a Myc3-CDC5 strain expressing Mtrm-3XFLAG under the *GAL1* promoter were induced with galactose or repressed with dextrose, immunoaffinity purified using either FLAG or Myc beads and subjected to Western analysis. Panels A and B show analysis of Mtrm-3XFLAG expressed in a WT strain. Panels C and D show analysis in a Myc3-CDC5 background. Panel A Lane 1 shows that Mtrm-3XFLAG non-specifically binds to Myc beads, rendering the co-immunoprecipitation results in panels C and D, Lane 1 likely artifactual. A small amount of Myc3-Cdc5, however, appears to co-immunoprecipitate with Mtrm-3XFLAG (panels C and D, Lane 3). The lanes marked M shows the Bio-Rad Precision Plus Pre-stained Protein Ladder used. (Other bands marked with an asterisk at approximately 55 kDa and 25 kDa represent residual heavy and light chains from the immunoaffinity purification.)

2.4.2 MudPIT analysis of Mtrm expressed in yeast

In order to address whether other yeast proteins including the yeast homolog of Polo, Cdc5, co-purified with Mtrm in yeast, we performed multi-dimensional protein identification technology (MudPIT) mass spectrometry

analysis on a Mtrm-3XFLAG fusion protein inducibly expressed and FLAG-purified from yeast also containing Myc-tagged version of Cdc5 under the control of its endogenous promoter (SLJ97). The details of MudPIT will be described more in more detail in Chapter 3. As shown in Figure 2-3, we did not visualize any pertinent bands other than that corresponding to Mtrm-3XFLAG by silver staining 5% of protein eluates after galactose induction, anti-FLAG agarose immunoaffinity purification and subsequent 3XFLAG peptide elutions (see panel A, Lanes 6-8).

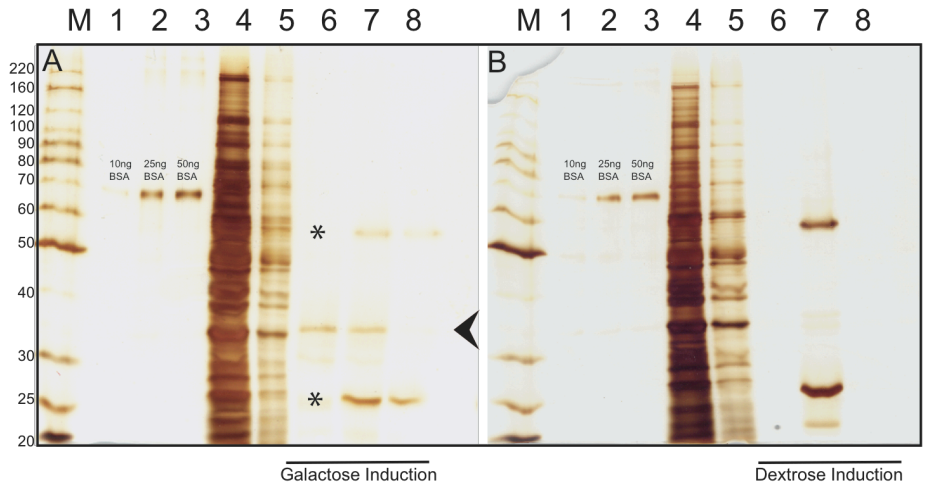

Figure 2-4 Silver stain of Mtrm-3XFLAG immunoaffinity purified from yeast.

Cell lysates from a *Myc3-CDC5* strain expressing Mtrm-3XFLAG under the control of the *GAL1* promoter induced with galactose or repressed with dextrose (panels A and B, respectively) and subjected to FLAG immunoaffinity purification and silver staining (Invitrogen SilverExpress). Lane 4 represents flow through following FLAG immunoaffinity purification. Lane 5 represents the first wash following purification. Lanes 6-8 represent 5% of the first, second and third 3XFLAG peptide elutions following purification washes, respectively. Mtrm-3XFLAG protein is eluted following galactose induction (~37 kDa band). However, no other pertinent bands were visible via silver stain. The lane marked M shows the Invitrogen BenchMark Protein Ladder used. (Other bands in Lanes 6-8 at approximately 55 kDa and 25 kDa represent residual heavy and light chains from the immunoaffinity purification.)

We performed MudPIT analysis on the remaining 95% of the first and second eluates following galactose induction and dextrose repression. Two sequential elutions for each case were analyzed to allow for one technical replicate each. Consistent with the silver stain, MudPIT analysis revealed that no proteins of interest differentially co-purified with the samples induced with galactose (containing Mtrm-3xFLAG protein) versus the dextrose only (No FLAG protein) control. Also, no peptides were detected that covered Myc3-Cdc5.

Table 2-1 MudPIT analysis of Mtrm-3XFLAG expressed in yeast.

Cell lysates from a *Myc3-CDC5* strain expressing Mtrm-3XFLAG under the control of the *GAL1* promoter induced with galactose or repressed in dextrose, subjected to FLAG immunoaffinity purification and MudPIT mass spectrometry. The table shows the number of peptides (P), spectra (S), sequence coverage (SC) and normalized spectral abundance factor (NSAF) for the top 25 iteracting proteins detected. In total, 4 samples were analyzed: two sequential elutions following galactors induction (blue) and two sequential elutions following dextrose induction (gray). Mtrm-3XFLAG was, by far, the most abundant protein identified in the mixture, with the majority of other interacting proteins being ribosomal in nature.

			Elution 1				Elution 2				Elution 1				Elution 2			
Protein Rank	Protein Name	Protein symbol	P	S	SC	NSAF	P	S	SC	NSAF	P	S	SC	NSAF	P	S	SC	NSAF
1	Mtrm-3xFlag	MTRM	28	363	58.9	0.081	30	371	59.3	0.081	1	4	13.3	0.010	x	x	x	x
2	Peroxiredoxin TSA1	TSA1	11	71	62.2	0.020	12	63	61.7	0.017	x	x	x	x	x	x	x	x
3	Single-stranded DNA-binding protein RIM1, mitochondrial	RIM1	6	58	32.6	0.023	5	32	43.7	0.012	x	x	x	x	x	x	x	x
4	40S ribosomal protein S12	RPS12	4	26	33.6	0.010	7	30	42.7	0.011	x	x	x	x	1	4	13.3	0.005
5	60S ribosomal protein L4-A	RPL4A	16	69	47.8	0.010	17	54	45.3	0.008	x	x	x	x	3	4	10.2	0.002
6	60S ribosomal protein L4-B	RPL4B	16	69	49.4	0.010	15	52	45.3	0.008	x	x	x	x	3	4	10.2	0.002
7	60S ribosomal protein L8-A	RPL8A	13	48	43	0.010	11	35	47.3	0.007	x	x	x	x	1	2	5.5	0.001
8	Galactokinase	GAL1	20	83	46.4	0.008	23	80	44.3	0.008	x	x	x	x	x	x	x	x
9	60S ribosomal protein L12	RPL12	6	23	44.8	0.008	6	27	46.7	0.009	x	x	x	x	2	3	17	0.003
10	60S ribosomal protein L1	RPL1	7	40	18.9	0.010	6	23	24	0.006	x	x	x	x	1	3	6	0.002
11	60S ribosomal protein L8-B	RPL8B	13	43	46.9	0.009	11	31	47.3	0.006	x	x	x	x	2	3	10.9	0.002
12	40S ribosomal protein S20	RPS20	3	18	39.7	0.008	4	16	39.7	0.007	x	x	x	x	1	2	10.7	0.003
13	40S ribosomal protein S10-B	RPS10b	3	15	50.5	0.008	4	13	50.5	0.007	x	x	x	x	x	x	x	x
14	60S ribosomal protein L10	RPL10	7	30	33.5	0.007	4	28	24.9	0.007	x	x	x	x	3	5	24	0.004
15	60S acidic ribosomal protein P2-alpha	RPP2A	3	13	31.1	0.007	2	14	23.6	0.007	x	x	x	x	2	6	31.1	0.009
16	40S ribosomal protein S19-B	RpS19b	4	20	31.9	0.008	6	16	45.1	0.006	x	x	x	x	x	x	x	x
17	Guanine nucleotide-binding protein subunit beta-like protein	ASC1	10	32	63.3	0.005	9	46	48.6	0.008	x	x	x	x	1	1	6.9	0.001
18	60S ribosomal protein L22-A	RPL22A	3	16	41.3	0.007	3	13	41.3	0.006	x	x	x	x	x	x	x	x
19	60S acidic ribosomal protein P0	RPP0	7	36	27.9	0.006	8	27	27.6	0.005	x	x	x	x	2	3	14.1	0.002
20	40S ribosomal protein S5	RPS5	6	24	33.8	0.006	7	21	38.7	0.005	x	x	x	x	1	1	6.7	0.001
21	Heat shock protein 26	HSP26	6	23	42.1	0.006	8	19	36.4	0.005	x	x	x	x	x	x	x	x
22	Mitochondrial acidic protein MAM33	MAM33	7	30	33.5	0.006	8	21	37.2	0.004	x	x	x	x	x	x	x	x
23	60S ribosomal protein L14-B	RPL14B	6	13	34.1	0.005	5	13	28.3	0.005	x	x	x	x	x	x	x	x
24	60S ribosomal protein L6-A	RPL6A	5	18	27.3	0.006	6	14	38.6	0.004	x	x	x	x	1	1	8.5	0.001
25	60S ribosomal protein L19	RPL19	9	21	30.7	0.006	5	13	16.4	0.004	x	x	x	x	x	x	x	x

2.4.3 Post-translational modification analysis of Mtrm expressed in yeast

By combining the two MudPIT runs expressing Mtrm3x-FLAG following galactose induction, we were able to achieve approximately 72% sequence coverage of the protein. This allowed us to perform post-translational analysis of Mtrm to determine whether the protein is phosphorylated similarly in yeast and fly. While MtrmT40 was not phosphorylated on Mtrm3X-FLAG purified from the *Myc3-CDC5* yeast strain, MtrmS52 was reproducibly phosphorylated, which is consistent with previous PTM studies of Mtrm purified from ovarian lysates [60]. Furthermore, the phosphorylation status of MtrmS52 is intriguing in light of our Y2H results, which demonstrate that mutation of this residue to non-phosphorylatable alanine renders the protein unable to interact with *Drosophila* Polo in yeast.

Table 2-2 Phosphorylated sites detected on Mtrm-3XFLAG expressed in yeast.

MtrmS52 was found reproducibly phosphorylated when Mtrm is expressed in yeast. Because this residue is also found highly phosphoyrlated in the fly [60]

Residue Position	NetPhos2_ Probability	Kinase	Kinase_ Score	Modified _Spc	Modified_Spc /Total_Spc Avg	Modified_Spc /Total_Spc Stdev	Times Detected
S48	0.016	GSK3	0.52	2	2.56	0	1
S52	0.996	cdk5/GSK3	0.55/0.51	**10**	**12.82**	**3.62**	**2**
S121	0.745	n/a		1	1.2	0	1
S123	0.973	n/a		1	1.43	0	1
S124	0.717	cdc2	0.51	4	4.82	0	1
T127	0.718	n/a		2	2.41	0	1
S129	0.026	CKII/cdc2	0.54/0.51	2	2.41	0	1

2.5 Discussion

The Y2H experiments described in Chapter 2 of this thesis provide the first evidence that Mtrm may interact with Polo in a fashion that does not solely depend on the core PBD-binding motif. Analysis of various Mtrm mutants revealed that the physical interaction may also depend on the C-terminal SAM domain and other phosphorylatable residues such as MtrmS48 and MtrmS52. Interestingly (in the context of the Y2H assays), MtrmT40, which falls within an absolutely conserved PBD binding motif appears to be dispensable. Whether or not this reflects the sensitive nature of the assay itself or is a consequence of analyzing the interaction in a heterologous system remains unclear.

Additional evidence supporting the view that Mtrm and Polo may interact in a non-canonical mechanism includes the analysis of various Polo mutants via Y2H. The results described in Figure 2-2 suggest that Mtrm may interact with Polo via a surface that is distinct from the canonical PBD binding pocket as the 'pincer mutant' predicted to ablate PBD specificity is still able to interact with Mtrm. This intriguing finding suggests that Mtrm and Polo may interact by some mechanism, perhaps similar to that described between Dbf4 and the yeast Polo homolog, Cdc5, where Dbf4 is thought to bind to a distinct binding surface on the PBD.

Of note, the PoloT182A mutant has a reduced ability to bind Mtrm, while the PoloTHK triple mutant appears to engage in robust interaction. An explanation for this may be obtained if we consider the current model by which Polo is

thought to fold into a ‘closed’ configuration state, where the PBD interacts with the kinase domain when the T-loop is not phosphorylated. Perhaps PoloT182A is folded into its ‘closed’ configuration state, thereby rendering it unable to interact with Mtrm. Intriguingly, the PoloTHK triple can still robustly bind to Polo, begging the speculation that the triple mutant is open configuration state. If so, then the data suggest that perhaps PoloH518 and PoloK520 contribute to establishing or maintaining the mutual inhibitory ‘closed’ configuration of Polo.

In this chapter, we also addressed the possibility that Mtrm is able to physically interact with the yeast homolog of Polo, Cdc5. Multidimensional protein identification technology (MudPIT) mass spectrometry analysis definitively showed that Mtrm does not appear to robustly interact with Cdc5. More importantly, MudPIT analysis also demonstrated that Mtrm-3XFLAG likely does not interact with any other yeast protein, supporting the view that the interaction between Mtrm and Polo is likely direct. However, it should be noted that the reciprocal MudPIT study was not performed on an epitope tagged version of *Drosophila* Polo expressed in yeast. Additionally, we cannot rule out the possibility that wash conditions were too stringent to maintain any pertinent weak interactions. Finally, post-translational modification analysis of Mtrm-3XFLAG purified from yeast reveals that Mtrm is at least partially similar the same analysis of Mtrm purified from ovarian lysates. Taken together, these data ultimately help to validate our Y2H studies and support the view that the Y2H interaction between Mtrm and Polo likely reflects a direct, physical interaction.

2.6 Acknowledgments

I would like to especially thank Dr. Sue Jaspersen and members of the Jaspersen Lab for their help and guidance. In addition, thank you to Kimberly Collins and Cathleen M. Lake for their helpful discussions. I am grateful to Laurence Florens of the Stowers Proteomics core facility for collaborating with me on the MudPIT and PTM analysis.

2.7 Materials and Methods

Plasmid Construction

For construction of Y2H plasmids, *mtrm* cDNA was amplified with ExTaq DNA Polymerase using primers 5'-cgggatccgaatggagaattctc-3' and 5'-tccctcgagttaaagagtgtggagcac-3'. The PCR reaction steps included an initial denaturation step (94°C for 2 min), followed by 30 synthesis cycles (94°C for 30 sec, 65°C for 45 sec, and 72°C for 2 min), and a final 10-min extension step at 72°C. The PCR fragment was then purified before and after co-digestion with *BamHI* and *XhoI* using the QIAGEN QIAquick PCR Purification Kit. The purified, digested fragment was then subcloned into the *pGADT7* gel purified (QIAGEN QIAquick Gel Extraction Kit) vector digested with the same enzymes. *polo* cDNA was amplified with primers 5'-cgggatcctaatggccgcgaag-3' and 5'-tccctcgagttatgtgaacatcttctc-3' using the PCR settings described above. The PCR fragment was then purified before and after co-digestion with *BamHI* and *XhoI* using the QIAGEN QIAquick PCR Purification Kit. The purified, digested

fragment was then subcloned into the *pGBKT7* gel purified (QIAGEN QIAquick Gel Extraction Kit) vector digested sequentially with *SalI* then *BamHI.* (*XhoI* and *SalI* produce compatible cohesive ends.) *mtrm* and *polo* sequences within their respective vectors were then confirmed with Sanger sequencing (MolSeq13102 and 13132). (Note: *pGADT7-polo* and *pGBKT7-mtrm* were also generated using similar strategies, however, expression of *pGBKT7-mtrm* within the Y2H system exhibited a significant amount of self activation with the *pGADT7* vector alone.)

For construction of an integrating plasmid for inducible expression of *mtrm* in yeast using the *GAL1* promoter, *mtrm-3XFLAG* template was amplified with ExTaq Polymerase using primers 5'-ccgctcgaggatggagaattctcgca-3' and 5'-tccccgcggttacttgtcatcgtcgt-3' using the PCR method described previously. The PCR fragment was then purified before and after co-digestion with *XhoI* and *SacII* using the QIAGEN QIAquick PCR Purification Kit. The purified, digested fragment was then subcloned into *pDK20* that was gel purified (QIAGEN QIAquick Gel Extraction Kit) following digestion with the same enzymes, and the sequence of the resulting plasmid was confirmed by Sanger Sequencing. The *pDK20-mtrm-3XFLAG* vector was then linearized with *StuI* for subsequent transformation into the *URA3* locus

Generation of site directed mutants

Mutations in *pGADT7-mtrm* and pGBKT7-*polo* were made using the Quik Change II XL Site-Directed Mutagenesis Kit (Stratagene, CA). Changes were

made according to the codon preferences of *S. cerevisiae*. DNA fragments containing the mutations were then amplified via PCR with the primers described above using the PCR settings described in the Y2H section above. The PCR fragments were then subcloned back into clean *pGADT7* or *pGBKT7* vector as described above. *mtrm* mutant and *polo* mutant sequences were then re-confirmed with Sanger sequencing.

Yeast Transformations

Yeast transformations were performed according to the Jaspersen Lab protocol. A 50 ml overnight culture was grown in YPD. The following day, an OD600 measurement was taken. If OD600 was greater than 1.0, cells were diluted back to 0.1 and allowed to grow for an additional 4-6 hrs. If OD600 was 0.2-1.0, cells were used immediately or diluted for use later in the day. If OD600 was less than 0.2, cells were allowed to grow for an additional amount of time. At the appropriate cell density, cells were centrifuged in a 50 ml conical for 3 min at approximately 1500xg. Following removal of the media, the pellet was then washed/resuspended in 5 ml of TE by vortexing. Cells were then spun down, and following removal of the TE, cells were then washed/resuspended in 5 mL of LiOAc mix by vortexing. Cells were then spun down, and following removal of the LiOAc, pellet was resuspended in .5 – 1 ml of LiOAc mix. In a 1.5 ml microfuge tube, 100 µl cells in LiOAc mix, 10 µl freshly boiled salmon sperm, and 1-5 ug of plasmid DNA in H_2O was combined. 700 µl of PEG mix was then added and mix was resuspended in the microfuge tube by vortexing. The mix

was subsequently incubated for 30 min at room temperature. 48 µl of DMSO was added followed by a brief vortex, and the mix was then incubated for 15 min at 42°C. Mix was then centrifuged at 5K in a microcentrifuge and gently resuspended in 200-500 µl YPD. Transformed cells were then plated on appropriate selective plates and grown up for 2 days at 30°C. Note: It is important to simultaneously perform a negative transformation control in which no plasmid DNA is added. Secondly, 2-micron, Cen-based plasmids and PCR products can be directly transformed; integrating plasmids must be cut with a restriction enzyme to target them for integration into the yeast genome.

Yeast Two-hybrid analysis

Yeast two-hybrid assays were performed using the Matchmaker two-hybrid system 3 (Clontech). *pGADT7-mtrm* and various *pGADT7-mtrm* mutants were transformed into yeast strain AH109. *pGBKT7-polo* and various *pGBKT7-polo* mutants were transformed into yeast strain Y187 (Clontech). The transformed strains were mated on YPD overnight, and diploids containing both constructs were then selected on SD plates lacking tryptophan and leucine. These were then spotted at 10-fold serial dilutions on the same plates and also on reporter plates lacking histidine and cultured for 4 days at 30°C.

Co-immunoprecipitations

Two 50 ml starter cultures in YP media supplemented with 2% raffinose (YP-raffinose) were inoculated with colonies of freshly-streaked a WT yeast

strain (SLJ001) transformed with *pDK20-mtrm-3XFLAG* vector and a *Myc3-CDC5* strain (SLJ917) transformed with *pDK20-mtrm-3XFLAG* vector. The inoculations were grown overnight at 30°C in a shaking incubator. Culture size was expanded to 100ml by dilution with YP-raffinose to an OD_{600} of 0.25 before incubation at 30°C. When the culture reached OD_{600} of 0.8, the two 100ml cultures were divided in half. For each genotype, 50ml cultures were induced for 3 hrs at 30°C by the addition of galactose to a final concentration of 2%. The remaining 50ml of each genotype were grown for 3 hrs at 30°C in the presence of 2% dextrose as our uninduced control. Following the induction period, the four 50ml cultures each divided into half, making eight 25ml cultures, which were then harvested by centrifugation (10 min, ~5,000xg, 4°C). Pellets were snap-frozen in liquid nitrogen and stored at -80°C prior to co-immunoprecipitations.

Lysates of the eight samples were prepared by bead beating at 4°C in 500µl yeast lysis buffer followed by centrufugation at 14,000RPM for 10 min at 4°C. For each genotype and induction type, FLAG immunoaffinity purification and Myc immunoaffinity purification was performed in parallel.

Western Analysis

Standard techniques were used for Western analysis. The primary antibodies used were mouse anti-FLAG M2 (Sigma) at a dilution of 1:2000 and rabbit anti-Myc A14 at a dilution of 1:1000. Immunoreactivity was detected using an alkaline phosphatase-conjugated mouse and rabbit secondary antibody

(Jackson ImmunoResearch) and the nitroblue tetrazolium and 5-bromo-4-chloro-3-indolyl phosphatase (NBT/BCIP, Invitrogen) reagents.

Purification of FLAG-epitope-tagged proteins and associated proteins from S. cerevisiae

50ml starter cultures in YP media supplemented with 2% raffinose (YP-raffinose) were inoculated with colonies of freshly-streaked a *Myc3-CDC5* strain (SLJ917) transformed with *pDK20-mtrm-3XFLAG* vector. The inoculations were grown overnight at 30°C in a shaking incubator. Culture size was expanded to 6 Liters total by dilution with YP-raffinose to an OD_{600} of 0.25 before incubation at 30°C. When the culture turbidity reached OD_{600} of 0.8, 3 Liters were induced for 3 hrs at 30°C by the addition of galactose to a final concentration of 2%. The remaining 3 Liters were grown for 3 hrs at 30°C in the presence of 2% dextrose to serve as our uninduced control. Following the induction period, the cultures were then harvested by centrifugation (10 min, ~5,000xg, 4°C). Pellets were snap-frozen in liquid nitrogen and stored at -80°C prior to FLAG purification.

FLAG purification was performed according to the specifications available online from the laboratory of Toshi Tsukiyama of the Fred Hutchinson Cancer Research Center***.***

MudPIT analysis

MudPIT analysis is described in the Materials and Methods section of Chapter 3.

Post-translational modification analysis

Post-translational modification analysis in conjunction with the Stowers proteomics core facility was performed according to the specifications previously described in [60].

Chapter 3. Analysis of physical interaction between Mtrm and Polo kinase during *Drosophila* female meiosis

3.1 Introduction

The results of the Y2H assays presented us with the intriguing finding that Mtrm may interact with Polo via a mechanism that does not solely depend on a canonical PBD binding motif. Thus, we returned to the fly as a model to determine whether these findings would hold true in the native organism. In order to achieve this, we took advantage of φC31 site-specific *Drosophila* transgenic techniques to create a large series of *3XFLAG-mtrm* mutant transgenic flies that are used throughout the remainder of this thesis [86]. Targeted integration is advantageous when comparing multiple transgenic lines. Since our transgenes of interest are integrated into the same site in the *Drosophila* genome, positional effects can be mitigated. Consistent with this view, we observed no gross differences in protein levels between the *mtrm* transgenes assayed by MudPIT analysis.

As highlighted before, MtrmS48 and MtrmS52 are reproducibly phosphorylated in flies, suggesting that those residues may also hold functional significance [60]. In addition, MtrmT40 is critical for Mtrm function during female meiosis as well as physical interaction with Polo kinase as assayed by co-immunoprecipitations from ovarian lysates [60]. Consistent with this view, the Y2H studies described in Chapter 2 demonstrate that MtrmS48 and Mtrm52 are

critical for physical interaction with Polo. However, these studies proved contradictory for MtrmT40. Unlike the studies in the fly, Y2H analysis suggested that MtrmT40 is dispensable for physical interaction with Polo. In order to address this, we performed MudPIT mass spectrometry on 3XFLAG-epitope-tagged versions of Mtrm purified from ovarian lysates. These tagged Mtrm mutants containing either single alanine substitutions targeting conserved residues or N or C-terminal truncations of Mtrm. MudPIT analysis allows not only for us to examine the ability of a particular Mtrm mutant interact with endogenous Polo, but also to identify other Mtrm interactors that could potentially play a role in the Mtrm-Polo interaction.

3.2 MudPIT analysis of Flag-tagged Mtrm purified from ovarian lysates

MudPIT mass spectrometry is a highly sophisticated technique that allows for the analysis of complex protein mixtures. The advantages over traditional mass spectrometry techniques are significant. By coupling high-pressure liquid chromatography and tandem mass spectrometry with sophisticated database software and automated data collection systems, the technique allows for a more unbiased proteomic analysis with a high degree of sensitivity allowing for the identification of both high and low abundance proteins.

The relative abundance of a given protein in the sample is best approximated by its normalized spectral abundance factor (NSAF) [87], which

may be calculated by the following equation, where SpC is spectral count and L is protein length:

$$NSAF_k = \frac{(SpC/L)_k}{\sum_{i=1}^{N}(SpC/L)_i}$$

In short, NSAFs are an estimate of protein abundance (SpC) adjusted for protein length (L) and the percentage of total spectra within a given run. Statistical analysis of runs from multiple biological replicates of data is made possible by Power Law Global Error Model (PLGEM) software [88], which calculates signal to noise (STN) ratios of NSAF datasets allowing us to identify differentially abundant proteins across samples.

As defined by NSAF, abundances of proteins from ovarian lysates that co-purify with 3XFLAG-Mtrm, 3XFLAG-MtrmT40A, 3XFLAG-MtrmS48A, 3XFLAG-MtrmSTPDEL and 3XFLAG-MtrmSAMDEL were compared to their levels in a set of negative control samples (*w1118* ovaries) that were also affinity purified. We then performed PLGEM analysis, we subsequently evaluated datasets of proteins selected by two relative NSAF p-value thresholds: $p \leq 0.001$ (Table 3.1) and ≤ 0.005 (Table 3.2).

As shown in Table 3.1, only five proteins co-purified with full-length 3XFLAG-Mtrm that filled the most stringent criteria of having a p-value ≤ 0.001: Polo kinase, vitilline membrane 26Aa, heat shock protein 26, heat shock protein 27 and heat shock protein 23. Moreover, Mtrm mutants 3XFLAG-MtrmT40A,

3XFLAG-MtrmS48A, 3XFLAG-MtrmSTPDEL, and 3XFLAG-MtrmSAMDE failed to co-purify Polo at the same level of significance. These results are congruent with our Y2H findings with the exception of the MtrmT40A result. In the fly, MtrmT40 is critical for physical interaction with endogenous Polo as assayed by MudPIT analysis. In addition, the data regarding MtrmT40A are consistent with previously published work [60].

The example of vitelline membrane 26Aa being called a Mtrm 'interactor' demonstrates one of the pitfalls in simply using p-values calculated by PLGEM for candidate selection. PLGEM evaluates how two data sets differ from each other: in this case the seven NSAF values for vitelline membrane 26Aa in the seven experimental runs (NSAF = {0, 0.0004, 0.0003, 0, 0, 0.0004, 0.1336}) versus the five in the control samples (NSAF = {0, 0.0010, 0, 0, 0}). Clearly, the exceedingly high, outlying NSAF in one Mtrm MudPIT run artifactually shifted the rank of vitelline membrane 26Aa from a non-significant to one of significance. By contrast, we may be more confident in stating that Mtrm and Polo interact due to a more consistent NSAF set with higher values from the experimental duplicates (NSAF = {0.0147, 0.009, 0.005, 0.0140, 0.0117, 0.0259}). Until a better algorithm is developed, compiling protein lists and determining potential binding partners will require not only filtering by p-value, but also manual assessment.

Table 3-1 Protein co-purified with 3XFLAG-Mtrm and 3XFLAGMtrm mutant proteins with statistical significance of p ≤ 0.001.

Ovarian lysates were made from 100 ovaries dissected from the *Drosophila* females expressing the version of 3XFLAG-epitope tagged Mtrm and subjected to immunoaffinity purification and MudPIT mass spectrometry. Relative abundance of proteins as described by the NSAF were calculated by *NSAF7*, and statistical significance (p-value) of a protein's NSAF for multiple MudPIT runs relative to a No-FLAG negative control was evaluated by PLGEM (Mtrm, n=7; Mtrm-T40A, n=4; Mtrm-S48A, n= 7; MtrmSTPDEL, n=2; MtrmSAMDEL, n=2; Control, n=5). The table shows a list of proteins (highlighted yellow) found in addition to Mtrm, MtrmT40A, MtrmS40A, MtrmSTPDEL, or MtrmSAMDEL that were detected at significant levels when the p-value threshold was set to p ≤ 0.001.

	Mtrm	MtrmT40A	MtrmS48A	MtrmSTPDEL	MtrmSAMDEL	
Description	**p-value**	**p-value**	**p-value**	**p-value**	**p-value**	**Locus GI**
heat shock protein 26	0.00E+00	0.00E+00	0.00E+00	2.00E-07	1.23E-02	17647519
vitelline membrane 26Aa	0.00E+00	3.60E-01	2.28E-03	3.32E-01	1.21E-01	17136584
polo, isoform B	1.20E-06	1.16E-02	1.38E-02	1.31E-02	6.13E-01	**62472270**
heat shock protein 27	2.79E-06	5.79E-06	9.38E-06	1.12E-03	1.27E-03	17647521
heat shock protein 23	9.25E-04	9.12E-04	8.72E-03	1.39E-03	5.56E-01	17737553
lethal -2 37Cg	4.83E-03	3.82E-02	3.12E-03	7.02E-04	4.73E-01	24585154
CG8928	2.28E-02	9.04E-02	9.82E-03	7.65E-03	6.84E-04	24642361
yolk protein 2	1.53E-01	1.93E-01	1.84E-01	2.33E-01	6.10E-04	161077703
actin 88F	3.89E-01	5.91E-04	5.56E-02	4.65E-02	4.65E-02	17975545
chorion protein 15	4.90E-01	1.93E-02	1.33E-02	1.39E-01	3.66E-04	17647277

Table 3-2 lists those interactors that were detected at significant levels when the p-value threshold was then increased to p ≤ .005 (including the previously presented proteins listed at a threshold of p ≤ 0.001). The putative binding partners of Mtrm or Mtrm mutants may shed light on the possible functions of specific Mtrm residues and domains as well as perhaps yet to be discovered roles that the Mtrm-Polo complex may play during *Drosophila* female meiosis. Intriguing interactors of the full length 3XFLAG-Mtrm include Dodo, Lodestar, Cdc2c, Belle, and Cdc16. Interestingly, Dodo is the *Drosophila* homologue of human PIN1 (peptidylprolyl cis/trans isomerase, NIMA-interacting 1), which is phosphorylated by human Plk1 [89]. Interestingly, PIN1 selectively

targets phosphorylated pS/pT-P motifs in order to facilitate the regulation of the phosphorylation state (among other post-translational modifications) of its substrates. Other proteins listed as significant when the threshold is set to $p \leq 0.005$ include several members of the Anaphase-Promoting Complex/Cyclosome (APC/C) complex: Cdc16, Cdc23, Shattered, and Imaginal discs arrested. The APC/C is an E3 ubiquitin ligase that is known for targeting cell cycle proteins for degredation by the proteasome. Indeed, these data may make biological sense as the current hypothesis holds that Mtrm is rapidly degraded upon or shortly after NEB.

Interestingly, the truncated version of Mtrm lacking its C-terminal SAM domain (MtrmSAMDEL) loses a vast number of protein associations. This result supports the view that a primary role of the SAM domain of Mtrm is to mediate protein-protein interactions. Curiously, the STP deletion of Mtrm (MtrmSTPDEL) appears to interact with an increased number of protein partners with a p value $\leq .005$. From these data, we speculate that the C-terminal SAM domain of Mtrm may function as the primary domain for protein-protein interactions while the STP region may facilitate specificity of binding. The few proteins that do co-purify with MtrmSTPDEL with a p value of $\leq .005$ appear to be associated with ubiquitination: CG10254, isoform B; cdc16; skpA; elongin C; hyperplastic discs; the NUB1 homolog; Apc 1, 5, and 8. From this data alone, it is not entirely clear whether Mtrm-STPDEL is involved in the ubiquitin-degradation pathway or is simply in the process of being degraded itself.

Table 3-2 Protein co-purified with 3XFLAG-Mtrm and 3XFLAG-Mtrm mutant proteins with statistical significance of p ≤ 0.005.

Ovarian lysates were made from 100 ovaries dissected from the *Drosophila* females expressing the version of 3XFLAG-epitope tagged Mtrm and subjected to immunoaffinity purification and MudPIT mass spectrometry. Relative abundance of proteins as described by the NSAF were calculated by *NSAF7*, and statistical significance (p-value) of a protein's NSAF for multiple MudPIT runs relative to a Flag-only negative control was evaluated by PLGEM (Mtrm, n=7; Mtrm-T40A, n=4; Mtrm-S48A, n= 7; MtrmSTPDEL, n=2; MtrmSAMDEL, n=2; Control, n=5). The table shows a list of proteins (highlighted yellow) found in addition to Mtrm, -T40A, -S40A, STPDEL, or SAMDEL that were detected at significant levels when the p-value threshold was set to p ≤ 0.005.

	Mtrm	MtrmT40A	MtrmS48A	MtrmSTPDEL	MtrmSAMDEL	
Description	**p-value**	**p-value**	**p-value**	**p-value**	**p-value**	**Locus GI**
heat shock protein 26	0.00E+00	0.00E+00	0.00E+00	2.00E-07	1.23E-02	17647519
vitelline membrane 26Aa	0.00E+00	3.60E-01	2.28E-03	3.32E-01	1.21E-01	17136584
polo, isoform B	1.20E-06	1.16E-02	1.38E-02	1.31E-02	6.13E-01	**62472270**
heat shock protein 27	2.79E-06	5.79E-06	9.38E-06	1.12E-03	1.27E-03	17647521
heat shock protein 23	9.25E-04	9.12E-04	8.72E-03	1.39E-03	5.56E-01	17737553
dodo	1.30E-03	2.60E-03	5.46E-03	8.67E-03	4.73E-01	17647355
CG6617	1.31E-03	7.29E-03	1.83E-03	2.20E-03	8.90E-02	24643081
lodestar	1.69E-03	3.75E-03	2.28E-03	1.70E-03	2.05E-01	24644932
Dpy-30-like 1	1.77E-03	4.93E-02	5.34E-03	1.38E-03	4.73E-01	24583515
CG7208, isoform B	2.53E-03	1.06E-02	4.83E-03	2.00E-03	1.04E-01	85816234
absent, small, or homeotic discs 2, isoform D	2.60E-03	7.72E-03	4.27E-03	1.99E-03	4.73E-01	221459037
CG31357	2.74E-03	2.81E-02	3.75E-03	4.56E-03	9.61E-02	24649795
CG10254, isoform B	2.99E-03	1.11E-02	1.42E-02	1.25E-02	3.72E-01	24649371
CG14207, isoform A	3.07E-03	3.51E-03	2.55E-03	1.61E-03	2.70E-02	19920346
cdc2c, isoform C	3.97E-03	8.97E-03	9.95E-03	5.17E-03	3.17E-02	281362157
heterogeneous nuclear ribonucleoprotein at 98DE, isoform A	4.02E-03	5.31E-01	1.67E-02	1.51E-02	9.10E-02	24650831
CG8368, isoform B	4.49E-03	1.15E-02	5.62E-03	1.98E-03	1.34E-01	24659458
CG10055	4.57E-03	9.61E-03	6.42E-03	1.56E-03	1.27E-01	24644770
belle	4.64E-03	7.90E-03	1.80E-03	2.53E-03	1.79E-01	17985987
cdc16	4.73E-03	4.70E-03	6.48E-03	3.05E-03	4.73E-01	17137612
lethal -2 37Cg	4.83E-03	3.82E-02	3.12E-03	7.02E-04	4.73E-01	24585154
skpA, isoform H	5.53E-03	4.13E-03	4.70E-03	1.37E-03	7.46E-02	85724772

Table 3-2 *(cont.)*

	Mtrm	MtrmT40A	MtrmS48A	MtrmSTPDEL	MtrmSAMDEL	
Description	**p-value**	**p-value**	**p-value**	**p-value**	**p-value**	**Locus GI**
hyperplastic discs	5.79E-03	8.61E-03	8.25E-03	4.13E-03	2.16E-01	24645474
lethal -1 G0156, isoform A	5.90E-03	3.03E-02	1.37E-01	3.44E-03	6.12E-03	24643268
CG15445, isoform A	6.05E-03	5.31E-01	1.29E-02	3.96E-03	4.73E-01	24643638
dynamin related protein 1	6.06E-03	9.16E-03	2.36E-02	4.11E-03	5.66E-01	24581168
RNA polymerase II 33kD subunit	6.34E-03	1.12E-02	1.04E-02	1.53E-03	1.96E-02	17137650
female sterile -1 young arrest	6.79E-03	2.31E-02	5.72E-03	3.55E-03	4.31E-01	24639404
ribosomal protein S14a, isoform A	7.10E-03	3.01E-03	9.16E-03	3.45E-02	5.44E-01	24640451
CG3295	7.31E-03	1.66E-02	1.56E-02	4.84E-03	4.73E-01	20130193
spindle defective 2	7.35E-03	4.61E-02	1.20E-02	4.97E-03	4.73E-01	21357057
vacuolar protein sorting 25	7.76E-03	4.91E-03	1.15E-02	3.62E-03	4.73E-01	19921830
CG10237, isoform B	7.89E-03	1.59E-02	7.30E-03	3.30E-03	4.73E-01	19921536
protein phosphatase V	8.06E-03	5.31E-01	2.18E-02	4.86E-03	4.73E-01	17737286
cdc23	9.22E-03	3.44E-02	4.56E-03	3.86E-03	4.73E-01	24585440
ribosomal protein S24	9.70E-03	4.49E-01	4.51E-03	4.83E-01	4.62E-01	20130247
shattered, isoform A	9.73E-03	2.83E-02	1.06E-02	4.92E-03	4.73E-01	24642175
adenylate kinase 6	1.02E-02	3.28E-02	1.02E-02	2.07E-03	4.73E-01	19922110
imaginal discs arrested, isoform A	1.04E-02	1.31E-01	1.54E-02	3.90E-03	4.73E-01	45550537
CG5604	1.04E-02	1.93E-02	6.11E-03	2.13E-03	9.57E-02	24583318
CG7945, isoform B	1.06E-02	3.06E-02	6.36E-03	2.44E-03	4.73E-01	24664648
CG13090	1.07E-02	5.82E-02	1.73E-02	4.84E-03	4.73E-01	24582879
CG12214, isoform B	1.11E-02	5.31E-01	3.78E-02	4.92E-03	4.73E-01	24652364
mediator complex subunit 10	1.32E-02	5.31E-01	1.41E-02	4.01E-03	4.73E-01	281366312
Chrac-14, isoform A	1.48E-02	5.31E-01	2.45E-02	2.39E-03	3.74E-02	78707308
DnaJ-like-1, isoform B	1.51E-02	3.33E-02	7.21E-03	3.24E-03	3.35E-01	24658562
cytoplasmic dynein light chain 2, isoform B	1.51E-02	1.35E-02	3.90E-03	1.27E-02	4.73E-01	24580844
CG5174, isoform A	1.57E-02	1.43E-01	2.46E-02	4.32E-03	1.03E-01	24655026
VhaAC39	1.61E-02	6.20E-02	4.23E-02	3.40E-03	4.73E-01	18543319
CG16734, isoform B	1.86E-02	5.31E-01	6.12E-01	4.45E-03	4.73E-01	281361435
CG7182	1.88E-02	6.16E-02	9.09E-02	3.43E-03	4.47E-01	21355965

Table 3-2 *(cont.)*

	Mtrm	MtrmT40A	MtrmS48A	MtrmSTPDEL	MtrmSAMDEL	
Description	**p-value**	**p-value**	**p-value**	**p-value**	**p-value**	**Locus GI**
Transcription-factor-IIA-S	1.93E-02	5.31E-01	3.83E-02	3.68E-03	4.73E-01	17738155
arrest, isoform C	2.02E-02	2.50E-02	4.23E-03	4.96E-03	4.73E-01	24583875
CG8928	2.28E-02	9.04E-02	9.82E-03	7.65E-03	6.84E-04	24642361
CG7686	2.34E-02	5.59E-02	2.39E-01	4.21E-03	4.73E-01	19921998
CG1637, isoform B	2.37E-02	3.26E-02	6.12E-01	9.01E-03	4.57E-03	24641134
ribosomal protein L38	3.02E-02	2.04E-02	4.47E-03	1.86E-02	9.96E-02	116007488
transport and golgi organization 7	4.09E-02	7.07E-02	7.08E-02	4.06E-03	1.03E-01	19922220
elongin C, isoform A	5.49E-02	1.90E-02	1.08E-01	4.16E-03	4.73E-01	24655726
death caspase-1	8.97E-02	1.53E-01	1.28E-01	3.73E-03	3.30E-01	17352459
yolk protein 2	1.53E-01	1.93E-01	1.84E-01	2.33E-01	6.10E-04	161077703
Ski6	1.66E-01	1.76E-01	3.54E-01	9.94E-02	3.01E-03	24584046
chorion protein 19	2.09E-01	4.76E-01	9.15E-02	3.75E-02	2.20E-03	17986137
ribosomal protein L23	2.10E-01	4.28E-03	8.00E-02	3.52E-01	1.93E-01	17647883
CG1637, isoform C	2.79E-01	1.37E-01	4.09E-01	4.06E-02	4.75E-03	20129007
actin 87E, isoform B	3.36E-01	4.39E-03	2.11E-02	1.13E-02	1.13E-02	24646579
mitochondrial ribosomal protein L12	3.54E-01	4.73E-02	3.86E-01	1.97E-01	4.06E-03	17864338
actin 88F	3.89E-01	5.91E-04	5.56E-02	4.65E-02	4.65E-02	17975545
chorion protein 15	4.90E-01	1.93E-02	1.33E-02	1.39E-01	3.66E-04	17647277
mitochondrial ribosomal protein S18C	6.12E-01	5.31E-01	1.25E-01	4.64E-02	4.76E-03	24651373
chorion protein 18	6.12E-01	5.31E-01	3.25E-03	4.73E-01	2.88E-03	17647281
Neb-cGP	6.12E-01	2.09E-03	6.12E-01	4.73E-01	4.73E-01	21358399

3.3 Relative abundance ratios of Polo versus various Mtrm mutants

The sensitivity of MudPIT analysis provides a means by which to quantitate how interactions between Mtrm and Polo are affected by mutation. We compared average NSAF values of the two proteins across a series of Mtrm mutations – MtrmSTPDEL, MtrmSAMDEL, MtrmS39A, MtrmT40A, MtrmF46A, MtrmS48A, MtrmS52A, and MtrmS137A –the results of which are summarized in Figure 3.1.

All Mtrm mutants studied appeared to affect interaction with Polo, albeit to varying degrees. Both the N and C-terminal truncations of Mtrm greatly disrupted Mtrm-Polo interaction as did alanine substitution of MtrmT40, MtrmS48, and MtrmS52. By contrast, substitution of MtrmS39 and MtrmF46, and MtrmS137 with alanine allowed partial binding. These findings are worthy of note, and their significance will be discussed in relation to results of the *Drosophila* genetic studies described in Chapters 4 and 5.

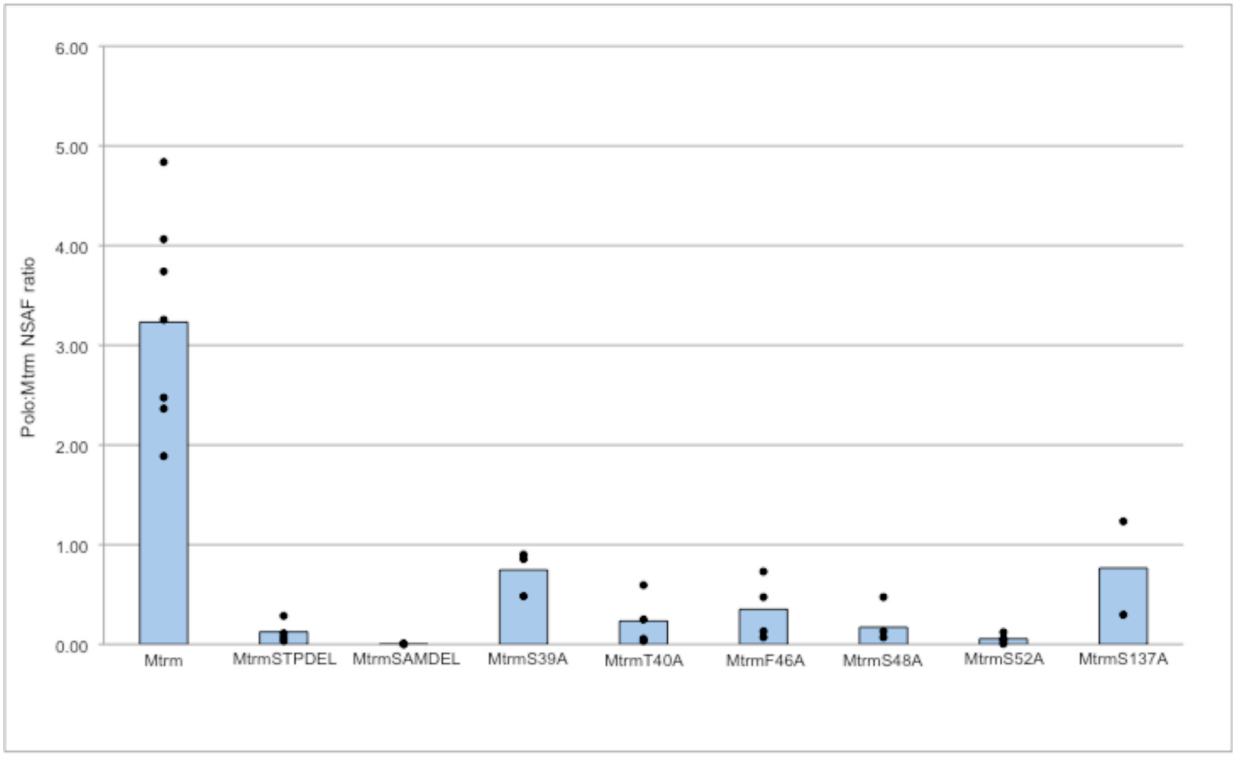

	Domain Affected	Average Polo:Matrimony NSAF ratio (n)
Mtrm		3.23 (7)
MtrmSTPDEL	PBD binding motif	0.13 (4)
MtrmSAMDEL	SAM domain	0.00 (3)
MtrmS39A	PBD binding motif	0.75 (3)
MtrmT40A	PBD binding motif	0.23 (4)
MtrmF46A		0.35 (4)
MtrmS48A	GSKß phosphorylation motif	0.17 (3)
MtrmS52A	GSKß phosphorylation motif	0.06 (3)
MtrmS137A	Polo phosphorylation motif	0.77 (2)

Figure 3-1 Average Polo versus Mtrm/Mtrm mutant NSAF Ratios.

Ovarian lysates were made from 100 ovaries dissected from the *Drosophila* females expressing the version of 3XFLAG-epitope tagged Mtrm and subjected to immunoaffinity purification and MudPIT mass spectrometry. Relative abundance of proteins as described by the NSAF were calculated by *NSAF7*. Bars represent the average Polo:Mtrm NSAF ratio, which is also summarize in the adjoining table. Points represent the distribution of NSAF ratios over *n* samples.

3.4 Discussion

This chapter describes the most detailed biochemical analysis of the Mtrm:Polo interaction to date. Strikingly, the results confirm much of what was observed in the Y2H analysis of Mtrm mutants and also address the incongruent finding regarding interaction between MtrmT40A and Polo predicted by Y2H.

In addition, we present proteomic analysis of additional potential Mtrm-interacting proteins. While the PLGEM algorithm provides an unbiased evaluation of MudPIT datasets, it is clear that more work is required to design a computational method to filter data. Regardless, our efforts have yielded a number of candidate proteins that may be studied in the context of *Drosophila* female meiosis.

3.5 Acknowledgments

Thanks to the Stowers molecular biology core facility for the mutagenesis of Mtrm. I would like to thank the members of the Stowers proteomics core facility including our collaborators Laurence Florens and Selene Swanson. Thanks to the I would also like to thank Charles Banks and Stephanie Kong for helpful discussions, support and expertise.

3.6 Materials and Methods

Generation of site-directed mutants

Mutations in the *mtrm* gene were generated using the Quik Change II XL

Site-Directed mutagenesis Kit (Stratagene, CA) in conjunction with the Stowers molecular biology core facility. A 3.1 kb *ScaI* fragment containing the *mtrm* gene flanked by its regulatory elements derived from the Bac clone *BACR13D12* was isolated via gel purification and sequentially subjected to enzymatic digestion and then subcloned into *pBS-KSII+* (Clonetech, CA), which was then used for site directed mutagenesis. (The 3.1 kb fragment was used so that genomic mutant versions of *mtrm* could be easily generated in the future if desired.) The resultant *pBS-mtrm* containing the engineered mutation was then utilized as the PCR template for generating the transgene to be integrated in the fly as described in the below. All mutational changes were specifically designed to comply with *D. melanogaster* codon usage bias.

Generation of fly transgenes

A single strategy was employed for the generation of all *3XFLAG-mtrm* mutant transgenes used in Chapters 3, 4 and 5. All *mtrm* PCR products were amplified by the primers listed below. The resulting products were digested with *NotI* and *BamHI* and then subcloned into the *pUASp-attB-5'FLAG* vector (gift from S. Takeo) digested with the same enzymes. Following verification with Sanger sequencing.

Both the full length and alanine substitution versions of the *mtrm* gene were amplified via PCR with primers 5'-cggcggccgcatggagaattctcgcacgc -3' and 5'-cggggatccttaaagagtgtggagcacatccatg -3.' The N-terminal *mtrm* truncation

deleting the first 53 amino acids of Mtrm was amplified from full length *mtrm* with primers 5'- cggcggccgcatgcccatcgagaatatgggcacg -3' and 5'- cggggatccttaaagagtgtggagcacatccatg-3. The C-terminal *mtrm* truncation deleting the last 64 amino acids of Mtrm was amplified from full length *mtrm* with primers 5'- cggcggccgcatggagaattctcgcacgc -3' and 5'- gccggatccttacgagtggttcgatgc -3.

φ*C31 site-specific integration into the Drosophila genome*

φC31 site-specific integration was utilized to introduce the fly transgenes into the *D. melanogaster* genome. This system uses φC31 integrase, which mediates recombination between the bacterial and phage attachment sites, *attB* and *attP*. Expression of φC31 integrase allows for efficient integration of *attB*-containing plasmids including the transgene of interest into *attP* loci that have been previously inserted into the *D. melanogaster* genome. For this work, we used the *attP40 D. melanogaster* line for insertion on Chromosome *2* [86]. Because all fly transgenes are inserted into the same locus, any positional effects that would otherwise result via traditional transgenesis techniques are mitigated, thus allowing for a comparative analysis between transgenes. Embryo injection of *pUASp-attB-5'FLAGmtrm* DNAs into *attP40* embryos expressing φC31 integrase were performed by Genetic Services, Inc.

Immunoprecipitation of FLAG-epitope tagged proteins from Drosophila ovarian lysates

Ovaries from approximately 100 *Drosophila* females per FLAG IP were

dissected in 1X PBS and homogenized with an IP buffer (50 mM Tris-HCl pH 6.8, 150 mM NaCl, 2.5mM EGTA, 2.5mM EDTA, 0.1% Triton X-100, 1 mM protease inhibitor cocktails). Lysates were cleared by centrifugation twice at 14,000 rpm for 15 min at 4°C. Lysates were added to 100 µl of equilibrated EZview Red ANTI-FLAG M2 Affinity 5 hrs at 4°C. The beads were washed with cold IP buffer 5 times for 10 min each at 4°C. Proteins were eluted with 100 µl of 200 ng/µl 3XFLAG peptide in TBS pH 7.4 by incubating for 1 hr at 4°C on a rocker. After collecting the supernatant, proteins were eluted again with another 100 µl of 200 ng/µl 3XFLAG peptide. 5µl (or 95%) of both elution 1 and 2 were run on SDS-PAGE (4-12% NuPAGE gradient gel) and silver-stained (Invitrogen, SilverExpress) The remainder of the eluates were then TCA-precipitated.

TCA precipitation of eluates

Each sample was brought to 400 µl with 100 mM Tris-HCL, pH 8.5. 100 µl TCA (final concentration of 20%) was added, and the reactions were carried out o/n at 4°C. The samples were then spun down at 14,000 rpm 30 min at 4°C, pellets were washed with cold acetone and spun at 14,000 rpm 10 min at 4°C twice. Pellets were subsequently air dried and submitted to the Stowers proteomics core facility as a dried pellet.

MudPIT analysis of proteins purified from Drosophila ovarian lysates

MudPIT analysis was performed in collaboration with the Stowers proteomics core facility. TCA-precipitated proteins were resuspended in 30 µl of

100 mM Tris-HCl, pH 8.5, 8 M urea, reduced with 5 mM TCEP (Tris(2-Carboxylethyl)-Phosphine Hydrochloride, Pierce), and alkylated with 10 mM CAM (Chloroacetamide, Sigma). Endoproteinase Lys-C (Roche) was added to a final concentration of 0.1 ug/µl for at least 6 hours at 37°C; then the sample was diluted to 2 M urea with 100 mM Tris-HCl, pH 8.5. Calcium chloride was added to a final concentration of 2 mM, and the digestion with trypsin (0.1 ug/µl) was let to proceed overnight at 37°C while shaking. The reaction was quenched by adding formic acid to 5% and the peptide mixture was loaded onto a 100 µm fused silica microcapillary column packed with 8 cm of reverse phase material (Aqua, Phenomenex), followed by 3 cm of 5-µm Strong Cation Exchange material (Partisphere SCX, Whatman) and 2 cm of 5-µm C_{18} reverse phase.

The loaded microcapillary column was placed in-line with a Quaternary Agilent 1100 series HPLC pump. Overflow tubing was used to decrease the flow rate from 0.1 ml/min to about 200–300 nl/min. Fully automated 10-step chromatography runs were carried out. Three different elution buffers were used: 5% acetonitrile, 0.1% formic acid (Buffer A); 80% acetonitrile, 0.1% formic acid (Buffer B); and 0.5 M ammonium acetate, 5% acetonitrile, 0.1% formic acid (Buffer C). Peptides were sequentially eluted from the SCX resin to the reverse phase resin by increasing salt steps, followed by an organic gradient. The last two chromatography steps consisted in a high salt wash with 100% Buffer C followed by the acetonitrile gradient. The application of a 2.5 kV distal voltage electrosprayed the eluting peptides directly into a LTQ ion trap mass

spectrometer equipped with a nano-LC electrospray ionization source (ThermoFinnigan). Full MS spectra were recorded on the peptides over a 400 to 1,600 *m*/*z* range, followed by three tandem mass (MS/MS) events sequentially generated in a data-dependent manner on the first, second, and third most intense ions selected from the full MS spectrum (at 35% collision energy). Mass spectrometer scan functions and HPLC solvent gradients were controlled by the Xcalibur data system (ThermoFinnigan).

SEQUEST was used to match MS/MS spectra to peptides in a database of 37016 sequences, consisting of 18331 *Drosophila melanogaster* proteins (downloaded from NCBI on 2009-12-23), 177 usual contaminants such as human keratins, IgGs, and proteolytic enzymes. To estimate false discovery rates (FDR), each protein sequence was randomized (keeping the same amino acid composition and length) and the resulting 18508 "shuffled" sequences were added to the database used for the SEQUEST searches. The validity of peptide/spectrum matches was assessed using the SEQUEST-defined parameters, cross-correlation score (XCorr) and normalized difference in cross-correlation scores (DeltCn). Spectra/peptide matches were only retained if they had a DeltCn of at least 0.08 and,minimum XCorr of 1.8 for singly-, 2.5 for doubly-, and 3.5 for triply-charged spectra. In addition, the peptides had to be fully-tryptic and at least 7 amino acids long. Combining all runs, proteins had to be detected by at least 2 such peptides, or 1 peptide with 2 independent spectra. Under these criteria the final FDRs at the protein and peptide levels were % ±

and % ± , respectively. DTASelect was used to select and sort peptide/spectrum matches passing this criteria set. Peptide hits from multiple runs were compared using CONTRAST. To estimate relative protein levels, spectral counts were normalized; using an in-house developed script (*NSAF7*): for each protein *k* detected in a particular MudPIT analysis, Normalized Spectral Abundance Factors (NSAFs) were calculated as shown in the chapter.

Chapter 4. Residues and regions of Mtrm critical for proper homologous achiasmate segregation

4.1 Introduction

As discussed in Chapter 1, *mtrm* is critical for homologous achiasmate segregation—a well characterized process in *Drosophila* that ensures the faithful segregation of chromosome pairs that do not recombine during female meiosis. Females heterozygous for a null allele of *mtrm* display high levels of achiasmate chromosome nondisjunction (NDJ). Importantly, this phenotype is genetically linked to *polo* as the high levels of achiasmate chromosome NDJ can be fully suppressed by simultaneous reduction of the *polo* gene [60]. As mentioned previously, mutating the central residue of the Polo-box domain (PBD) binding motif, MtrmT40, to alanine ablates both the physical interaction of Mtrm with Polo and Mtrm's function as assayed by homologous achiasmate segregation [60]. Thus, we hypothesized that Mtrm negatively regulates Polo during *Drosophila* female meiosis via physical interaction. As outlined in Chapter 2, our Y2H data suggest that the physical interaction is direct. Moreover, analysis in both the fly and in yeast (Chapters 2 and 3) suggest that physical interaction between these two proteins does not solely depend on the PBD binding motif. Several additional residues/regions within Mtrm, such as the C-terminal SAM domain and conserved phosphorylation sites including MtrmS48 and MtrmS52 appear to be important for its physcial association with Polo.

This chapter tests the hypothesis of whether additional Mtrm residues/regions critical for physical interaction with Polo are also critical for Mtrm function as assayed by homologous achiasmate segregation during *Drosophila* female meiosis. We first independently verify the genetic interaction between *mtrm* and *polo* as it relates to homologous achiasmate segregation. We then take advantage of *mtrm* homolog sequences representing 30 million years of divergence by testing their ability to rescue the homologous achiasmate segregation defects observed in *Drosophila* females heterozygous for a null allele of *mtrm*. These results allowed us to narrow our focus to three blocks of conserved sequence within the *mtrm* gene. In addition to truncation analysis, we also performed an alanine-scanning mutagenesis of those conserved residues in an effort to identify additional specific mutations in Mtrm that are required for homologous achiasmate segregation.

4.2 Co-suppression of defect using multiple mutant alleles of *mtrm* and *polo*

The work described by Xiang *et al.* in 2007 primarily used a null allele of *mtrm* (*mtrm*^{126}) made by imprecise excision of the *P* element insertion *KG08051*, which deletes 80 bp upstream of the start codon in *mtrm* and 123 bp downstream of the *mtrm* start codon [60]. Using this allele, Xiang *et al.* demonstrated that females heterozygous for *mtrm*^{126} displayed high levels of achiasmate NDJ as assayed by *FM7/X* and fourth chromosome segregation. (As mentioned in Chapter 1, *FM7* is a balancer chromosome that fully suppresses recombination

between the *Xs*, and the fourth chromosomes of *Drosophila* females are always achiasmate.) Xiang *et al.* also demonstrated that this phenotype is fully suppressed by simultaneous reduction of the *polo* gene by using several mutant alleles of *polo* including the *P* element insertion site mutants $polo^{KG03033}$ and $polo^{16\text{-}1}$ and a deficiency that uncovers the *polo* gene (*Df(3L)rdgC-co2*) [60].

We confirmed these results by testing whether the NDJ phenotype of an independently derived deficiency that uncovers the *mtrm* gene (*Df(3L)66C-T2-T10*) could be suppressed by simultaneous reduction of the *polo* gene using the $polo^{KG03033}$ and $polo^{16\text{-}1}$ mutants. We found that *FM7/X* females heterozygous for *Df(3L)66C-T2-T10* displayed a high level of achiasmate NDJ: approximately 23% and 15% *X* and fourth chromosome NDJ respectively, which is consistent with previously published work utilizing this particular deficiency allele [59]. Reduction of the *polo* function using either $polo^{KG03033}$ or $polo^{16\text{-}1}$ greatly suppressed this phenotype. Females trans-heterozygous for *Df(3L)66C-T2-T10* and $polo^{KG03033}$ exhibited approximately 1% and .5% *X* and fourth achiasmate NDJ respectively, and females trans-heterozygous for *Df(3L)66C-T2-T10* and $polo^{16\text{-}1}$ exhibited approximately 0% and .5% *X* and fourth achiasmate NDJ (Table 4-1). Taken together, these results confirm that *mtrm* and *polo* genetically interact, and their function is required to ensure proper segregation of achiasmate chromosomes.

Oocyte genotype	Paternal genotype	*FM7/X*	*FM7/X; Df(3L)66CT2-T10/+*	*FM7/X; Df(3L)66CT2-T10/ polo^{KG03033}*	*FM7/X; Df(3L)66CT2-T10/ polo$^{16-1}$*
Normal					
X; 4	*XY; 44*	502.	288.	186.	144.
X; 4	*0; 44*	369.	254.	663.	291.
X Nondisjunction					
0; 4	*XY; 44*	0.	27.	1.	0.
XX; 4	*0; 44*	2.	42.	0.	0.
4th Chromosome Nondisjunction					
X; 0	*XY; 44*	1.	38.	0.	2.
X;0	*0;44*	0.	9.	0.	0.
X; 44	*XY; 0*	1.	14.	0.	0.
X; 44	*0; 0*	1.	11.	2.	0.
X:4 Nondisjunction					0.
0; 0	*XY; 44*	0.	3.	0.	0.
XX; 44	*0; 0*	0.	8.	0.	0.
0; 44	*XY; 0*	0.	8.	0.	0.
XX; 0	*0; 44*	0.	5.	1.	0.
Total Progeny		876.	707.	853.	437.
Adjusted Total		878.	800.	855.	437.
% Nullo-*X*		0.	9.5	0.47	0.
% Diplo-*X*		0.46	13.75	0.47	0.
Total % *X* Nondisjunction		**0.46**	**23.25**	**0.94**	**0.**
% Nullo-*4*		0.11	7.88	0.23	0.46
% Diplo-*4*		0.23	7.13	0.23	0.
Total % *4th* Chromosome Nondisjunction		**0.34**	**15.**	**0.47**	**0.46**

Table 4-1 Detailed segregational effects of simultaneous heterozygosity for a deficiency that uncovers *mtrm* and two mutant alleles of *polo.*

FM7/X; spa^{pol} females containing a deficiency that uncovers *mtrm* (*Df(3L)66C-T2-T10)* exhibit levels of achiasmate *X* and fourth chromosome NDJ consistent with previously published work [59]. When females of this genotype are also heterozygous for *polo^{KG03033}* or *polo$^{16-1}$*, the levels of NDJ are greatly reduced. These co-suppression results are consistent with previously published work [60], and confirm using an independently derived null allele of *mtrm* that *mtrm* and *polo* genetically interact to govern homologous achiasmate segregation.

4.3 Evolutionarily conserved residues are critical for proper homologous achiasmate segregation

As described in Chapter 1 and shown in Figure 1-3, *mtrm* is conserved throughout the genus *Drosophila*. A sequence alignment of the predicted Mtrm protein from 12 sequenced *Drosophila* species revealed three highly conserved blocks of sequence. One block surrounds an S-T^{40}-P sequence that fits a canonical PBD consensus motif, one is located just proximal to the C-terminal sterile alpha SAM domain of Mtrm. In addition, critical residues within the SAM domain are also evolutionarily conserved. Aside from these domains, the sequence of Mtrm in the *Drosophila* species is quite divergent, with 38.6% identity between Mtrm of *D. melanogaster* Mtrm and *D. grimshawi* Mtrm (see Figure 4-1 for phylogram of sequenced *Drosophila* species.) Because of this divergence, it was not clear if the evolutionarily divergent *mtrm* homologs would be able to rescue the meiotic defects observed in *D. melanogaster* females heterozygous for a null allele of *mtrm.* Such a finding would be beneficial, however, because it would allow us to narrow our focus to those residues that are evolutionarily conserved.

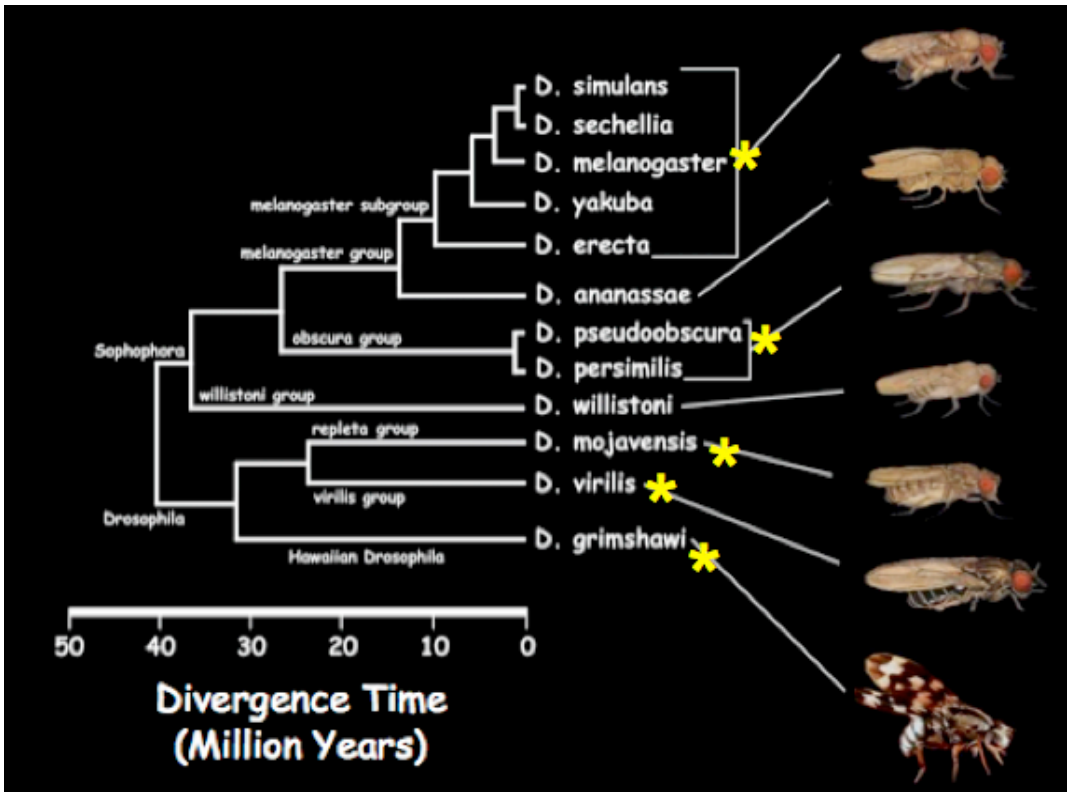

Figure 4-1 Phylogram of 12 sequenced species of *Drosophila*.

mtrm homologs are identified in 12 sequenced species of *Drosophila*. In addition to *D. melanogaster mtrm*, *D. pseudoobscura*, *D virilis, D. mojavensis* and *D. grimshawi mtrm* (yellow asterisks) were all functional when expressed in a *D. melanogaster* host. These results allow us to narrow our focus on those Mtrm residues/regions that have been conserved for approximately 30 million years.

In order to determine the functionality of various *mtrm* homologs in a *D. melanogaster* host, constructs containing various *mtrm* homologs N-terminally tagged with 3XFLAG were integrated into the *Drosophila* genome at the *attP40* site and expressed in the germline using the *nanos-GAL4* driver. As a control, we expressed *D. melanogaster mtrm* tagged in an identical manner, integrated at the same site and driven by the *nanos-Gal4* promoter. The transgenes were crossed into an *FM7/X* genetic background also containing one copy of a

recombinant third chromosome containing both the *nanos-GAL4* driver and the *mtrm*^{126} null *mtrm* allele.

As shown in Table 4-2, expression of wild type *D. melanogaster mtrm* fully rescues the homologous achiasmate segregation defects observed in *mtrm* null heterozygotes, indicating that the transgene driven by the *nanos-Gal4* driver is functional as assayed by homologous achiasmate segregation. Importantly, we found that *D. pseudoobscura mtrm, D. virilis mtrm, D. mojavensis mtrm* and *D. grimshawi mtrm* are all able to rescue the homologous achiasmate segregation defects to levels comparable to *D. melanogaster mtrm* when expressed in the *FM7/X; nanos-Gal4-mtrm*^{126} mutant females. The fact that even the most divergent homolog, *D. grimsahwi mtrm*, is functional in *D. melanogaster* suggests that the functionally significant areas of sequence sufficient to ensure proper chromosome segretaion (and perhaps control of Polo) are likely to involve those that are evolutionarily conserved—the STP region, a short region just proximal to the SAM domain, and/or the SAM domain itself.

Table 4-2 Detailed segregational effects of various *mtrm* homologs in *Drosophila* species.

FM7/X; spa^{pol} females also containing a recombinant third chromosome with both the *nanos-GAL4* driver and the *mtrm*^{126} allele exhibit high levels of achiasmate *X* and fourth chromosome NDJ consistent with previously published work [60]. Females expressing various *mtrm* homologs in this genetic background were all able to rescue the observed homologous achiasmate segregation defects, indicating that those Mtrm residues that are functionally important are also those that have been evolutionarily conserved.
[a] Transgenes expressed in a *FM7/X; nanos-GAL4-mtrm126/+; spa*^{pol} background

Oocyte genotype	Paternal genotype	*FM7/X*	*FM7/X; nanosGal4-mtrm^{126}/+*	*D. melanogaster*[a]	*D. psuedoobscura*[a]	*D. virilis*[a]	*D. mojavensis*[a]	*D. grimshawi*[a]
Normal								
X; 4	*XY; 44*	15310.	5390.	386.	267.	59.	599.	371.
X; 4	*0; 44*	12211.	4062.	251.	277.	82.	612.	248.
X Nondisjunction								
0; 4	*XY; 44*	56.	1695.	10.	12.	1.	10.	5.
XX; 4	*0; 44*	96.	2206.	9.	15.	1.	12.	17.
4th Chromosome Nondisjunction								
X; 0	*XY; 44*	60.	1099.	11.	17.	5.	21.	12.
X;0	*0;44*	29.	553.	4.	11.	5.	21.	3.
X; 44	*XY; 0*	80.	1976.	14.	28.	4.	45.	15.
X; 44	*0; 0*	45.	1414.	16.	24.	7.	31.	4.
X:4 Nondisjunction								
0; 0	*XY; 44*	9.	619.	2.	1.	0.	6.	5.
XX; 44	*0; 0*	4.	934.	7.	2.	1.	4.	5.
0; 44	*XY; 0*	6.	1066.	4.	3.	0.	4.	4.
XX; 0	*0; 44*	4.	647.	1.	3.	1.	0.	0.
Total Progeny		27910.	21661.	715.	660.	166.	1365.	689.
Adjusted Total		28085.	28828.	748.	696.	170.	1401.	725.
% Nullo-*X*		0.51	6.48	1.87	0.57	1.18	0.57	1.38
% Diplo-*X*		0.74	23.45	4.28	4.6	1.18	2.86	3.86
Total % *X* Nondisjunction		**1.25**	**49.72**	**8.82**	**10.34**	**4.71**	**5.14**	**9.93**
% Nullo-*4*		0.41	11.21	2.54	3.3	2.94	2.07	2.76
% Diplo-*4*		0.52	19.55	4.81	6.47	6.47	6.14	5.24
Total % *4th* Chromosome Nondisjunction		**0.93**	**40.15**	**9.76**	**14.08**	**14.71**	**10.42**	**8.55**

4.4 Truncation analysis: the SAM domain of Mtrm appears dispensable for homologous achiasmate segregation

In Chapter 3, we demonstrated that both the N-terminal region and the C-terminal SAM domain of Mtrm are critical for the physical interaction with Polo that is robust enough to be detected by immunoaffinity purifications and subsequent MudPIT analysis. We also wanted to examine whether these regions of Mtrm were required for Mtrm function as assayed by homologous achiasmate segregation (below) and oocyte development (discussed in Chapter 5).

Using the same strategy for integration and expression, we introduced truncated versions of *mtrm* into *FM7/X* females also heterozygous for *nanos-Gal4-mtrm*^{126}. The N-terminal deletion, MtrmSTPDEL, deleting amino acids 2 – 53 of Mtrm (including the conserved S-T^{40}-P sequence) was not able to rescue the meiotic defect (Table 4-3). Compared to control females heterozygous for a null allele of *mtrm* with no rescue construct, which displayed approximately 50% and 40% achiasmate *X* and fourth chromosome NDJ respectively, females expressing the MtrmSTPDEL truncation in this genetic background displayed approximately 38% and 28% *X* and fourth chromosome NDJ respectively. These results are not surprising, as previous work has demonstrated that MtrmT40 is critical for Mtrm function as assayed by homologous achiasmate segregation [60]—a truncated version of Mtrm that results in the deletion of this residue would not be expected to rescue functionality in this context.

The C-terminal deletion, MtrmSAMDEL, which deletes the last 64 amino acids of the protein including the SAM domain, however, is able to complement the meiotic defects (Table 4-3). Females heterozygous for a null allele of *mtrm* expressing the MtrmSAMDEL truncation displayed approximately 11% and 7% *X* and fourth chromosome NDJ respectively. These results are quite unexpected since the SAM domain of Mtrm appears to be critical for robust physical interaction with Polo in both flies and yeast (Chapter 2 and Chapter 3). This intriguing result suggests that perhaps a transient interaction exists between Polo and a region of Mtrm that is proximal to the SAM domain, and this transient interaction that goes otherwise undetected is sufficient to ensure proper homologous achiasmate segregation.

A number of different reasons might account for the apparent discrepancy between the physical and genetic data regarding the importance of the SAM domain for Mtrm function. First, our immunopurification conditions may have been too stringent to detect a weak or transient interaction between Polo and MtrmSAMDEL. Secondly, the affinity of MtrmSAMDEL for Polo may be reduced, which could also account for why we did not detect an association. Alternatively, the ability of MtrmSAMDEL to rescue NDJ may occur through a mechanism that is Polo-independent. Mtrm binds to a number of proteins in an oocyte extract, and alteration in binding to one of these, rather than Polo, may lead to the decreased rate of achiasmate NDJ. Additional studies aimed at testing MtrmSAMDEL binding to Polo and other meiotic regulators will help distinguish

between these possibilities.

Based on the observation that creation of a single point mutant (MtrmT40A) in the PBD abrogates its ability to robustly interact with Polo and its ability to function as assayed by homologous chromosome segregation as described in Chapters 2 and 3 and previously [60], even when the SAM domain is present, we propose that Mtrm primarily binds to Polo via the PBD binding motif and the surrounding region. Consistent with this hypothesis, we identify other Mtrm point mutants (with an intact SAM domain) that behave similarly to MtrmT40A with regard to their ability to bind to Polo and to result in defects in homologous achiasmate segregation (see Section 4.5). Taken together with the results demonstrated in the previous section, Section 4.3, we hypothesize that those residues are likely the evolutionarily conserved motifs within Mtrm that are most important for its interaction with Polo during female meiosis.

Table 4-3 Detailed segregational effects of N and C-terminal *mtrm* truncations expressed in females heterozygous for a null allele of *mtrm.*

FM7/X; spa^{pol} females containing a recombinant third chromosome with both *nanos-GAL4* and *mtrm*^{126} expressing an N-terminally truncated version of Mtrm are not able to engage in proper homologous achiasmate segregation. By contrast, females expressing a C-terminally truncated versionof Mtrm (MtrmSAMDEL) are able to ensure proper homologous achiasmate segregation.

[a] Transgenes expressed in a *FM7/X; nanos-GAL4-mtrm*^{126}*/+; spa*^{pol} background.

Oocyte genotype	Paternal genotype	*FM7/X*	*FM7/X; nanosGal4-mtrm*^{126}*/+*	*FLMtrm*[a]	*STPDEL*[a]	*SAMDEL*[a]
Normal						
X; 4	*XY; 44*	15310.	5390.	386.	197.	334.
X; 4	*0; 44*	12211.	4062.	251.	130.	209.
X Nondisjunction						
0; 4	*XY; 44*	56.	1695.	10.	30.	16.
XX; 4	*0; 44*	96.	2206.	9.	43.	11.
4th Chromosome Nondisjunction						
X; 0	*XY; 44*	60.	1099.	11.	17.	9.
X;0	*0;44*	29.	553.	4.	9.	3.
X; 44	*XY; 0*	80.	1976.	14.	32.	11.
X; 44	*0; 0*	45.	1414.	16.	24.	4.
X:4 Nondisjunction						
0; 0	*XY; 44*	9.	619.	2.	8.	1.
XX; 44	*0; 0*	4.	934.	7.	10.	1.
0; 44	*XY; 0*	6.	1066.	4.	21.	4.
XX; 0	*0; 44*	4.	647.	1.	15.	3.
Total Progeny		27910.	21661.	715.	536.	606.
Adjusted Total		28085.	28828.	748.	663.	642.
% Nullo-*X*		0.51	23.45	4.28	17.8	6.54
% Diplo-*X*		0.74	26.27	4.55	20.51	4.67
Total % *X* Nondisjunction		**1.25**	**49.72**	**8.82**	**38.31**	**11.21**
% Nullo-*4*		0.41	14.51	2.81	10.86	3.12
% Diplo-*4*		0.52	25.63	6.95	17.8	3.89
Total % *4*th Chromosome Nondisjunction		**0.93**	**40.15**	**9.76**	**28.66**	**7.01**

4.5 Dissecting the conserved regions proximal to the SAM domain of Mtrm via alanine-scanning mutagenesis

In order to identify conserved Mtrm residues that are required for homologous achiasmate segregation, we performed an alanine-scanning mutagenesis of the two blocks of conservation proximal to the SAM domain. Specifically, we mutated residues within the STP region, which contains a canonical Polo PBD binding motif surrounded by a larger region of evolutionary conservation and the region of conservation just proximal to the C-terminal SAM domain (see Figure 1-2). The results from our mutational analysis by Y2H in Chapters 2 and *in vivo* in the fly (Chapter 3) suggest that in addition to the canonical PBD binding motif, other residues within these regions of Mtrm play a role in its physical interaction with Polo. Additionally, analysis of post-translational modifications (PTM) on Mtrm demonstrated that, in addition to MtrmT40, MtrmS48 and MtrmS52 are phosphorylated in the fly [60]. Together, these observations raise the possibility that, in addition to residues falling within the canonical PBD binding motif (S-T^{40}-P), other conserved residues may be required for Mtrm function.

Using the same approach for assaying achiasmate NDJ as described above, we first examined the functional role of the S-T^{40}-P sequence itself. As shown in Table 4-4, our results suggest that only the last two residues of the S-T^{40}-P PBD binding site are required for Mtrm function. Expression of a MtrmS39A mutant disrupting the serine at the – 1 position relative to the central

threonine within the PBD binding motif fully rescued the meiotic defect relative to the Full-length (FL) Mtrm control, while expression of a MtrmT40A mutant or a MtrmP41A mutant were unable to rescue the meiotic defect observed in *nanos-GAL4-mtrm*^{126}/+ heterozygote females (Table 4-4). The fact that the mutant MtrmS39A protein is functional with regard to homologous achiasmate segregation is somewhat surprising, as the serine at the – 1 position has been predicted to be absolutely required for interaction with the PBD [46,54]. However, as noted in Chapter 1, cases also exist where PBD binding sites have been defined that lack a serine at the –1 position relative to the phosphorylatable residue [55].

We expanded our analysis to include other conserved residues both within and surrounding the STP region. Of the 26 amino acids we mutated to alanine between positions 29 and 66 (including the S-T^{40}-P residues), 15 point mutants appeared to fully rescue Mtrm function relative to the FLMtrm control. 3 mutants appeared to partially rescue Mtrm function (MtrmV31A, MtrmV36A, and MtrmF46A), and 8 mutants failed to rescue functionality as assayed by homologous achiasmate segregation (MtrmT40A, MtrmP41A, MtrmS48A, MtrmP49A, MtrmL51A, MtrmS52A, MtrmP53A and MtrmI54A) (Table 4-4).

An additional 10 conserved residues proximal to the SAM domain were examined. MtrmE141 and MtrmN151 appear to be critical for function as assayed by homologous achiasmate segregation (Table 4-4). Taken together, these results indicate that multiple Mtrm residues appear critical for homologous chromosome segregation.

Table 4-4 Detailed segregational effects of amino acid to alanine Mtrm mutants expressed in females heterozygous for a null allele of *mtrm.*

FM7/X; spa^{pol} females containing a recombinant third chromosome with both *nanos-GAL4* and *mtrm*^{126} expressing mutant versions of *mtrm* where conserved amino acids are individually mutated to alanine are tested for their ability to function as assayed by homologous achiasmate segregation

[a] Transgenes expressed in a *FM7/X; nanos-GAL4-mtrm*^{126}*/+; spa*^{pol} background.

Table 4-4

Oocyte genotype	Paternal genotype	*V36A*[a]	*R37A*[a]	*C38A*[a]	*S39A*[a]	*T40A*[a]	*P41A*[a]	*I42A*[a]	*F43A*[a]	*G44A*[a]
Normal										
X; 4	*XY; 44*	616.	511.	448.	517.	178.	379.	447.	356.	494.
X; 4	*0; 44*	549.	312.	277.	194.	118.	305.	353.	259.	299.
X Nondisjunction										
0; 4	*XY; 44*	42.	0.	7.	6.	41.	45.	5.	2.	6.
XX; 4	*0; 44*	61.	3.	15.	7.	37.	84.	11.	4.	8.
4[th] Chromosome Nondisjunction										
X; 0	*XY; 44*	74.	39.	21.	19.	27.	66.	7.	11.	16.
X;0	*0;44*	39.	12.	7.	9.	17.	13.	4.	6.	6.
X; 44	*XY; 0*	120.	88.	38.	11.	53.	63.	11.	19.	33.
X; 44	*0; 0*	70.	32.	17.	2.	43.	39.	9.	17.	12.
X:4 Nondisjunction										
0; 0	*XY; 44*	19.	1.	1.	1.	21.	73.	1.	0.	1.
XX; 44	*0; 0*	34.	0.	2.	0.	13.	23.	3.	0.	2.
0; 44	*XY; 0*	16.	0.	2.	3.	8.	11.	1.	1.	1.
XX; 0	*0; 44*	12.	0.	6.	0.	17.	17.	1.	1.	3.
Total Progeny		1652.	998.	841.	769.	573.	1118.	853.	676.	881.
Adjusted Total		1836.	1002.	874.	786.	710.	1371.	875.	684.	902.
% Nullo-*X*		8.39	0.2	2.29	2.54	19.72	18.82	1.6	0.88	1.77
% Diplo-*X*		11.66	0.6	5.26	1.78	18.87	18.09	3.43	1.46	2.88
Total % *X* Nondisjunction		**20.04**	**0.8**	**7.55**	**4.33**	**38.59**	**36.91**	**5.03**	**2.34**	**4.66**
% Nullo-*4*		9.53	5.29	4.81	3.82	16.9	18.89	1.71	2.78	3.33
% Diplo-*4*		15.8	11.98	7.21	2.42	19.44	12.4	3.2	5.56	5.65
Total % *4*[th] Chromosome Nondisjunction		**25.33**	**17.27**	**12.01**	**6.23**	**36.34**	**31.29**	**4.91**	**8.33**	**8.98**

Table 4-4 *(cont.)*

Oocyte genotype	Paternal genotype	*V36A*[a]	*R37A*[a]	*C38A*[a]	*S39A*[a]	*T40A*[a]	*P41A*[a]	*I42A*[a]	*F43A*[a]	*G44A*[a]
Normal										
X; 4	*XY; 44*	616.	511.	448.	517.	178.	379.	447.	356.	494.
X; 4	*0; 44*	549.	312.	277.	194.	118.	305.	353.	259.	299.
X Nondisjunction										
0; 4	*XY; 44*	42.	0.	7.	6.	41.	45.	5.	2.	6.
XX; 4	*0; 44*	61.	3.	15.	7.	37.	84.	11.	4.	8.
4[th] Chromosome Nondisjunction										
X; 0	*XY; 44*	74.	39.	21.	19.	27.	66.	7.	11.	16.
X;0	*0;44*	39.	12.	7.	9.	17.	13.	4.	6.	6.
X; 44	*XY; 0*	120.	88.	38.	11.	53.	63.	11.	19.	33.
X; 44	*0; 0*	70.	32.	17.	2.	43.	39.	9.	17.	12.
X:4 Nondisjunction										
0; 0	*XY; 44*	19.	1.	1.	1.	21.	73.	1.	0.	1.
XX; 44	*0; 0*	34.	0.	2.	0.	13.	23.	3.	0.	2.
0; 44	*XY; 0*	16.	0.	2.	3.	8.	11.	1.	1.	1.
XX; 0	*0; 44*	12.	0.	6.	0.	17.	17.	1.	1.	3.
Total Progeny		1652.	998.	841.	769.	573.	1118.	853.	676.	881.
Adjusted Total		1836.	1002.	874.	786.	710.	1371.	875.	684.	902.
% Nullo-*X*		8.39	0.2	2.29	2.54	19.72	18.82	1.6	0.88	1.77
% Diplo-*X*		11.66	0.6	5.26	1.78	18.87	18.09	3.43	1.46	2.88
Total % *X* Nondisjunction		**20.04**	**0.8**	**7.55**	**4.33**	**38.59**	**36.91**	**5.03**	**2.34**	**4.66**
% Nullo-*4*		9.53	5.29	4.81	3.82	16.9	18.89	1.71	2.78	3.33
% Diplo-*4*		15.8	11.98	7.21	2.42	19.44	12.4	3.2	5.56	5.65
Total % *4*[th] Chromosome Nondisjunction		**25.33**	**17.27**	**12.01**	**6.23**	**36.34**	**31.29**	**4.91**	**8.33**	**8.98**

Table 4-4 *(cont.)*

Oocyte genotype	Paternal genotype	*N45A*[a]	*F46A*[a]	*R47A*[a]	*S48A*[a]	*P49A*[a]	*N50A*[a]	*L51A*[a]	*S52A*[a]	*P53A*[a]	*I54A*[a]
Normal											
X; 4	*XY; 44*	330.	306.	352.	49.	155.	370.	188.	241.	265.	120.
X; 4	*0; 44*	222.	213.	266.	43.	135.	202.	152.	165.	209.	118.
X Nondisjunction											
0; 4	*XY; 44*	9.	22.	10.	10.	32.	9.	48.	39.	37.	43.
XX; 4	*0; 44*	7.	35.	13.	21.	43.	11.	38.	47.	59.	34.
4[th] Chromosome Nondisjunction											
X; 0	*XY; 44*	13.	25.	21.	10.	47.	18.	35.	42.	40.	22.
X;0	*0;44*	1.	9.	9.	9.	28.	4.	20.	22.	20.	26.
X; 44	*XY; 0*	11.	29.	30.	16.	56.	16.	62.	99.	61.	32.
X; 44	*0; 0*	14.	28.	9.	7.	42.	3.	38.	39.	53.	32.
X:4 Nondisjunction											
0; 0	*XY; 44*	3.	13.	6.	6.	15.	8.	19.	16.	22.	16.
XX; 44	*0; 0*	2.	12.	2.	12.	31.	2.	9.	19.	18.	19.
0; 44	*XY; 0*	2.	7.	0.	1.	16.	1.	27.	21.	20.	13.
XX; 0	*0; 44*	2.	4.	4.	0.	9.	6.	14.	20.	9.	12.
Total Progeny		616.	703.	722.	184.	609.	650.	650.	770.	813.	487.
Adjusted Total		641.	796.	757.	234.	755.	687.	805.	932.	978.	624.
% Nullo-*X*		4.37	10.55	4.23	14.53	16.69	5.24	23.35	16.31	16.16	23.08
% Diplo-*X*		3.43	12.81	5.02	28.21	21.99	5.53	15.16	18.45	17.59	20.83
Total % *X* Nondisjunction		**7.8**	**23.37**	**9.25**	**42.74**	**38.68**	**10.77**	**38.51**	**34.76**	**33.74**	**43.91**
% Nullo-*4*		3.74	8.54	6.61	13.25	16.29	7.28	15.03	14.59	12.47	16.67
% Diplo-*4*		5.15	11.93	5.68	20.94	25.43	3.64	21.37	23.39	19.43	20.51
Total % *4*[th] Chromosome Nondisjunction		**8.89**	**20.48**	**12.29**	**34.19**	**41.72**	**10.92**	**36.4**	**37.98**	**31.9**	**37.18**

Table 4-4 *(cont.)*

Oocyte genotype	Paternal genotype	*S66A*[a]	*S129N*[a]	*S137A*[a]	*E141A*[a]	*S142A*[a]	*R143A*[a]	*R145A*[a]	*S146A*[a]	*N151A*[a]	*H152A*[a]	*S153A*[a]
Normal												
X; 4	*XY; 44*	398.	335.	510.	235.	1075.	24.	387.	133.	164.	314.	266.
X; 4	*0; 44*	345.	228.	351.	172.	693.	30.	193.	89.	137.	214.	182.
X Nondisjunction												
0; 4	*XY; 44*	18.	11.	7.	53.	26.	1.	8.	4.	62.	15.	5.
XX; 4	*0; 44*	27.	18.	8.	77.	27.	0.	16.	5.	82.	22.	4.
4[th] Chromosome Nondisjunction												
X; 0	*XY; 44*	36.	30.	31.	43.	45.	3.	8.	12.	29.	31.	11.
X;0	*0;44*	21.	8.	10.	24.	20.	2.	1.	5.	22.	8.	1.
X; 44	*XY; 0*	61.	46.	44.	76.	59.	2.	19.	7.	65.	26.	18.
X; 44	*0; 0*	50.	22.	22.	58.	36.	2.	4.	5.	35.	12.	5.
X:4 Nondisjunction												
0; 0	*XY; 44*	1.	4.	5.	28.	10.	0.	5.	0.	24.	5.	7.
XX; 44	*0; 0*	4.	7.	7.	24.	4.	0.	3.	0.	15.	7.	5.
0; 44	*XY; 0*	3.	4.	4.	31.	8.	0.	0.	0.	30.	5.	2.
XX; 0	*0; 44*	3.	3.	3.	30.	10.	0.	0.	0.	20.	2.	2.
Total Progeny		967.	716.	1002.	851.	2013.	64.	644.	260.	685.	661.	508.
Adjusted Total		1023.	763.	1036.	1094.	2098.	65.	676.	269.	918.	717.	533.
% Nullo-*X*		4.3	4.98	3.09	20.48	4.19	3.08	3.85	2.97	25.27	6.97	5.25
% Diplo-*X*		6.65	7.34	3.47	23.95	3.91	0.	5.62	3.72	25.49	8.65	4.13
Total % *X* Nondisjunction		**10.95**	**12.32**	**6.56**	**44.42**	**8.1**	**3.08**	**9.47**	**6.69**	**50.76**	**15.62**	**9.38**
% Nullo-*4*		6.35	6.82	5.5	16.73	5.	7.69	2.81	6.32	15.14	7.39	5.63
% Diplo-*4*		12.22	11.8	8.49	22.3	5.67	6.15	4.29	4.46	20.7	8.65	6.94
Total % *4*[th] Chromosome Nondisjunction		**18.57**	**18.61**	**14.**	**39.03**	**10.68**	**13.85**	**7.1**	**10.78**	**35.84**	**16.04**	**12.57**

4.6 Discussion

The results described in this Chapter demonstrate that evolutionarily conserved residues appear to be sufficient for Mtrm function in the context of homologous achiasmate segregation. A strong correlation appears to exist between the ability of different versions of Mtrm to rescue chromosome segregation defects and their physical interaction with Polo, which was discussed in Chapters 2 and 3. Mutants able to bind Polo also rescued achiasmate NDJ, while mutants that failed to interact with Polo resulted in high levels of achiasmate NDJ. The MtrmSAMDEL construct there is only exception to this correlation. While required for robust physical interaction, MtrmSAMDEL appears dispensable in the context of homologous chromosome segregation. Therefore we propose that the interaction between Mtrm and Polo is first established by residues proximal to the SAM domain, which is sufficient for function as assayed by homologous achiasmate segregation, but that maintenance of this interaction must also involve the C-terminal SAM domain, which may be required for some other meiotic process (discussed in Chapter 5).

The data described in this chapter suggest that the transient establishment of interaction between Mtrm and Polo that is required for homologous chromosome segregation is in part due MtrmT40 and its corresponding proline, MtrmS48 and its corresponding proline, and a four amino acid sequence spanning MtrmL51 to MtrmI54 (which includes MtrmS52 and its corresponding

proline). Since MtrmT40, MtrmS48 and MtrmS52 are all phosphorylated, it seems likely that phosphorylation regulates binding between Mtrm and Polo.

The identity of those kinases that phosphorylate MtrmT40A, MtrmS48A and MtrmS52A remains unclear, but the fact that each phosyporylatable residue is followed by a proline suggests the task is performed by a proline directed kinases such as Cdk5, Cdk1 or MAPK kinases as predicted by the NetPhosK algorithm [62]. Furthermore, the inability of MtrmP41A, MtrmP49A or MtrmP53A to rescue the defects in chromosome segregation could be interpreted in two ways: it could mean that phosphorylation at each corresponding phosphorylatable serine or threonine is critical for function and may indeed depend upon proline-directed kinase phosphorylation or that disruption of these prolines may simply affect the protein structurally.

Since phosphorylation at these sites likely plays a role in Mtrm function, we examined the functionality of the phospho-mimic mutants MtrmT40E, MtrmS48E, and MtrmS52E with respect to homologous achiasmate segregation. None of the phospho-mimic Mtrm mutants were able to rescue functionality (data not shown). These data suggest that either the phospho-mimetic was not successful or perhaps that phosphorylation at MtrmT40, MtrmS48 and MtrmS52 must be dynamic for proper protein functionality.

Finally, we demonstrate that residues that fall within the region of conservation just proximal to the SAM domain also appear critical for Mtrm

function. Whether or not these mediate a transient interaction between Mtrm and Polo remains unclear, but it appears that many levels of complexity remain to be elucidated regarding Mtrm functionality.

4.7 Acknowledgments

Many thanks to Jenny Chisholm, Amanda Wilson and Kavya Nandanan for assistance with subcloning, scoring of nondisjunction, and fly husbandry. Thank you to Cathleen Lake for the helpful comments and suggestions, Genetic services, Inc. for the embryo injections and the Stowers Molecular Biology core facililty for help with site-directed mutagenesis.

4.8 Materials and Methods

Site directed mutants and fly transgenes were generated as described in Chapter 3.

Drosophila stocks

Throughout this chapter, *y w ; spa*^{pol} was used as the wild-type strain. For achiasmate *X* chromosome studies, *y w/FM7* was used as our wild-type control, and a recombinant version of chromosome *3* where the *nanos-GAL4* driver and *mtrm*^{126} were recombined together [60]. The deficiency stock *Df(3L)66C-T2-T10* [59], and the mutant *polo* alleles, *polo*^{KG03033} and *polo*$^{16-1}$ (available from the Bloomington *Drosophila* Stock Center), were used for the co-suppression assays.

Achiasmate Chromosome NDJ assays

Transgene-bearing males from each transgenic line were crossed to *y w ; spa^{pol}* and resulting *y w ; transgene/+ ; spa^{pol}* females were then crossed to either *FM7/y+Y ; nanos-GAL4-mtrm^{126} ; spa^{pol}* males or *FM7/y+Y ; nanos-GAL4 ; spa^{pol}* males to generate *y w/FM7 ; transgene/+ ; nanos-GAL4-mtrm^{126}/+ ; spa^{pol}* tester females or *y w/FM7 ; transgene/+ ; nanos-GAL4/+ ; spa^{pol}* tester females. Corresponding internal control female siblings of the same genotype but lacking the transgene were also collected and tested for each case, and those internal controls are reflected cumulatively. For each line, we scored at least 10 such tester females individually crossed to *attached –XY, y+ v f B; C(4), ci ey^{R}* males, and assessed the frequency of *X* chromosome nondisjunction at meiosis I as described in [59,76].

Chapter 5. Residues and regions of Mtrm critical for proper oocyte development

5.1 Introduction

With the exception of the MtrmSAMDEL mutant, the results presented in Chapters 2, 3 and 4 suggest a strong correlation between the ability of various mutant versions of Mtrm to physically interact with Polo and their ability to rescue homologous achiasmate segregation defects in *mtrm* heterozygotes. By in large, mutants able to interact with Polo kinase also rescued achiasmate NDJ, while mutants that failed to bind Polo resulted in high levels of chromosome mis-segregation. However, analysis of the MtrmSAMDEL mutant revealed that while the C-terminal SAM domain is required together with specific Mtrm residues for robust physical interaction with Polo, it is dispensable in the context of chromosome segregation. Taken together, these observations suggest that a transient interaction between the region proximal to the SAM domain of Mtrm and Polo may be sufficient for the process of homologous achiasmate segregation. But what, then, is the purpose of the robust interaction observed between Mtrm and Polo during *Drosophila* female meiosis?

This chapter addresses this question by examining whether our series of site-specifically integrated *mtrm* transgenes rescue the failure of fertilized eggs to hatch from females completely lacking endogenous *mtrm*, —a phenotype initially reported in 2003 [59]. The defect in egg hatchability is not definitively linked to

Polo kinase mis-regulation. However, previous work has demonstrated that females lacking sufficient doses of *mtrm* exhibit a dosage-dependent early onset of nuclear envelope breakdown (NEB) that is suppressed by simultaneous reduction of the *polo* gene [60]. Precocious NEB at this stage may result in release of an incompletely or inappropriately re-compacted karyosome—a spherical cluster that meiotic chromosomes form within the oocyte nucleus that is thought to normally facilitate proper spindle formation following NEB. Consistent with this view, *mtrm* heterozygotes also exhibit karyosome defects both before and after NEB that can be rescued by simultaneous reduction in the *polo* gene [60]. Intriguingly, abnormal karyosome morphology is highly correlated with female sterility [90,91]. Therefore, the sterility observed in females lacking *mtrm* could be due karyosome defects so severe that the oocyte is unable to recover and build a spindle. Alternatively, early onset of NEB could also cause other deleterious problems for the chromosomes of the oocyte related to the lack of or persistence of incorrect cell cycle factors present or absent at that time.

5.2 Components of all three conserved regions of Mtrm are required for proper oocyte development

In order to determine whether our mutant versions of *mtrm* are able to rescue the sterility observed in females lacking endogenous *mtrm*, we introduced our transgenes into females trans-heterozygous for two null alleles of *mtrm*: the *nanos-GAL4, mtrm*^{126} chromosome and a deficiency that uncovers the *mtrm* gene (*Df(3L)66C-T2-T10*). As a negative internal control, we also tested siblings

lacking the transgene from each cross confirm the sterility phenotype. The results of this analysis are shown in Table 5.1. In general, the data demonstrate a strong correlation between the ability of specific Mtrm mutants to physically interact with Polo with their ability to rescue sterility in *mtrm* trans-heterozygotes. Components of all three regions of evolutionary conservation—the STP region, the region proximal to the SAM domain, and the C-terminal SAM domain are critical for fertility. We interpret these data to mean that robust physical interaction between Mtrm and Polo is required for female fertility, perhaps by facilitating proper maintenance of karyosome morphology and/or ensuring proper timing of NEB.

Table 5-1 Fertility screen of Mtrm truncations and amino acid to alanine Mtrm mutants expressed in females lacking endogenous *mtrm.*

Females trans-heterozygous for the *nanos-GAL4, mtrm*^{126} chromosome and a deficiency that uncovers the *mtrm* gene (*Df(3L)66C-T2-T10*) expressing *mtrm* transgenes with the indicated mutations were screened for fertility. Siblings from each cross lacking the transgene were used as internal controls.

	FLMtrm	**STPDEL**	**SAMDEL**	L29A	V31A	N32A	T33A	S34A	N35A	V36A	R37A	C38A	S39A	**T40A**	**P41A**	I42A	F43A	G44A	N45A	F46A	R47A	**S48A**	**P49A**	N50A	**L51A**	**S52A**	**P53A**	**I54A**	S66A	S129N	S137A	E141A	S142A	R143A	**R144A**	R145A	S146A	**N151A**	H152A	S153A
Transgene	+	-	-	+	+	+	+	+	+	+	+	+	+	-	-	+	+	+	+	+	+	-	-	+		-	-	-	+	+	+	+	+	+	-	+	+	-	-	+
No Transgene	-	-	-	-	-	-	-	-	-	-	-	-	-	-	-	-	-	-	-	-	-	-	-	-	-	-	-	-	-	-	-	-	-	-	-	-	-	-	-	-

In addition to examining this phenotype in a *mtrm* null background, we were also interested in knowing whether *mtrm* heterozygotes displayed reduced fertility. We determined egg hatchability rates from females of the following genotypes *w1118* (control), *y w ; nanos-GAL4, mtrm*^{126}*/+* and various *mtrm*

transgenes in a *y w ; nanos-GAL4*, *mtrm*^{126}*/(Df(3L)66C-T2-T10)* background (Table 5-2). Perhaps not surprisingly, the fertility of *mtrm* heterozygotes was reduced by approximately half compared to wild type. This finding is consistent with previous work that demonstrated that *mtrm* heterozygotes displayed defects in both proper timing of NEB and maintenance of karyosome architecture [60]. Perhaps the NEB and/or karyosome defects lead to a reduced egg hatch rate. In a *mtrm* null background, introduction of a 3XFLAG-FLMtrm transgene rescues the defects in fertility to a rate similar to that of the *mtrm* heterozygotes. Importantly, consistent with our general screen, neither point mutations in key Mtrm residues nor deletion of the C-terminal SAM domain restores fertility.

Table 5-2 Egg Hatchability rates of females heterozygous for a null allele of *mtrm* and of key Mtrm mutants expressed in females lacking endogenous *mtrm*.

Egg hatch rates were determined for the genotypes listed below

Maternal genotype	Egg Hatchability %	N
w1118	96	113
nanos-GAL4, mtrm^{126}*/+*	57	341
3XFLAGMtrm; nanos-GAL4-mtrm^{126}*/Df(3L)66CT2-T10*	52.5	206
3XFLAGMtrmSAMDEL; nanos-GAL4-mtrm^{126}*/Df(3L)66CT2-T10*	0	100
3XFLAGMtrmSTPDEL; nanos-GAL4-mtrm^{126}*/Df(3L)66CT2-T10*	0	100

5.3 Discussion

The results described in this chapter suggest that we have identified a separation-of-function mutant involving the C-terminal SAM domain of Mtrm. While dispensable for homologous achiasmate segregation, the C-terminal SAM domain appears critical for proper oocyte development as assayed by its inability

to rescue female fertility in a *mtrm* trans-heterozygote background. Females heterozygous for a null allele of *mtrm* display both improper timing of NEB and abnormal karyosome morphology, which is highly correlated with female sterility. Hence, we speculate that the sterility observed in females trans-heterozygous for *mtrm* may be due to severe, irreversible karyosome defects and/or early onset of NEB resulting in the release of an improperly compacted karyosome that cannot recover. Because these phenotypes are in fact observed in *mtrm* heterozygotes and both can be rescued by simultaneously decreasing the dosage of *polo* [60], we speculate that the sterility observed in females lacking *mtrm* may be linked to Polo mis-regulation.

Several conserved Mtrm residues proximal to the SAM domain in addition to the SAM domain itself are required together for robust interaction with Polo *in vivo*. We speculate that this robust interaction between Mtrm and Polo is necessary for maintenance of the karyosome, and complete failure of physical interaction with Polo results in karyosome instability and sterility. However, future studies to address this will be necessary. We propose that the interaction between Mtrm and Polo is first established by residues proximal to the SAM domain, which is sufficient for function as assayed by homologous achiasmate segregation. However, maintenance of this interaction must also involve the C-terminal SAM domain, which may be required for some other meiotic process such as karyosome maintenance as speculated in this chapter.

5.4 Acknowledgments

Many thanks to Jennifer Chisholm and Amanda Wilson of the Hawley Lab who performed many of the necessary crosses in order to determine the functionality of our series of *mtrm* mutants as assayed by female fertility and egg hatchability.

5.5 Materials and Methods

Fertility assays

To screen for the ability of our mutant lines to rescue sterility, transgene-bearing females from each transgenic line also balanced for Chromosome *3* were crossed to *y w/y+Y ; Df(3L)66C-T2-10/TM3 ; spa*^{pol} males. Resulting *y w ; transgene/+ ; Df(3L)66C-T2-10/TM3 ; spa*^{pol} females were then crossed to y w*/y+Y ; nanos-GAL4, mtrm*^{126} *; spa*^{pol} males to generate *y w; transgene/+ ; nanos-GAL4, mtrm*^{126}*/ Df(3L)66C-T2-10; spa*^{pol} tester females and *y w ; nanos-GAL4-mtrm*^{126}*/ Df(3L)66C-T2-10; spa*^{pol} control siblings. At least 10 females per genotype per mutant line were placed in vials with wild type *w*^{1118} males, and fertility was determined 7 days later by presence or absence of larvae.

Egg hatchability assays

To determine egg hatch rate, tester females either with or without a *mtrm* transgene in a *nanos-GAL4, mtrm*^{126}*/Df(3L)66C-T2-10* trans-heterozygote background were yeasted and placed with wild type males for 2 days. Males and

females were then placed in grape plate cages and allowed to lay eggs for 8 hours, at which point the adults were removed and the eggs were counted. Two days later unhatched eggs were counted.

Chapter 6. Conclusions, Perspectives and Future Directions

This thesis examines the detailed mechanism by which Mtrm physically interacts with Polo kinase to regulate Polo function during *Drosophila* female meiosis to ensure proper homologous achiasmate segregation and oocyte development. We are interested in understanding the nature of this interaction, since a more complex view of how Polo kinase is controlled by its protein partners has recently emerged. This view is consistent with the observation that Polo kinase promotes a diverse set of molecular events during cell division—likely a consequence of its complex regulation as exemplified by the sheer number of regulatory partners that have been discovered and the varied mechanisms of interaction that have been found. From a clinical standpoint, understanding the intricacies of post-translational Polo kinase regulatory interactions may help drive innovative strategies for targeted Polo kinase inhibition in cancer cells.

Previous work demonstrated that a physical interaction exists between Mtrm and Polo involving the central residue of a Polo PBD binding motif within Mtrm [60]. This led to the speculation that Mtrm and Polo may engage in a canonical mechanism of interaction, where phosphorylation of the central residue, MtrmT40, allows for subsequent Polo PBD binding through a well characterized positively charged cleft at the interface of the two C-terminal Polo

boxes, PB1 and PB2, mediated by two residues essential for PBD selectivity—namely PoloH518 and PoloK520. Post-translational modification (PTM) analysis of Mtrm supported this view, as MtrmT40 is phosphorylated at high levels in the fly ovary. However, PTM analysis also demonstrated that other absolutely conserved residues are also phosphorylated at high levels *in vivo,* including MtrmS48 and MtrmS52. These observations raise the intriguing possibility that additional sites play a role in mediating the physical interaction between Mtrm and Polo. Since these residues may be phosphorylated by a distinct kinase, regulation of Polo binding due to phosphorylation of these residues adds an additional layer of complexity to the control of meiotic processes by Polo. Furthermore, little was known about the functionality of the C-terminal SAM domain of Mtrm, specifically whether it played a role in mediating the physical interaction with Polo or other proteins (including Mtrm itself), or whether it mediated some other role independent of Polo binding during *Drosophila* female meiosis.

Prior work also demonstrated that *mtrm* and *polo* were genetically linked, and that this interaction was important for ensuring proper homologous achiasmate segregation and oocyte development [60]. Interestingly, these phenotypes were possibly separable, albeit both potentially Polo-mediated. However, a separation-of-function mutant allele of *mtrm* or *polo* had not been identified, and it remained unknown as to whether disruption of chromosome segregation results in defects in oocyte development or vice versa. Alternatively,

the phenotypes observed in *mtrm* and *polo* mutants may simply reflect the dependency of the two pathways.

The results presented in this thesis have shed light on a number of these questions. First, we demonstrate that Mtrm may engage in a novel mechanism of interaction with Polo kinase. Not only are additional Mtrm residues such as MtrmS48 and Mtrm52 required for robust physical interaction with Polo kinase, but Mtrm may interact with Polo kinase by a novel mechanism that fails to be perturbed by ablation of Polo residues known to be required for canonical PBD specificity. This finding is reminiscent of a report that describes the interaction between Dbf4 and the yeast Polo homolog, Cdc5 [56]. However, unlike the Dbf4-Cdc5 interaction, the Mtrm-Polo interaction appears to be phospho-dependent.

Second, we have made several interesting findings regarding the functionality of the C-terminal SAM domain of Mtrm. We demonstrate that at least one role of the SAM domain is to mediate the vast majority of protein-protein interactions observed during *Drosophila* female meiosis as identified by MudPIT analysis. The SAM domain also appears critical for the physical interaction of Mtrm with Polo. Furthermore, we present the first evidence that Mtrm may interact with itself via the SAM domain and speculate that perhaps this self-interaction may play a role in the ability of Mtrm to robustly interact with Polo kinase and/or Mtrm's role in oocyte development. Further experiments are necessary to elucidate whether this is the case. In a general sense, the

interaction between Mtrm and Polo can be considered to join a growing list of regulatory proteins including Map205, Dbf4 and Bora, which interact with Polo via some non-canonical mechanism (see Figure 6-1 for working model).

Finally, we were able to identify a separation-of-function allele of *mtrm* that involves the SAM domain. While dispensable for proper chromosome segregation, this domain is critical for oocyte development, raising an entirely new array of intriguing questions regarding Mtrm function during *Drosophila* female meiosis. Additionally, the identification of a separation-of-function mutant

Figure 6-1 A working model for how Mtrm may regulate Polo kinase through physical interaction.

Depicted is a working model to explain the relationship between Mtrm and Polo and how they may coordinate homologous achiasmate segregation and proper oocyte development during Drosophila female meiosis. The affinity for Polo to Mtrm is first initiated by the region proximal to the C-terminal SAM domain. This transient interaction is sufficient for ensuring proper homologous achiasmate segregation. It is also a necessary step for allowing the subsequent more robust physical interaction facilitated by the C-terminal SAM domain, which is required for proper oocyte development as assayed by female fertility.

could potentially be an extremely useful tool for elucidating the mechanisms by which Polo can activate different pathways at different times during cell division. We have recently begun fluorescence cross-correlation studies of fluorescently labelled versions of Mtrm, including a truncated version of Mtrm that deletes the SAM domain, and Polo expressed under their respective native promoters in the fly germline. Due to the anatomy of the *Drosophila* ovariole and distinct morphology of oocytes at different stages of development, we will be able to examine the physical interaction between Mtrm and Polo throughout meiotic progression—identifying the exact stage when Mtrm and Polo appear to interact, as well as to potentially be able to detect more transient interactions that might otherwise go unidentified between Polo and Mtrm. These experiments and others will certainly further our understanding of the mechanism of the interaction between Mtrm and Polo.

6.1 Unravelling the intricate Mtrm regulation of Polo with simple yeast

The first evidence demonstrating that Mtrm may interact with Polo by a non-canonical mechanism came from our Y2H studies. Indeed, the fact that our findings in yeast largely correlate with our findings in the fly support the view that heterologous expression of Mtrm and Polo in yeast is a valid method for future studies of the mechanism of interaction between these two proteins. Furthermore, while mutational studies of Polo kinase in the fly are ongoing, the

analogous studies in yeast presented here can be used to predict the probable outcomes of those experiments.

Pending the correlation of those outcomes and given the relative speed of the system, it would be feasible to consider returning to Y2H as a means to dissect at a finer scale the residues and regions of both Mtrm and Polo that are critical for their physical interaction. Incorporating the point mutations discussed in this work would provide additional opportunities by which to confirm that the data collected using these two systems are largely congruent. Furthermore, it would be advantageous to utilize the Y2H as a rapid means to perform additional truncation analyses in parallel. These analyses may identify more precisely the regions of Polo and Mtrm that are capable of interacting. These experiments may give rise to likely candidates for post-translational modifications or identify novel regulatory domains through a scanning mutagenesis approach. However, this type of approach is not without caveats. The strategy to replace any residue with an alanine or remove peptide stretches may grossly alter the overall structure of the protein. At least for Mtrm, this caveat may be minimized, as much of the protein is predicted to be intrinsically unstructured. We may also fail to predict important aspects of regulation if the molecular mechanisms responsible for some post-translational modifications do not occur properly in S. cerevisiae; our observation that MtrmT40 is not phosphorylated in yeast exemplifies this point. However, the fact that the yeast system was able to accurately predict virtually all of the important binding interactions between Mtrm and Polo that we

later verified in the fly demonstrates the utility of the Y2H system for rapid screening and analysis of Mtrm and Polo binding

6.2 *In vivo* studies of Mtrm and Polo associations

While the yeast system was valuable to understand the fundamentals of the Mtrm-Polo interaction, it was essential to validate and extend our findings within the context *Drosophila* female meiosis. We did this by extensive proteomic analysis of Mtrm, and our proteomic results of Mtrm posed interesting questions in addition to validating the interaction between Mtrm and Polo characterized via the Y2H assay. While our MudPIT analysis of Mtrm expressed in *S. cerevisiae* exposed no new protein partners, albeit that Mtrm was expressed in the absence of *Drosophila* Polo. Mass spectroscopy of samples purified from transgenic flies indicated that Mtrm-Polo intermingle with an array of complexes. What is the significance of each of these associations? Are they required for the correct folding of Mtrm and Polo, either as separate identities or together as a joint complex? Do they act as co-activators or inhibitors stimulating/hindering a specific activity (and what is that activity)? Or does the Mtrm-Polo complex somehow modulate their cellular roles? For example, PLGEM analysis of Mtrm purified from the fly ovary revealed that only four proteins co-purified with a p value of less than or equal to .001—Polo kinase, Heat shock protein 23, Heat shock protein 26, and Heat shock protein 27. Are chaperones required to

facilitate the formation and/or stabilization of the Mtrm-Polo complex? These questions and others could be addressed in future studies.

In parallel to the experiments described in this thesis, we initiated the ground work for *in vitro* studies by establishing recombinant Mtrm and Polo expression in *Drosophila* Schneider (S2) cells as well as in the Sf9 cell – baculovirus system. Preliminary experiments for these approaches gave unanticipated results--Mtrm and Polo could be not co-purified from transfected S2 cell extract nor from a mixture of two Sf9 extracts, each from a single infection of either Mtrm or Polo. Consistent with trends seen by others using baculovirus for recombinant protein expression, a Mtrm-Polo complex could be isolated if insect cells were co-infected with both Mtrm and Polo containing virus. While encouraged by this outcome, we were puzzled when we could co-purify Polo with a several of Mtrm mutants including MtrmT40A and MtrmS48A that were predicted not to be binding partners in the Y2H assay or by MudPIT analysis and could not rescue achiasmic chromosome segregation defect nor sterility phenotype of *Drosophila mtrm* mutants.

If Mtrm-Polo interaction depends on the cell cycle, we may reconcile the seemingly incongruent observations described above. Transfection of S2 cells is performed when cells are highly confluent and hence expression of proteins occurs as confluency-induced cell cycle exit occurs or as they are arrested in G0/G1. Infection of Sf9 cells with baculovirus also halts growth of cells, but the cell cycle arrests in G2/M. In this light, Polo-associated Mtrm may be able to be

purified from starting material sourced from transfected *Drosophila* S2 cells that have been synchronised and are in G2/M.

6.3 Genetic screens to identify dominant suppressors of female sterility and homologous achiasmate segregation

We speculate that phosphorylation plays a key role in controlling the interaction between Mtrm and Polo. Additionally, other interactors likely play a role in facilitating the functional interaction between these two proteins. Identifying regulators that modify Mtrm or Polo thus facilitating their affinity for one another or other proteins that somehow play a role in mediating this interaction would elucidate another layer of Polo regulation as well as advance our efforts to examine *Drosophila* female meiotic processes such as homologous achiasmate segregation at a molecular level. One extremely powerful way to identify such regulators is to perform genetic screens for dominant suppressors of our phenotypes of interest. Because the homologous chromosome segregation defect is so severe in females heterozygous for a null allele of *mtrm*, one could feasibly design a screen to look for modifiers that suppresses this phenotype. Additionally, one could imagine performing a selection for suppressors of the oocyte development phenotype that results in eggs that do not hatch. Furthermore, it would be interesting to perform a selection that suppresses the sterility females lacking endogenous *mtrm* but containing MtrmSAMDEL mutant protein. Such a selection may identify interactors that are involved in the sterility defect but not the achiasmate NDJ phenotype.

The ease of screening for suppressors of sterility cannot be over stated. One caveat to this selection however, would be recovering non-specific suppressors. This could be circumvented by the use of appropriate secondary screens, such as examination of achiasmate NDJ in heterozygotes, which is a common phenotype in meiotic regulators and has been used extensively as a criterion for isolation of mutants that affect meiotic progression.

6.4 From yeast and flies to humans

We have an opportunity to look to nature for as a source of inspiration to solve problems faced by humans involving the fundamental process chromosome segregation. Here we examine Mtrm, a negative regulator of highly conserve Polo kinase during *Drosophila* female meiosis. Our hope is that these studies will eventually lead to new insights into the varied mechanisms of human Polo regulation and perhaps contribute to new and innovative strategies for targeted inhibition of Polo as an anti-cancer therapeutic.

In addition, aneuploidy is a critical issue in human reproductive biology. We have linked Polo regulation to the special process of homologous achiasmate segregation. Because Chromosome 21 in humans has been reported to fail to recombine at a much higher frequency than expected, we suspect that, like flies, human female meiosis also engages in homologous achiasmate segregation. Perhaps this system is perturbed as women age, leading to the observed increased rate of births of children with trisomy 21. This research raises many

questions. Although Mtrm orthologs have not been found in humans, does Polo kinase play a similar role in humans and if so, what regulatory protein plays the analogous role of Mtrm? Clearly, novel approaches are needed to address this question. However, using power of well-established model organisms such as yeast and fly, clever genetic analysis and cutting-edge proteomic technology will certainly drive us forward toward this end.

References

[1] Barr F. a, Silljé H. H. W., and Nigg E. a, 2004, “Polo-like kinases and the orchestration of cell division.,” Nature reviews. Molecular cell biology, **5**(6), pp. 429-40.

[2] Petronczki M., Lénárt P., and Peters J.-M., 2008, “Polo on the Rise-from Mitotic Entry to Cytokinesis with Plk1.,” Developmental cell, **14**(5), pp. 646-59.

[3] Archambault V., and Glover D. M., 2009, “Polo-like kinases: conservation and divergence in their functions and regulation.,” Nature reviews. Molecular cell biology, **10**(4), pp. 265-75.

[4] Lowery D. M., Lim D., and Yaffe M. B., 2005, “Structure and function of Polo-like kinases.,” Oncogene, **24**(2), pp. 248-59.

[5] Lane H. a, and Nigg E. a, 1996, “Antibody microinjection reveals an essential role for human polo-like kinase 1 (Plk1) in the functional maturation of mitotic centrosomes.,” The Journal of cell biology, **135**(6 Pt 2), pp. 1701-13.

[6] Spänkuch-Schmitt B., Bereiter-Hahn J., Kaufmann M., and Strebhardt K., 2002, “Effect of RNA silencing of polo-like kinase-1 (PLK1) on apoptosis and spindle formation in human cancer cells.,” Journal of the National Cancer Institute, **94**(24), pp. 1863-77.

[7] Wolf G., Solbach C., Loibl S., Knecht R., Stegmu M., Minckwitz G. V., Kaufmann M., and Strebhardt K., 2002, “Downregulation of human polo-like kinase activity by antisense oligonucleotides induces growth inhibition in cancer cells Birgit Spa,” Oncogene, pp. 3162-3171.

[8] Kappel S., Matthess Y., Zimmer B., Kaufmann M., and Strebhardt K., 2006, “Tumor inhibition by genomically integrated inducible RNAi-cassettes.,” Nucleic acids research, **34**(16), pp. 4527-36.

[9] Sunkel C. E., and Glover D. M., 1988, “polo, a mitotic mutant of Drosophila displaying abnormal spindle poles.,” Journal of cell science, **89 (Pt 1)**, pp. 25-38.

[10] Llamazares S., Moreira a, Tavares a, Girdham C., Spruce B. a, Gonzalez C., Karess R. E., Glover D. M., and Sunkel C. E., 1991, “polo encodes a protein kinase homolog required for mitosis in Drosophila.,” Genes & Development, **5**(12a), pp. 2153-2165.

[11] Strebhardt K., and Ullrich A., 2006, “for cancer therapy,” Cancer, **6**(April), pp. 321-330.

[12] Pawson T., and Nash P., 2003, “Assembly of cell regulatory systems through protein interaction domains.,” Science (New York, N.Y.), **300**(5618), pp. 445-52.

[13] Thompson S. L., Bakhoum S. F., and Compton D. a, 2010, “Mechanisms of chromosomal instability.,” Current biology : CB, **20**(6), pp. R285-95.

[14] Pavelka N., Rancati G., and Li R., 2010, “Dr Jekyll and Mr Hyde: role of aneuploidy in cellular adaptation and cancer.,” Current opinion in cell biology, **22**(6), pp. 809-815.

[15] Wolf G., Elez R., Doermer a, Holtrich U., Ackermann H., Stutte H. J., Altmannsberger H. M., Rübsamen-Waigmann H., and Strebhardt K., 1997, “Prognostic significance of polo-like kinase (PLK) expression in non-small cell lung cancer.,” Oncogene, **14**(5), pp. 543-9.

[16] Knecht R., Elez R., Oechler M., Solbach C., Ilberg C. V., and Strebhardt K., 1999, “Prognostic Significance of Polo-like Kinase (PLK) Expression in Squamous Cell Carcinomas of the Head and Neck Advances in Brief Prognostic Significance of Polo-like Kinase (PLK) Expression in Squamous Cell Carcinomas of the Head and Neck 1,” Cancer Research, pp. 2794-2797.

[17] Feng Y.-B., Lin D.-C., Shi Z.-Z., Wang X.-C., Shen X.-M., Zhang Y., Du X.-L., Luo M.-L., Xu X., Han Y.-L., Cai Y., Zhang Z.-Q., Zhan Q.-M., and Wang M.-R., 2009, “Overexpression of PLK1 is associated with poor survival by inhibiting apoptosis via enhancement of survivin level in esophageal squamous cell carcinoma.,” International journal of cancer. Journal international du cancer, **124**(3), pp. 578-88.

[18] Weichert W., Ullrich A., Schmidt M., Gekeler V., Noske A., Niesporek S., Buckendahl A.-C., Dietel M., and Denkert C., 2006, “Expression patterns of polo-like kinase 1 in human gastric cancer.,” Cancer science, **97**(4), pp. 271-6.

[19] Kneisel L., Strebhardt K., Bernd A., Wolter M., Binder A., and Kaufmann R., 2002, “Expression of polo-like kinase (PLK1) in thin melanomas: a novel marker of metastatic disease.,” Journal of cutaneous pathology, **29**(6), pp. 354-8.

[20] Rizki A., Mott J. D., and Bissell M. J., 2007, “Polo-like kinase 1 is involved in invasion through extracellular matrix.,” Cancer research, **67**(23), pp. 11106-10.

[21] Weichert W., Denkert C., Schmidt M., Gekeler V., Wolf G., Köbel M., Dietel M., and Hauptmann S., 2004, “Polo-like kinase isoform expression is a prognostic factor in ovarian carcinoma.,” British journal of cancer, **90**(4), pp. 815-21.

[22] Zhang Y., Liu Y., Yang Y.-X., Xia J.-H., Zhang H.-X., Li H.-B., and Yu C.-Z., 2009, “The expression of PLK-1 in cervical carcinoma: a possible target for enhancing chemosensitivity.,” Journal of experimental & clinical cancer research : CR, **28**, p. 130.

[23] Takahashi T., Sano B., Nagata T., Kato H., Sugiyama Y., Kunieda K., Okano Y., and Saji S., 2002, “colorectal cancers,” Cancer Science, **1**.

[24] Jachau K., and Mawrin C., with von Bossanyi, 2001, “Increased human polo-like kinase-1 expression in gliomas.,” Journal of neuro-oncology, **53**(1), pp. 1-11.

[25] Ito Y., Miyoshi E., Sasaki N., Kakudo K., Yoshida H., Tomoda C., Uruno T., Takamura Y., Miya a, Kobayashi K., Matsuzuka F., Matsuura N., Kuma K., and Miyauchi a, 2004, “Polo-like kinase 1 overexpression is an early event in the progression of papillary carcinoma.,” British journal of cancer, **90**(2), pp. 414-8.

[26] Yu C., Zhang X., Sun G. U., and Guo X., 2008, “Original Article - Received 7 October 2007 - Accepted 18 January 2008 RNA Interference-Mediated Silencing of the Polo-like Kinase 1 Gene Enhances Chemosensitivity to Gemcitabine in Pancreatic,” October, (October 2007).

[27] Gray P. J., Bearss D. J., Han H., Nagle R., Tsao M.-sound, Dean N., and Hoff D. D. V., 2004, “Identification of human polo-like kinase 1 as a potential therapeutic target in pancreatic cancer Identification of human polo-like kinase 1 as a potential therapeutic target in pancreatic cancer,” Cell, pp. 641-646.

[28] Weichert W., Schmidt M., Gekeler V., Denkert C., Stephan C., Jung K., Loening S., Dietel M., and Kristiansen G., 2004, “Polo-like kinase 1 is overexpressed in prostate cancer and linked to higher tumor grades.,” The Prostate, **60**(3), pp. 240-5.

[29] Reagan-Shaw S., and Ahmad N., 2005, “Polo-like kinase (Plk) 1 as a target for prostate cancer management.,” IUBMB life, **57**(10), pp. 677-82.

[30] Uckun F. M., Ozer Z., Qazi S., Tuel-Ahlgren L., and Mao C., 2010, “Polo-like-kinase 1 (PLK1) as a molecular target to overcome SYK-mediated resistance of B-lineage acute lymphoblastic leukaemia cells to oxidative stress.,” British journal of haematology, **148**(5), pp. 714-25.

[31] Gleixner K. V., Ferenc V., Peter B., Gruze A., Meyer R. a, Hadzijusufovic E., Cerny-Reiterer S., Mayerhofer M., Pickl W. F., Sillaber C., and Valent P., 2010, “Polo-like kinase 1 (Plk1) as a novel drug target in chronic myeloid leukemia: overriding imatinib resistance with the Plk1 inhibitor BI 2536.,” Cancer research, **70**(4), pp. 1513-23.

[32] Stutz N., Nihal M., and Wood G. S., 2011, “Polo-like kinase 1 (Plk1) in cutaneous T-cell lymphoma.,” The British journal of dermatology, **164**(4), pp. 814-21.

[33] Nogawa M., Yuasa T., Kimura S., Tanaka M., Kuroda J., Sato K., Yokota A., Segawa H., Toda Y., Kageyama S., Yoshiki T., Okada Y., and Maekawa T., 2005, “Intravesical administration of small interfering RNA targeting PLK-1 successfully prevents the growth of bladder cancer,” Journal of Clinical Investigation, **115**(4).

[34] Nappi T. C., Salerno P., Zitzelsberger H., Carlomagno F., Salvatore G., and Santoro M., 2009, “Identification of Polo-like kinase 1 as a potential therapeutic target in anaplastic thyroid carcinoma.,” Cancer research, **69**(5), pp. 1916-23.

[35] Lu L.-Y., and Yu X., 2009, “The balance of Polo-like kinase 1 in tumorigenesis.,” Cell division, **4**, p. 4.

[36] Takai N., Hamanaka R., Yoshimatsu J., and Miyakawa I., 2005, “Polo-like kinases (Plks) and cancer.,” Oncogene, **24**(2), pp. 287-91.

[37] Eckerdt F., Yuan J., and Strebhardt K., 2005, “Polo-like kinases and oncogenesis.,” Oncogene, **24**(2), pp. 267-76.

[38] Lu L.-Y., Wood J. L., Minter-Dykhouse K., Ye L., Saunders T. L., Yu X., and Chen J., 2008, “Polo-like kinase 1 is essential for early embryonic development and tumor suppression.,” Molecular and cellular biology, **28**(22), pp. 6870-6.

[39] Steegmaier M., Hoffmann M., Baum A., Lénárt P., Petronczki M., Krssák M., Gürtler U., Garin-Chesa P., Lieb S., Quant J., Grauert M., Adolf G. R., Kraut N., Peters J.-M., and Rettig W. J., 2007, “BI 2536, a potent and selective inhibitor of polo-like kinase 1, inhibits tumor growth in vivo.,” Current biology : CB, **17**(4), pp. 316-22.

[40] Santamaria A., Eberspa U., Eis K., Husemann M., Mumberg D., Prechtl S., Schulze V., Siemeister G., Wortmann L., Barr F. A., and Nigg E. A., 2007, “Use of the Novel Plk1 Inhibitor ZK-Thiazolidinone to Elucidate Functions of Plk1 in Early and Late Stages of Mitosis □,” Molecular Biology of the Cell, **18**(October), pp. 4024 - 4036.

[41] Strebhardt K., 2010, “Multifaceted polo-like kinases: drug targets and antitargets for cancer therapy.,” Nature reviews. Drug discovery, **9**(8), pp. 643-60.

[42] Reindl W., Yuan J., Krämer A., Strebhardt K., and Berg T., 2008, “Inhibition of polo-like kinase 1 by blocking polo-box domain-dependent protein-protein interactions.,” Chemistry & biology, **15**(5), pp. 459-66.

[43] Reindl W., Yuan J., Krämer A., Strebhardt K., and Berg T., 2009, “A pan-specific inhibitor of the polo-box domains of polo-like kinases arrests cancer cells in mitosis.,” Chembiochem : a European journal of chemical biology, **10**(7), pp. 1145-8.

[44] Watanabe N., Sekine T., Takagi M., Iwasaki J.-ichi, Imamoto N., Kawasaki H., and Osada H., 2009, “Deficiency in chromosome congression by the inhibition of Plk1 polo box domain-dependent recognition.,” The Journal of biological chemistry, **284**(4), pp. 2344-53.

[45] Elia A. E. H., Cantley L. C., and Yaffe M. B., 2003, “Proteomic screen finds pSer/pThr-binding domain localizing Plk1 to mitotic substrates.,” Science (New York, N.Y.), **299**(5610), pp. 1228-31.

[46] Elia A. E. H., Rellos P., Haire L. F., Chao J. W., Ivins F. J., Hoepker K., Mohammad D., Cantley L. C., Smerdon S. J., and Yaffe M. B., 2003, “The molecular basis for phosphodependent substrate targeting and regulation of Plks by the Polo-box domain.,” Cell, **115**(1), pp. 83-95.

[47] Kothe M., Kohls D., Low S., Coli R., Cheng A. C., Jacques S. L., Johnson T. L., Lewis C., Loh C., Nonomiya J., Sheils A. L., Verdries K. a, Wynn T. a, Kuhn C., and Ding Y.-H., 2007, “Structure of the catalytic domain of human polo-like kinase 1.,” Biochemistry, **46**(20), pp. 5960-71.

[48] Seong Y.-S., Kamijo K., Lee J.-S., Fernandez E., Kuriyama R., Miki T., and Lee K. S., 2002, “A spindle checkpoint arrest and a cytokinesis failure by the dominant-negative polo-box domain of Plk1 in U-2 OS cells.,” The Journal of biological chemistry, **277**(35), pp. 32282-93.

[49] Archambault V., D’Avino P. P., Deery M. J., Lilley K. S., and Glover D. M., 2008, “Sequestration of Polo kinase to microtubules by phosphopriming-independent binding to Map205 is relieved by phosphorylation at a CDK site in mitosis.,” Genes & development, **22**(19), pp. 2707-20.

[50] Park J.-E., Soung N.-K., Johmura Y., Kang Y. H., Liao C., Lee K. H., Park C. H., Nicklaus M. C., and Lee K. S., 2010, “Polo-box domain: a versatile mediator of polo-like kinase function.,” Cellular and molecular life sciences : CMLS, **67**(12), pp. 1957-70.

[51] Qi W., Tang Z., and Yu H., 2006, “Phosphorylation- and Polo-Box – dependent Binding of Plk1 to Bub1 Is Required for the Kinetochore Localization of Plk1 □,” Molecular Biology of the Cell, **17**(August), pp. 3705-3716.

[52] Baumann C., Körner R., Hofmann K., and Nigg E. a, 2007, “PICH, a centromere-associated SNF2 family ATPase, is regulated by Plk1 and required for the spindle checkpoint.,” Cell, **128**(1), pp. 101-14.

[53] García-Alvarez B., Cárcer G. de, Ibañez S., Bragado-Nilsson E., and Montoya G., 2007, “Molecular and structural basis of polo-like kinase 1 substrate recognition: Implications in centrosomal localization.,” Proceedings of the National Academy of Sciences of the United States of America, **104**(9), pp. 3107-12.

[54] Huggins D. J., McKenzie G. J., Robinson D. D., Narváez A. J., Hardwick B., Roberts-Thomson M., Venkitaraman A. R., Grant G. H., and Payne M. C., 2010, “Computational Analysis of Phosphopeptide Binding to the Polo-Box Domain of the Mitotic Kinase PLK1 Using Molecular Dynamics Simulation,” PLoS Computational Biology, **6**(8), p. e1000880.

[55] Neef R., Preisinger C., Sutcliffe J., Kopajtich R., Nigg E. a, Mayer T. U., and Barr F. a, 2003, “Phosphorylation of mitotic kinesin-like protein 2 by

polo-like kinase 1 is required for cytokinesis.," The Journal of cell biology, **162**(5), pp. 863-75.

[56] Chen Y.-C., and Weinreich M., 2010, "Dbf4 regulates the Cdc5 Polo-like kinase through a distinct non-canonical binding interaction.," The Journal of biological chemistry, **285**(53), pp. 41244-54.

[57] Seki A., Coppinger J. a, Jang C.-Y., Yates J. R., and Fang G., 2008, "Bora and the kinase Aurora a cooperatively activate the kinase Plk1 and control mitotic entry.," Science (New York, N.Y.), **320**(5883), pp. 1655-8.

[58] Lowery D. M., Mohammad D. H., Elia A. E. H., and Yaffe M. B., 2004, "The Polo-Box Domain: A Molecular Integrator of Mitotic Kinase Cascades and Polo-like Kinase Function," Cell Cycle, **3**(2), pp. 128-131.

[59] Harris D., Orme C., Kramer J., Namba L., Champion M., Palladino M. J., Natzle J., and Hawley R. S., 2003, "A deficiency screen of the major autosomes identifies a gene (matrimony) that is haplo-insufficient for achiasmate segregation in Drosophila oocytes.," Genetics, **165**(2), pp. 637-52.

[60] Xiang Y., Takeo S., Florens L., Hughes S. E., Huo L.-J., Gilliland W. D., Swanson S. K., Teeter K., Schwartz J. W., Washburn M. P., Jaspersen S. L., and Hawley R. S., 2007, "The inhibition of polo kinase by matrimony maintains G2 arrest in the meiotic cell cycle.," PLoS biology, **5**(12), p. e323.

[61] Formstecher E., Aresta S., Collura V., Hamburger A., Meil A., Trehin A., Reverdy C., Betin V., Maire S., Brun C., Jacq B., Arpin M., Bellaiche Y., Bellusci S., Benaroch P., Bornens M., Chanet R., Chavrier P., Delattre O., Doye V., Fehon R., Faye G., Galli T., Girault J.-A., Goud B., Gunzburg J. de, Johannes L., Junier M.-P., Mirouse V., Mukherjee A., Papadopoulo D., Perez F., Plessis A., Rossé C., Saule S., Stoppa-Lyonnet D., Vincent A., White M., Legrain P., Wojcik J., Camonis J., and Daviet L., 2005, "Protein interaction mapping: a Drosophila case study.," Genome research, **15**(3), pp. 376-84.

[62] Blom N., Sicheritz-Pontén T., Gupta R., Gammeltoft S., and Brunak S., 2004, "Prediction of post-translational glycosylation and phosphorylation of proteins from the amino acid sequence.," Proteomics, **4**(6), pp. 1633-49.

[63] Wojcik E. J., 2008, "A mitotic role for GSK-3β kinase in Drosophila," Cell Cycle, **7**(December), pp. 3699-3708.

[64] Qiao F., and Bowie J. U., 2005, “The many faces of SAM.,” Science’s STKE : signal transduction knowledge environment, **2005**(286), p. re7.

[65] Kim C. a, and Bowie J. U., 2003, “SAM domains: uniform structure, diversity of function.,” Trends in biochemical sciences, **28**(12), pp. 625-8.

[66] Hall T. M. T., 2003, “SAM breaks its stereotype,” Nature Structural Biology, **10**(9), pp. 677-679.

[67] Galea CA, Wang Y, Sivakolundu SG K. R., 2008, “Regulation of cell division by intrinsically unstructured proteins: intrinsic flexibility, modularity, and signaling conduits.,” Biochemistry, **47**(29), pp. 7598-7609.

[68] Prilusky J., Felder C. E., Zeev-Ben-Mordehai T., Rydberg E. H., Man O., Beckmann J. S., Silman I., and Sussman J. L., 2005, “FoldIndex: a simple tool to predict whether a given protein sequence is intrinsically unfolded.,” Bioinformatics (Oxford, England), **21**(16), pp. 3435-8.

[69] Geddie ML, O’Loughlin TL, Woods KK M. I., 2005, “Rational Design of p53, an Intrinsically Unstructured Protein, for the Fabrication of Novel Molecular Sensors,” J Biol Chem, **22**(5), pp. 35641-35646.

[70] Whitaker M., 1996, “Control of meiotic arrest.,” Reviews of reproduction, **1**(2), pp. 127-35.

[71] Masui Y., 2001, “From oocyte maturation to the in vitro cell cycle: the history of discoveries of Maturation-Promoting Factor (MPF) and Cytostatic Factor (CSF).,” Differentiation; research in biological diversity, **69**(1), pp. 1-17.

[72] Nicklas R. B., 1974, “Chromosome segregation mechanisms.,” Genetics, **78**(1), pp. 205-13.

[73] Hawley R. S., 1988, “Exchange and Chromosomal Segregation in Eukaryotes,” Genetic Recombination, Kucherlapati R., ed., ASM Press, Washington, DC., pp. 497-527.

[74] Page S. L., and Hawley R. S., 2003, “Chromosome choreography: the meiotic ballet.,” Science (New York, N.Y.), **301**(5634), pp. 785-9.

[75] Grell R. F., 1962, “A new model for secondary nondisjunction: the role of distributive pairing.,” Genetics, **47**(December), pp. 1737-54.

[76] Hawley R. S., Irick H., Zitron A. E., Haddox D. A., Lohe A., New C., Whitley M. D., Arbel T., Jang J., McKim K., and Childs G., 1993, “There are two mechanisms of achiasmate segregation in Drosophila females, one of which requires heterochromatic homology,” Developmental genetics, **13**, pp. 440-467.

[77] Oliver T. R., Feingold E., Yu K., Cheung V., Tinker S., Yadav-Shah M., Masse N., and Sherman S. L., 2008, “New insights into human nondisjunction of chromosome 21 in oocytes.,” PLoS genetics, **4**(3), p. e1000033.

[78] Fledel-Alon A., Wilson D. J., Broman K., Wen X., Ober C., Coop G., and Przeworski M., 2009, “Broad-scale recombination patterns underlying proper disjunction in humans.,” PLoS genetics, **5**(9), p. e1000658.

[79] Koehler K. E., and Hassold T. J., 1998, “Human aneuploidy: lessons from achiasmate segregation in Drosophila melanogaster.,” Annals of human genetics, **62**(Pt 6), pp. 467-79.

[80] Smith S. K., Jaspersen S. L., and Hawley R. S., 2008, “Matrimony ties Polo down: Can this kinase get free?,” Cell Cycle, **7**(6), pp. 698-701.

[81] Tanaka K., Petersen J., MacIver F., Mulvihill D. P., Glover D. M., and Hagan I. M., 2001, “The role of Plo1 kinase in mitotic commitment and septation in Schizosaccharomyces pombe.,” The EMBO journal, **20**(6), pp. 1259-70.

[82] Lee K. S., Park J.-E., Asano S., and Park C. J., 2005, “Yeast polo-like kinases: functionally conserved multitask mitotic regulators.,” Oncogene, **24**(2), pp. 217-29.

[83] Liu J., and Maller J. L., 2005, “Xenopus Polo-like kinase Plx1: a multifunctional mitotic kinase.,” Oncogene, **24**(2), pp. 238-47.

[84] Chase D., Serafinas C., Ashcroft N., Kosinski M., Longo D., Ferris D. K., and Golden a, 2000, “The polo-like kinase PLK-1 is required for nuclear envelope breakdown and the completion of meiosis in Caenorhabditis elegans.,” Genesis (New York, N.Y. : 2000), **26**(1), pp. 26-41.

[85] Qian Y. W., Erikson E., Taieb F. E., and Maller J. L., 2001, “The polo-like kinase Plx1 is required for activation of the phosphatase Cdc25C and cyclin B-Cdc2 in Xenopus oocytes.,” Molecular biology of the cell, **12**(6), pp. 1791-9.

[86] Bischof J., Maeda R. K., Hediger M., Karch F., and Basler K., 2007, “An optimized transgenesis system for Drosophila using germ-line-specific phiC31 integrases.,” Proceedings of the National Academy of Sciences of the United States of America, **104**(9), pp. 3312-7.

[87] Zybailov B., Mosley A. L., Sardiu M. E., Coleman M. K., Florens L., and Washburn M. P., 2006, “Statistical analysis of membrane proteome expression changes in Saccharomyces cerevisiae.,” Journal of proteome research, **5**(9), pp. 2339-47.

[88] Pavelka N., Pelizzola M., Vizzardelli C., Capozzoli M., Splendiani A., Granucci F., and Ricciardi-Castagnoli P., 2004, “A power law global error model for the identification of differentially expressed genes in microarray data.,” BMC bioinformatics, **5**, p. 203.

[89] Eckerdt F., Yuan J., Saxena K., Martin B., Kappel S., Lindenau C., Kramer A., Naumann S., Daum S., Fischer G., Dikic I., Kaufmann M., and Strebhardt K., 2005, “Polo-like kinase 1-mediated phosphorylation stabilizes Pin1 by inhibiting its ubiquitination in human cells.,” The Journal of biological chemistry, **280**(44), pp. 36575-83.

[90] Lancaster O. M., Cullen C. F., and Ohkura H., 2007, “NHK-1 phosphorylates BAF to allow karyosome formation in the Drosophila oocyte nucleus.,” The Journal of cell biology, **179**(5), pp. 817-24.

[91] Orsi G. a, Joyce E. F., Couble P., McKim K. S., and Loppin B., 2010, “Drosophila I-R hybrid dysgenesis is associated with catastrophic meiosis and abnormal zygote formation.,” Journal of cell science, **123**(Pt 20), pp. 3515-24.